UNIVERSITÀ DEGLI STUDI DI MILANO – BICOCCA
Facoltà di Scienze Matematiche, Fisiche e Naturali
Corso di Dottorato in Biologia, XXV ciclo

The protein kinase Swe1: new players in its regulatory pathway and analysis of its involvement in mitotic spindle dynamics

Tutor: Dott.ssa Roberta FRASCHINI

Tesi di Dottorato di:
Erica RASPELLI
Matr. n. 064126

Anno Accademico 2011 - 2012

The protein kinase Swe1: new players in its regulatory pathway and analysis of its involvement in mitotic spindle dynamics

Erica Raspelli

matricola 064126

Tutor: Dott.ssa Roberta FRASCHINI

Università degli Studi di Milano Bicocca,

Piazza dell'ateneo Nuovo 1,20126 Milano

Dipartimento di Biotecnologie e Bioscienze

Piazza della Scienza 2, 20126 Milano

A tutti voi

che mi siete sempre accanto...

Contents

Abstract

Abstract

Swe1 is the effector kinase of the morphogenesis checkpoint that, in budding yeast, provides a link between cell morphology and entry into mitosis. Although there are some differences due to the particular kind of cell division established by the budding, Swe1 functions and regulators are evolutionarily conserved, indicating that this is an ancient cell cycle control strategy that has been adapted to respond to cytoskeletal signals in vertebrate as well as in *S. cerevisiae* cells. Swe1 blocks entry into mitosis through inhibitory phosphorylation of the catalytic subunit of the cyclin-dependent kinase Cdk1, Cdc28, and this modification is reversed by the protein phosphatase Mih1. Cdc28 activity is required both for entry into mitosis and for the switch from polar to isotropic bud growth, so when Cdc28 is phosphorylated on Tyr19 (Y19) both these events are inhibited.

Timely degradation of Swe1 is important for cell survival in case of DNA replication stress, while it is inhibited by the morphogenesis checkpoint in response to alterations in actin cytoskeleton or septins' structure. We show here that the lack of the Dma1 and Dma2 ubiquitin ligases, which moderately affects Swe1 localization and degradation during an unperturbed cell cycle with no apparent phenotypic effects, is toxic for cells that are partially defective in Swe1 down-regulation. Interestingly Swe1 is stabilized, but differently from morphogenesis checkpoint activation, restrained at

the bud neck and hyperphosphorylated in *dma1Δ dma2Δ* cells subjected to DNA replication stress, indicating that the mechanism stabilizing Swe1 under these conditions is different from the one triggered by the morphogenesis checkpoint. Finally, the Dma proteins are required for proper Swe1 ubiquitylation. Altogether, our data highlight a previously unknown role of these proteins in the complex regulation of Swe1 degradation and suggest that they might contribute to control, directly or indirectly, Swe1 ubiquitylation.

As already said, Swe1 stabilization prevents mitotic entry in response to different problems. In addition, elevated Swe1 levels inhibits mitotic spindle formation and elongation and several data indicate that, apart Cdc28, other Swe1 targets are likely involved in this process. In fact, the expression of Cdc28 alleles that could escape from Swe1 inhibition is not sufficient neither to restore proper spindle elongation nor progression through mitosis of cells that overexpress Swe1. We tried to identify new Swe1 targets acting in mitotic spindle dynamics and progression through mitosis by performing a genetic screen and by analyzing putative candidates among factors known to be involved in these processes. About the genetic screen, we found twelve recessive spontaneous suppressors that are able to restore spindle elongation and viability of *SWE1* overespressing cells that lack the APC regulatory subunit *CDH1.* Interestingly, the suppression phenotype is due to inactivation of the

same gene in all the suppressors. We are now trying to identify this gene and to characterize the suppression mechanism.

In parallel, we pursued the identification of Swe1 targets by analyzing spindle associated factors and proteins involved in spindle dynamycs. In particular, the MAP Bik1 was found in a proteome chip array as a protein phosphorylated by Swe1. We found that, differently from what is published, high Swe1 levels reduce Bik1 phosphorylation independently of Swe1 inhibitory activity on Cdc28. Further analysis will be required to better understand the molecular details of the indirect Swe1 action on Bik1 phosphorylation. In addition, we found that high levels of the Polo kinase *CDC5* partially restore spindle elongation and viability of *SWE1* overexpressing cells, but only in the presence of functional Mih1. In particular, high Swe1 levels cause the accumulation of fully phosphorylated Mih1, that is not functional, and *CDC5* overexpression in these cells restores the proper balance between Mih1 phosphorylation forms, and so its functionality. Further analysis will be required to better understand the interaction between Swe1, Cdc5 and the protein phosphatase Mih1.

Altogether our data shed new light on Swe1 regulation mechanism and put the basis for the identification its new target(s) .

Riassunto

Riassunto

Swe1 è la chinasi effettrice del checkpoint morfogenetico che, in lievito, coordina la formazione e la crescita della gemma con la divisione mitotica. Nonostante le differenze dovute al particolare tipo di divisione di *S. cerevisiae*, che si divide per gemmazione, le funzioni e i regolatori di Swe1 sono evolutivamente conservati; questo implica l'esistenza di un meccanismo di controllo comune per rispondere ad alterazioni del citoscheletro sia nei vertebrati che in lievito. Swe1 impedisce l'ingresso delle cellule in mitosi mediante una fosforilazione inibitoria su Cdc28, la subunità catalitica dei complessi CDK-ciclina; la fosfatasi Mih1 controbilancia l'azione di Swe1 rimuovendo la fosforilazione da Cdc28 e riportandola così nello stato attivo. Dal momento che l'attività dei complessi CDK-ciclina è richiesta sia per l'ingresso in mitosi che per il passaggio da crescita polarizzata a crescita isotropica, quando Cdc28 è fosforilata sul residuo Tyr19 (Y19) entrambi questi eventi sono inibiti.

Una rapida degradazione di Swe1 è importante per la sopravvivenza delle cellule in caso di stress replicativo, mentre Swe1 viene stabilizzato dal checkpoint morfogenetico in caso di alterazioni al citoscheletro di actina o all'anello di septine. In questo lavoro, mostriamo che l'assenza delle ubiquitina ligasi Dma1 e Dma2, che non ha grosse ripercussioni sulla localizzazione di Swe1 e sulla sua degradazione in un ciclo cellulare non perturbato, è tossica per le cellule che sono parzialmente difettive nella degradazione di Swe1.

Per di più, Swe1 è stabilizzata, mantenuta al bud neck e iperfosforilata in cellule *dma1Δ dma2Δ* sottoposte a stress replicativo, ad indicare che il meccanismo che porta alla stabilizzazione di Swe1 in queste condizioni è differente da quello attivato dal checkpoint morfogenetico. Infine, le proteine Dma sono richieste per una corretta ubiquitinazione di Swe1. Nel complesso, i nostri dati evidenziano un nuovo ruolo per le proteine Dma nel processo che porta alla degradazione di Swe1 e suggeriscono che possano contribuire, direttamente o indirettamente, all'ubiquitinazione di Swe1.

La stabilizzazione di Swe1 impedisce l'ingresso in mitosi in risposta a diversi problemi morfologici, inoltre alti livelli di Swe1 inibiscono la formazione e l'allungamento del fuso mitotico, e diversi dati indicano che Swe1 potrebbe agire su altri bersagli diversi da Cdc28 per la regolazione di questi processi. Infatti, l'introduzione di alleli di Cdc28 che non possono essere inibiti da Swe1 non è sufficiente a ripristinare un corretto allungamento del fuso nè una corretta mitosi in cellule che overesprimono *SWE1*. Abbiamo quindi tentato di identificare nuovi targets di Swe1 coinvolti nella dinamica del fuso mitotico e nella progressione della mitosi sia attraverso uno screening genetico che analizzando possibili candidati tra i fattori coinvolti nella dinamica del fuso mitotico. Per quanto riguarda lo screening, abbiamo identificato diversi soppressori spontanei, di cui 12 sono recessivi e sono in grado di ripristinare l'allungamento del

fuso e la vitalità di cellule che overesprimono *SWE1* e che portano le delezione della subunità regolativa dell'APC *CDH1.* E' da notare che tutti e 12 i soppressori, pur essendo indipendenti tra loro, sono mutati tutti nello stesso gene, che è responsabile per il fenotipo di soppressione. Stiamo cercando di identificare questo gene per meglio caratterizzare il meccanismo di soppressione e le eventuali interazioni con Swe1. Per quanto riguarda l'analisi di fattori associati al fuso mitotico, la MAP Bik1 è stata identificata in un proteome chip array come proteina fosforilata da Swe1. Abbiamo trovato che, a differenza di quanto è pubblicato, alti livelli di Swe1 riducono la fosforilazione di Bik1 e che questo è indipendente dall'attività inibitoria che Swe1 esercita su Cdc28. Saranno quindi necessarie altre analisi per approfondire il meccanismo dell'azione indiretta di Swe1 su Bik1. Inoltre, abbiamo dimostrato che alti livelli della Polo chinasi Cdc5 ripristinano in parte sia l'allungamento del fuso che la vitalità di cellule che overesprimono *SWE1* ma solo in presenza di Mih1 funzionale. Inoltre, alti livelli di Swe1 causano un accumulo di Mih1 completamente fosforilata, che è inattiva, e l'overespressione di *CDC5* in queste cellule ripristina il corretto bilanciamento tra le diverse forme fosforilate di Mih1. Ulteriori analisi saranno quindi necessarie per meglio comprendere le interazioni tra la chinasi Swe1 e la fosfatasi Mih1.

Nel complesso i nostri dati contribuiscono a chiarire il meccanismo di regolazione di Swe1 e aprono la strada all'identificazione di altri target di Swe1 diversi da Cdc28.

Introduction

The morphogenesis checkpoint and the protein kinase Swe1

In all eukaryotic cells, entry and progression into mitosis are controlled by the cyclin-dependent kinase Cdk1 bound to B-type cyclins. The activation of the mitotic CDK complexes is inhibited in case of damaged or not completely replicated DNA (Elledge et al., 1996), abnormal cell morphology or cytoskeletal problems (Huang and Ingber, 1999) by checkpoint pathways that mantain inhibitory phosphorylation of the catalitic subunit of Cdk1 on the conserved residues Thr14 and Tyr15 (Tyr19 in budding yeast), thus preventing entry into mitosis. In mammalian cells, these residues are phosphorylated by Wee1 and dephosphorylated by the phosphatase Cdc25, and checkpoint pathways act by inhibiting Cdc25 and promoting Wee1 function, thus ensuring the Wee1 inhibitory activity on Cdk1. The *Saccharomyces cerevisiae* homologous of Wee1 is the protein kinase Swe1, whose stability is controlled by the morphogenesis checkpoint, a conserved mechanism that provides a link between bud formation and mitosis (Keaton and Lew, 2006) by monitoring bud shape and actin cytoskeleton (Sia et al., 1996). This checkpoint inhibits entry into mitosis at least in part through Swe1 stabilization (Sia et al., 1998). Although these proteins are conserved among different organisms, *S. cerevisiae* Wee1 (Swe1) acts quite differently from its counterparts, probably because budding yeast mitosis begins early due to the unusual life cycle imposed by the budding. Swe1 inhibits entry into mitosis by phosphorylating the Y19

residue of the catalitic subunit of Cdk1, Cdc28 (Booher et al., 1993); this inhibitory phosphorylation is reversed by the Mih1 phosphatase (Russell *et al.*, 1989), leading to Cdk1 activation and entry into mitosis (Fig. 1). However, Y19 phosphorylation and its subsequent dephosphorylation are not essential for M-phase initiation in budding yeast (Amon et al., 1992). In fact, cells lacking either Swe1 or Mih1 display normal cell cycle in unperturbed condition, while Swe1 becomes essential for cell viability in response to perturbation in bud morphology or actin cytoskeleton (McMillan et al., 1998). Under these conditions, Swe1 inactivation is inhibited by the morphogenesis checkpoint, thus blocking entry into mitosis. Moreover, Swe1 overexpression from the *GAL1* promoter (*GAL1-SWE1*) is lethal for cells, because it inhibits Cdc28 totally, thus blocking both switch from polar to isotropic bud growth and separation of the microtubule organizing centers (Spindle Pole Bodies, SPBs, in yeast). As a consequence, cells arrest with elongated buds, undivided nuclei and monopolar spindles (Lim et al., 1996).

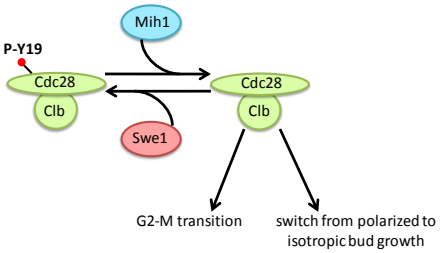

Figure 1: Schematic representation of CDK inhibition in budding yeast. Swe1 inhibits both entry into mitosis and transition from polarized to isotropic bud growth through phosphorylation of the Tyr19 (P-Y19) of the catalitic subunit of CDK complex, Cdc28. Its inhibitory activity is counteracted by the phosphatase Mih1 that removes the phosphate group from Tyr19 leading to CDK activation.

Swe1 has therefore a critical role in coordinating cell morphogenesis with nuclear division and it is subjected to multiple regulations that change its phosphorylation state (35-40 phosphorylated sites have been identified *in vivo*), subcellular localization and protein levels. During S phase, Swe1 accumulates in the nucleus, where it is phosphorylated by Clb-Cdc28 before being exported to the cytoplams, and then to the daughter side of the bud neck. Swe1 nuclear export is essential for its degradation in G2/M, as a Swe1 variant that cannot be exported from the nucleus is largely stabilized (Keaton et al., 2008). Clb-Cdc28 phosphorylates Swe1 at multiple sites (Harvey et al., 2005) and these events can occur in the nucleus, in the cytoplasm or at the bud neck. This multiple phosphorylation by Cdc28-Clb has different roles: on one hand it promotes Swe1 activity generating a feedback loop, while on the other hand it promotes Swe1 degradation (Keaton and Lew, 2006). At the mother-bud neck, filaments of evolutionarily conserved proteins called septins (Cdc3, Cdc10, Cdc11, Cdc12 and Shs1 in *S. cerevisiae*) form a dynamic ring structure (Versele and Thorner, 2004) that is essential for the recruitment of a number of proteins involved the control of cell cycle progression (Longtine and Bi, 2003; Gladfelter et al., 2005). Among these, the septin ring acts as a platform to recruit several Swe1 regulators, such as the Hsl1 protein kinase and its adaptor Hsl7, both essential for Swe1 localization to the bud neck and for its phosphorylation (Longtine et

al., 2000; Shulewitz et al., 1999). Hsl1, whose kinase activity requires assembled septins, undergoes autophosphorylation (Barral et al., 1999; McMillan et al., 1999) and phosphorylates Hsl7 (Shulewitz et al., 1999), but does not seem to phosphorylates Swe1 (Cid et al., 2001) although its kinase activity is required for Swe1 recruitment at the bud neck (Theesfeld et al., 2003). The fact that Hsl1 activation requires assembled septins ensures that Swe1 degradation does not begin until a bud has formed, thus providing a link between bud formation and entry into mitosis (Theesfeld et al., 2003). Also the PAK (p21-activated kinase) kinase Cla4 associates with the septin ring and is involved in Swe1 phosphorylation, probably during S phase (Sakchaisri et al., 2004). Moreover, Swe1 phosphorylation by Clb-Cdc28 promotes subsequent phosphorylation by the Polo-like kinase Cdc5 in M phase; in fact the synergistic phosphorylation that can be observed *in vitro* on Swe1 by Clb2-Cdc28 and Cdc5 is the result of priming Swe1 by Cdc28, with the resulting phosphorylated Swe1 becoming a better substrate for Cdc5 (Asano et al., 2005). An additional level of Swe1 regulation involves the Cdc55 regulatory subunit of protein phosphatase PP2A that has been implicated in Swe1 degradation, since Cdc55 loss of function causes Swe1 stabilization (Yang et al., 2000). However, the molecular details this control happens are not clear. In addition, a mathematical model for morphogenesis checkpoint activation suggested that a subset of Swe1 phosphorylations might inhibit its

activity whereas other phosphorylations may target Swe1 for degradation (Ciliberto et al., 2003). In any case, hyperphosphorylated Swe1 species are recognized by a still unidentified ubiquitin ligase and ubiquitylated (McMillan et al., 2002). Subsequently, Swe1 is degraded via the proteasome and this event allows mitotic entry (McMillan et al., 2002) (Fig.2).

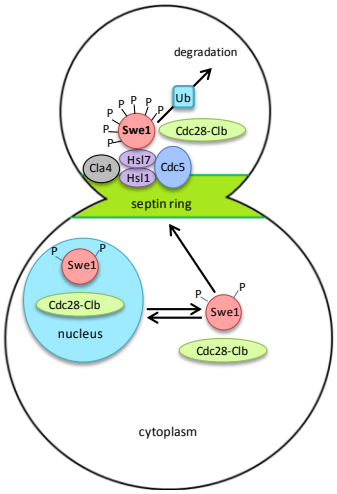

Figure 2: Swe1 localization and degradation in yeast. Swe1 accumulates in the nucleus of unbudded cells and is translocated to the daughter side of the bud neck following bud emergence through interaction with Hsl1-Hsl7. Once at the bud neck Swe1 undergoes multiple phosphorylation events that lead to its ubiquitylation and degradation via the proteasome (modified from Keaton and Lew, 2006). See text for details.

Successful bud formation leads to Swe1 degradation in G2, while morphological defects block this degradation, thus delaying entry into mitosis. Swe1 levels are controlled by the morphogenesis checkpoint, whose activation in response to alterations in actin cytoskeleton or septin organization causes Swe1 accumulation and subsequent delay in nuclear division (Lew, 2003) (Fig.3). This

checkpoint inhibits Swe1 degradation by interfering with Hsl1 localization at the bud neck, thus preventing Swe1 recruitment that is mandatory for modifications leading to its degradation (Longtine *et al.*, 2000). Accordingly, the lack of septin localization at the bud neck results in Swe1 stabilization (Barral *et al.*, 1999; Shulewitz *et al.*, 1999; Longtine *et al.*, 2000), and even subtle perturbations in septin structure interfere with Hsl1 and Swe1 localization at the bud neck (Longtine *et al.*, 2000). Moreover, actin depolymerization in budded cells causes both stabilization of Swe1 and its displacement from the bud neck without altering Hsl1 localization (Longtine *et al.*, 2000), indicating that morphogenesis checkpoint activation prevents Swe1 degradation by interfering with Swe1 localization at the bud neck, thus inhibiting the G2/M transition.

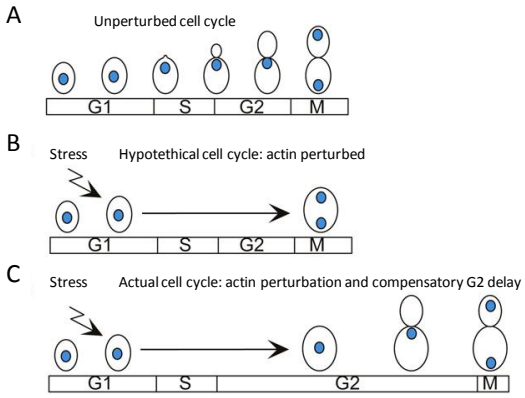

Figure 3: The morphogenesis checkpoint: The morphogenesis checkpoint. (A) During an unperturbed cell cycle, bud formation is coincident with DNA replication, and by the time of nuclear division, the bud is ready to receive the daughter nucleus. (B) Stresses can delay bud formation, and if the cell cycle continued uninterrupted, cells would become binucleate. (C) In reality, delays in bud formation trigger compensatory G2 delays in the cell cycle through the morphogenesis checkpoint, thus ensuring proper nuclear division (Lew, D.J., 2003).

However, how bud neck-localized Swe1 is targeted to degradation after phosphorylation is still obscure. There are Swe1 variants that do not undergo degradation although they show proper bud neck localization, phosphorylation and interaction with known Swe1 regulators (McMillan et al., 2002), indicating that still unknown Swe1 regulators exist. Moreover, the involvement of the ubiquitylation pathway and the identity of the related ubiquitin ligase(s) involved in Swe1 degradation are unknown. The *S. pombe* homologue of Swe1, Wee1, is ubiquitylated by the SCF (Skp, Cullin, F-box) complex (Ayad et al., 2003), a conserved multiprotein complex that is responsible for the ubiquitylation of a lot of cell cycle regulators. However, the single deletion of every known *S. cerevisiae* F-box protein does not cause accumulation of Y19 phosphorylated Cdc28, indicating that this complex is not responsible for Swe1 degradation in budding yeast or that more than a single F-box protein is involved in this process (McMillan et al., 2002). Another ubiquitin ligase that targets cell cycle regulators for degradation is the anaphase-promoting complex (APC) that works in association with either Cdc20 or Cdh1 regulatory subunits. Swe1 degradation is unaffected in nocodazole treated cells (Sia et al., 1998), a condition that keeps inactive both APC regulatory subunits, so it seems unlikely that this complex could mediate Swe1 degradation. Thus, the complex responsible for Swe1 ubiquitylation is not known yet and there are no obvious candidates to mediate this process.

Septins

Septins are a conserved family of GTP binding proteins that act as a scaffold for the recruitment of other proteins (Versele and Thorner, 2005). They were first identified in the budding yeast *S. cerevisiae* by temperature-sensitive mutations causing defective cytokinesis resulting in chains of multibudded and multinucleated cells at restrictive temperature (Hartwell, 1971). Subsequently, septins were found in all fungi and animals, but not in plants (Kinoshita, 2003). They share common functions in all the organisms where they were found, as they are involved in septum deposition during cytokinesis, in cell polarity establishment and in forming diffusion barrier (Cooper and Kiehart, 1996; Trimble, 1999; Caudron and Barral, 2009). *S. cerevisiae* septins are also implicated in bud site selection (Sanders et al., 1996; Longtine et al., 2003), chitin ring deposition (DeMarini et al., 1997), mitotic spindle positioning (Kusch et al., 2002), spindle positioning checkpoint (Fraschini et al., 2008) and morphogenesis checkpoint (Theesfeld et al., 2003; Gladfelter et al., 2005). Moreover, they are involved in monitoring cell cycle progression (Shulewitz et al., 1999; Barral et al., 1999) and form a diffusion barrier between the mother and the bud (Barral et al., 2000).

Seven genes encode *S. cerevisiae* septins: five of them, *CDC3, CDC10, CDC11, CDC12* and *SHS1/SEP7*, are expressed during the mitotic cell cycle, while *SPR3* and *SPR28* are expressed specifically during meiosis, where they replace Cdc12 and Shs1, respectively (De Virgilio

et al., 1996, Fares et al., 1996). All these proteins have conserved domains: a GTP binding domain homologous to Ras-like GTPases, an inositol-binding motif and a septin unique element of unknown function. Moreover, some septins, like Cdc3 and Cdc12, have a C-terminal coiled-coil domain (Versele and Thorner, 2005). Septins form hetero-oligomeric complexes that assemble into filaments, which then are organized into a ring that localizes at the future bud site in late G1. Once the bud emerges, the ring expands into a collar, forming an "hourglass structure" at the bud neck. During cytokinesis this structure splits into two rings that localize one to the mother cell cortex and the other to the bud cell cortex, before being disassembled during the next G1 (Longtine and Bi, 2003) (Fig.4).

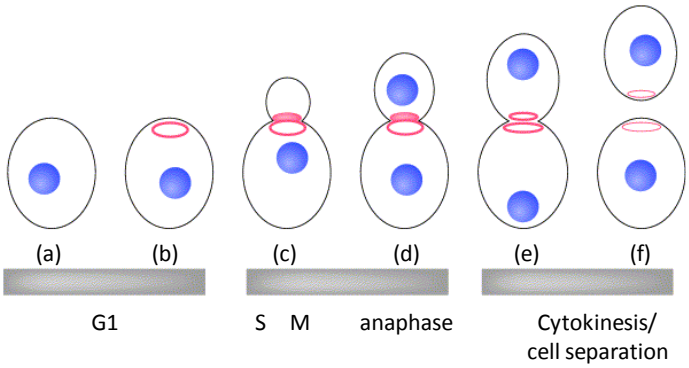

Figure 4: Septins dynamics in budding yeast. Early in G1 there is no specific localization of septins (a); they assemble into a ring at the presumptive bud site in late G1 (b); after bud emergence, the ring expands into a collar, forming an hourglass structure at the mother-bud neck (c), that persist until anaphase (d). Just before cytokinesis the collar splits into two rings (e) that are inherited one from the mother cell and the other from the daughter cell, and that are disassembled during the next G1 (f). (modified from Longtine and Bi, 2003).

These transitions in septins organization are due to an alternation between dynamism and stability, as supported by studies using fluorescence recovery after photobleaching (FRAP) (Dobbelaere et al., 2003). After bud emergence, septins switch from a dynamic state to a more stable state, which coincides with the switch from a ring to an hourglass structure. Around the time of cytokinesis, septins return dynamic, which coincides with the splitting of the septin hourglass into two rings (Dobbelaere et al., 2003; Cid et al., 2001), a step required for proper septum deposition.

The assembly of the septin ring and the transitions that take place throughout the cell cycle rely on many proteins. The small Rho-like GTPase Cdc42 has an essential role in septin ring assembly, and indeed septins are recruited to the future bud site in response to the polarization signal that comes from Cdc42 (Caviston et al., 2003). In fact, mutations affecting *CDC42*, *CDC24* (the latter encoding the Cdc42 GEF) or the GTP/GDP cycle of Cdc42 cause defects in septin ring assembly (Caviston et al., 2003; Gladfelter et al., 2002).

Septin ring dynamics during the cell cycle is regulated by different post-translational modifications, such as phosphorylation or SUMOylation. One of the effectors of Cdc42, the PAK kinase Cla4, is localized at the bud emergence site and is involved in the first steps of septin ring assembly and stabilization (Dobbelaere et al., 2003; Kadota et al., 2004). Cla4 phosphorylates Cdc10, Cdc3 and Cdc11 *in vitro*, and is responsible for a large part of Cdc10 phosphorylation *in*

vivo (Versele and Thorner, 2004). This event, which occurs in late G1, promotes and stabilizes septin complexes and filaments, thus ensuring proper ring assembly (Versele and Thorner, 2004). Cdc42 localizes at the future bud site and is involved, in addition to septins regulation, also in cell polarity establishment and maintenance. The fact that Cla4 needs to interact with Cdc42 in order to be active provides a space and time link between septin ring assembly, budding and polarity establishment. Another kinase involved in septin ring stabilization is Gin4, which localizes at the septin ring in late G1, playing a role in the formation of a rigid structure (Mortensen et al., 2002). Moreover Gin4 phosphorylates the septin Shs1 in mitosis, but the function of this modification is not clear (Dobbelaere et al., 2003; Mortensen et al., 2002). By the onset of cytokinesis, Shs1 is dephosphorylated by the protein phosphatase PP2A in association with its regulatory subunit Rts1 (Dobbelaere et al., 2003). After cell separation, the septin ring inherited is disassembled both in the mother and in the daughter cells, and the septin subunits are recycled in the next cell cycle (McMurray and Thorner, 2009). Cdc3 phosphorylation by Cdc28 in complex with G1 cyclins is required for this last step (Tang and Reed, 2002). Septins are subjected to a further kind of modification: they can be SUMOylated (i. e. conjugated with the ubiquitin-like peptide SUMO) on specific lysine residues. During mitosis, Cdc3, Cdc11 and Shs1 undergo this

modification, which promotes the destabilization of the hourglass structure, thus allowing its splitting (Johnson and Blobel, 1999).

As previously mentioned, budding yeast septins are involved in a number of different processes, which almost all rely on two septins features: the ability to form a diffusion barrier and to act as a scaffold for the recruitment of different proteins.

Septins' ability to form a diffusion barrier is very important throughout the cell cycle and is essential in cytokinesis. In fact, budding yeast septins control the compartmentalization of the cell cortex. This organization is required for several critical processes during the whole cell cycle: the septin ring/collar is required to maintain cell polarity and promote the restriction of growth to the bud, to help bud differentiation from the mother cell by accumulating different plasma membrane and cortical proteins, and to monitor the proper partition of SPBs between the mother and the bud at the end of mitosis (Caudron and Barral, 2009). Moreover, when the septin collar splits into two rings just before cytokinesis, each ring establishes a new diffusion barrier, with a new compartment between them. This compartmentalization restrains diffusible cortical factors involved in cell separation at the site of cell division, thus allowing proper cytokinesis (Dobbelaere and Barral, 2004).

Septins also act as a scaffold for the recruitment of a number of different proteins. Among others, they recruit the proteins that play a

role in the morphogenesis checkpoint (Gladfelter et al., 2005). In fact, the effettor kinase of this checkpoint, Swe1, must be localized to the bud neck to be degraded and this event depends on septins. Moreover, other proteins and kinases that act in this checkpoint, such as the Polo-like kinase Cdc5, the PAK kinase Cla4, Hsl1 and its adaptor Hsl7, are recruited to the bud neck through direct interaction with the septin ring, and all these localizations allow proper Swe1 inactivation and consequent entry into mitosis (Keaton and Lew, 2006). Finally, the septin ring has an asymmetry such that some proteins localize specifically to one side of the ring. For example, all the morphogenesis checkpoint proteins mentioned above localize specifically to the bud side of the septin collar (Keaton and Lew, 2006). How an asymmetric ring is generated out of non-polar filaments is unknown; however, this asymmetry is maintained also after bud emergence and after the transition from the ring into the hourglass-shaped collar. Thus, the septin ring and collar maintain the asymmetric distribution of different proteins both by acting as a scaffold for the recruitment of cytoplasmic proteins and as a diffusion barriers for protein compartmentalization. Through these general roles, septins influence many processes related to budding yeast cells' morphogenesis and division.

Spindle pole bodies separation and mitotic spindle elongation in budding yeast.

The spindle pole body (SPB) is the microtubule organizing center in the budding yeast *S. cerevisiae* and it is functionally equivalent to the centrosome in higher eukaryotes. Like chromosomes, the SPB is inherited from the mother cell and duplicates once in each division cycle during S phase. After duplication, sister SPBs move away from each other to assemble a short spindle upon initiation of mitosis. As budding yeast undergoes a close mitosis, SPBs are included in the nuclear envelope throughout the yeast life cycle and are therefore able to nucleate both nuclear and cytoplasmic microtubules. The SPB is a multiprotein complex that contains at least 30 different proteins (Jaspersen and Winey, 2004) and its structure was determined using electron microscopy (EM) (Adams and Kilmartin 1999). It appears as a cylindrical organelle that consists of three plaques: an outer plaque that faces the cytoplasm and binds cytoplasmic microtubules, an inner plaque that faces the nucleoplasm and is associated with nuclear microtubules, and a central plaque that is inside the nuclear membrane. One side of the central plaque is associated with an electron-dense region of the nuclear envelope termed the half-bridge. This is the site where the new SPB assembles during the G1 phase of the cell cycle (Adams and Kilmartin 1999).

SPB duplication can be divided into three steps based on EM studies of wild-type yeast cells and SPB duplication mutants, as described in

Figure 5. The first step occurs early in G1, when the half-bridge elongates and satellite material is deposited on its distal cytoplasmic tip. Next, the satellite expands into a duplication plaque, a structure that is similar to the cytoplasmic half of a mature SPB. The last step is insertion of the duplication plaque into the nuclear envelope and the assembly of nuclear SPB components. Yeast cells contain two duplicated side-by-side SPBs connected by a bridge at the end of G1. The bridge must be severed for the separation of SPBs, thus allowing proper spindle assembly (Fig.5). Microtubules and the kinesin-like motor proteins Cin8 and Kip1 are needed to move the SPBs apart (Jacobs et al., 1988; Roof et al., 1992); high CDK activity is also required for this step to occur (Fitch et al., 1992).

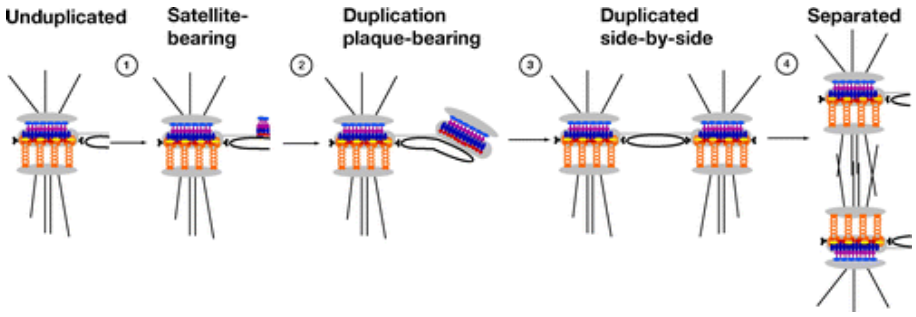

Figure 5: SPB duplication pathway. SPB duplication can be divided into three steps: (1) half-bridge elongation and deposition of satellite material, (2) expansion of the satellite into a duplication plaque, and (3) insertion of the duplication plaque into the nuclear envelope and assembly of the new SPB. Following SPB duplication, the bridge connecting the side-by-side SPBs is severed, and they move away from each other (4) (Jaspersen and Winey, 2004).

Plus-end directed kinesin motors Cin8 and Kip1 and the microtubule associated protein (MAP) Ase1 are involved in SPBs separation

(Crasta et al., 2006). Point mutations that abolish Cin8 motor activity but do not affect its ability to bind microtubules do not affect SPB separation (Gheber et al., 1999; Crasta et al., 2006). This observation, together with the involvement in SPBs separation of Ase1, that only binds microtubules but does not have motor activity, suggests that the shearing force generated by bundling action is sufficient to break the intra-SPB bridge. Cin8, Kip1 and Ase1 are targeted for degradation by the E3 ubiquitin ligase APC associated to its regulatory subunit Cdh1, which is active in G1. In order to be able to separate the SPBs and assemble a short spindle at the end of S phase, cells need to accumulate these microtubule-associated proteins by inhibiting their degradation through Cdh1 inactivation. In fact, the deletion of *CDH1* in cells that, for different reasons, are unable to separate the SPBs is sufficient to allow Cin8, Kip1 and Ase1 accumulation and SPBs separation (Crasta et al., 2006). Cdh1 is partially inactivated through phosphorylation by Cdc28/Clb (Cdk1) at multiple sites, and this step requires the dephosphorylation of the conserved Tyr19 of Cdc28 (Crasta et al., 2006; Lim et al., 1996). As dephosphorylation of Tyr19 of Cdc28 is required for Cdk1 activity, this means that this activity is required for SPBs separation. Cdh1 inactivation is very complex and involves multiple proteins (Fig. 6). In fact, Cdh1 phosphorylation by Cdc28 leads to partial Cdh1 inactivation, but is not sufficient to completely inactivate this factor. The Polo kinase Cdc5 and the stoichiometric Cdh1 inhibitor Acm1 are

also required for complete Cdh1 inactivation (Crasta et al., 2008). Cdh1 contains eleven Cdk1-phosphorylation sites, whose phosphorylation by Cdc28-Clb creates polo-box-binding (PBB) sites and allows the recruitment of Cdc5 to Cdh1 for further phosphorylation, suggesting that Cdk1 primes Cdh1 for subsequent Cdc5-mediated phosphorylation. Indeed, introduction of mutations in the Cdh1 PBB site abolishes the physical association between Cdh1 and Cdc5 and leads to reduced levels of Cin8 and Kip1, resulting in cells' failure to separate SPBs (Crasta et al., 2008). Thus, in addition to Cdk1, Cdc5 kinase activity is also required for fully inactivation of Cdh1 and SPBs separation. Moreover, Cdh1 is partially inhibited through physical interaction by a complex containing the Acm1, Bmh1 and Bmh2 proteins (Martinez et al., 2006). In fact, *cdc5* defective cells, although delayed in SPBs separation, are able to assemble a bipolar spindle and arrest in telophase with a long spindle, and this would not be possible without additional Cdh1 inhibitors. Indeed, cells deficient in both Cdc5 and Acm1 completely fail to break the intra SPBs bridge, suggesting that Cdc5 becomes essential for SPB separation in the absence of Acm1 complex (Crasta et al., 2008). In summary, Cdh1 inactivation involves Cdc28, Cdc5 and the Acm1 complex: sequential phosphorylation by Cdc28 and Cdc5 leads to Cdh1 inactivation allowing accumulation of Cin8, Kip1 and Ase1 and subsequent SPBs separation (Fig.6). In this process, Cdc28 acts as a priming kinase, because Cdc28-mediated phosphorylation

creates binding sites for Cdc5 resulting in further phosphorylation of Cdh1. Physical binding of the Acm1 complex to Cdh1 forms an additional inhibitory pathway. Thus, yeast cells use a multiple approach to inactivate the inhibitor Cdh1, which prevents accumulation of Cin8, Kip1 and Ase1, restraining cells to assemble a mitotic spindle.

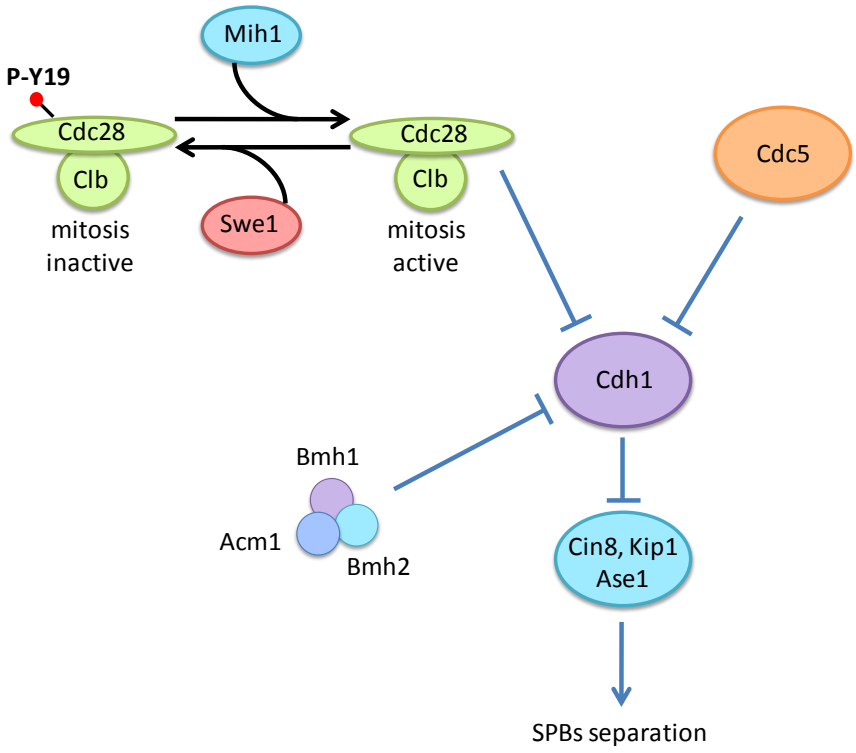

Figure 6: Model for Cdh1 inactivation. Cdk1, polo kinase Cdc5 and Acm1-Bmh1- Bmh2 complex cooperate to full Cdh1 inactivation. While Acm1-Bmh1-Bmh2 complex physically binds to Cdh1 to partially inactivate it, mitotically active Cdk1 phosphorylates Cdh1 and primes it for Cdc5 binding and additional phosphorylation. Complete inactivation of Cdh1 allows stabilization of microtubule binding proteins Cin8, Kip1 and Ase1 and mediates the formation of a short spindle (modified from Crasta et al., 2008).

The mitotic spindle is formed by sets of microtubules (MTs) that are composed by heterodimers of α- and β-tubulin assembled together in a head-to-tail fashion. As a result, each microtubule has two distinct ends with different properties: a dynamic fast growing one (plus end) and a slowly growing one (minus end). Microtubule polarity enables directional movement of motor proteins that are bound to MTs. Moreover, different microtubule-binding proteins show preference in binding plus or minus ends. The minus ends of MTs form spindle poles by nucleation in the SPBs. Depending on the placement of their plus end, microtubules are divided into different subsets: kinetochore MTs that attach the chromosomes to the spindle poles, astral MTs that are responsible for interactions between the spindle and the cell cortex and interpolar MTs that interdigitate between the two spindle poles to form an antiparallel microtubules array that is known as the spindle midzone. As soon as all of the chromosomes have bound microtubules emanating from either spindle pole through their kinetochores in order to achieve bi-orientation on the metaphase spindle, the spindle assembly checkpoint (SAC) is switched off, allowing the activation of the APC associated with its regulatory subunit Cdc20 (Zhou et al., 2002). This activates the protease separase, which cleaves the cohesin complex that holds sister chromatids together, thereby starting anaphase. Chromosome movement occurs in two steps: anaphase A, in which chromosomes move towards the spindle poles, and anaphase B, in which the

spindle poles move away from each other. Anaphase A is assumed to be dependent on shortening of the kinetochore microtubules that link centromeres to spindle poles. Anaphase B involves pushing forces generated at the spindle midzone through motor proteins that cause the sliding of interdigitating microtubules emanating from the opposite spindle poles (Fig. 7).

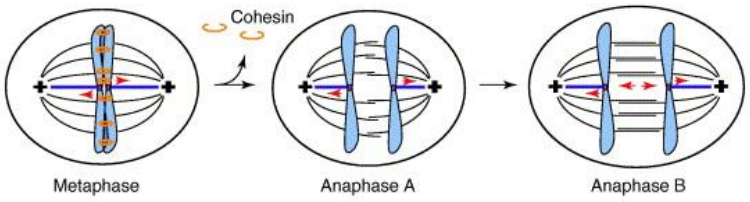

Figure 7: The metaphase to anaphase transition and anaphase forces. At the metaphase to anaphase transition, the removal of cohesin (orange rings) enables the kinetochore-associated microtubules (dark blue lines) to pull the sister chromatids apart. Forces exerted on chromosomes and on the anaphase spindle are shown in red. Note that in anaphase A the distance between the sister chromatids and the respective spindle pole is decreased, whereas in anaphase B the distance between the spindle poles is increased (de Gramont and Cohen-Fix, 2005).

Whereas metaphase is characterized by high Cdk1 activity, anaphase is marked by a reduction of Cdk1 activity that is counteracted by the phosphatase Cdc14. During most of the cell cycle, Cdc14 is kept inactive inside the nucleolus, from where it released and activated in two steps during anaphase. In early anaphase, the cdc-Fourteen Early Anaphase Release (FEAR) pathway triggers a partial and transient release of Cdc14 from the nucleolus to the nucleus (Stegmeier et al., 2002) (Fig. 8). FEAR-activated Cdc14 regulates processes such as microtubule dynamics and spindle stabilization that occur as cells

enter anaphase. There are several known spindle-associated targets of Cdc14 involved in these processes: the chromosomal passenger protein Sli15 (Pereira et al., 2003), the DASH complex component Ask1 (Higuchi et al., 2005), the spindle protein Fin1 (Woodbury et al., 2007) and the microtubule associated protein Ase1 (Khmelinskii et al., 2007). However, FEAR-controlled Cdc14 is not sufficient to promote mitotic exit, which is allowed only in late anaphase by full release of Cdc14, which counteracts and inactivates Cdk1. This full release is controlled by another regulatory pathway, the mitotic exit network (MEN) (Fig. 8). The MEN has at least two functions: it promotes mitotic exit and induces cytokinesis. These two functions are both controlled by Cdc14 and are largely independent from each other, as cells can exit mitosis while failing to complete cytokinesis (Yeong et al., 2002). The fact that cytokinesis occurrence needs MEN activation ensures that cell division will not take place before anaphase is completed.

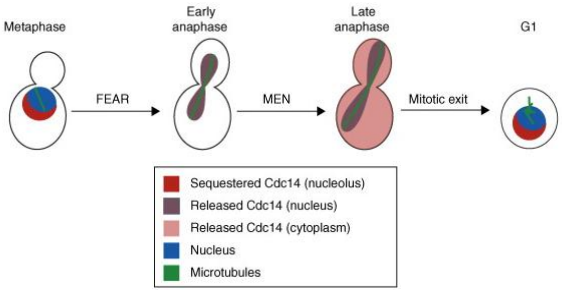

Figure 8: Cdc14 activity is regulated by changes in its intracellular localization. Cdc14 activation requires its release from the nucleolus; in early anaphase the FEAR pathway promotes Cdc14 transient release into the nucleus, while in late anaphase Cdc14 is fully released and activated trough the MEN pathway (see text for details) (DeWulf et al., 2009)

The spindle midzone, which is a key player in spindle stabilization and elongation, is also required to maintain the integrity of the anaphase spindle. In fact, the kinetics of pole separation and chromosome segregation is impaired in the absence of a stable overlap of antiparallel interpolar microtubules. Moreover, *S. cerevisiae* spindle elongation is driven mostly, if not only, by forces created within the spindle midzone. Indeed, genetic or physical perturbations of this structure result in inefficient separation of the spindle poles and collapse of the anaphase spindle (Schuyler et al., 2003).

FEAR-activated Cdc14 dephosphorylates several microtubule-associated proteins (MAPs) that form the spindle midzone and/or are required for microtubule stabilization observed in anaphase cells. Among other factors, Cdc14 dephosphorylates the MAPs Ase1, Stu1 and Fin1, the AuroraB kinase complex component Sli15, and the DASH kinetocore complex member Ask1. All these dephosphorylation events are required for proper midzone assembly and stability and/or for the reduced microtubules dynamics that is observed in anaphase cells (Higuchi and Uhlman, 2005; Woodbury and Morgan, 2006). Regulating midzone assembly by Cdc14 release provides a link between anaphase onset and changes in microtubule dynamics that are required for the assembly and the persistence of a stable midzone.

The microtubule associated protein Ase1 is a key player in spindle elongation as it is a core component of the spindle midzone and

regulates the localization of midzone and motor proteins. In particular, its midzone localization is independent of other midzone proteins, while the proper localization of almost all midzone proteins depends on Ase1 (Khmelinskii and Schiebel, 2008) . Ase1 is required for midzone formation, for promoting spindle elongation and stability in anaphase and plays also a role in cytokinesis. Cells without *ASE1* assemble a normal bipolar spindle in metaphase, but they show severe defects when progressing into anaphase. In fact, the spindle of *ase1Δ* cells collapses shortly after cells begin to elongate it (Schuyler et al., 2003), thus increasing the chromosome loss rate during cell division. Ase1 is regulated by phosphorylation during the cell cycle. In particular, its phosphorylation by Cdk1 in metaphase is required for spindle stability in anaphase, while Ase1 has to be dephosphorylated by Cdc14 at anaphase onset in order to assemble a spatially restricted spindle midzone. In fact, cells expressing either phosphomimic ($Ase1^{7D}$) or non-phosphorylatable ($Ase1^{7A}$) variants of Ase1 share defects in spindle stability and/or elongation (Khmelinskii et al., 2009). Phopsphorylation does not change Ase1 structure or microtubule binding activity, even though three out of seven Cdk1 phosphorylation sites are in the N-terminal part of the protein that is important for its dimerization (Khmelinskii et al., 2009). Instead, the different phosphorylation states of Ase1 contribute to the metaphase-anaphase transition through differential recruitment of motor proteins. In fact, the microtubule sliding forces are restrained

in metaphase, because phosphorylated Ase1 prevents the association of Cin8 with the overlapping microtubules of the spindle midzone. Dephosphorylation of Ase1 upon anaphase onset is necessary and sufficient to recruit the motor protein Cin8 to the midzone, therefore promoting active spindle elongation (Roostalu et al., 2010).

Ase1 is not the only midzone substrate of the Cdc14 phosphatase. The same balance of phosphorylation by Cdk1 and dephosphorylation by Cdc14 regulates the localization of many other proteins that promote spindle elongation and/or stabilization, such as Sli15, Ask1 and Fin1. Therefore, among other processes, the elongation of the mitotic spindle relies on a balance between phosphorylation and dephosphorylation events that have to occur sequentially and to be tightly coordinated to cell cycle progression.

The ubiquitin ligases Dma1 and Dma2

Modification of proteins by covalent attachment of ubiquitin molecules is a very common and conserved regulatory process. Usually, ubiquitylation targets proteins to degradation through the proteasome, but it may also regulate proteins through non-proteolytic mechanisms. These different fates of the target proteins are defined by the number and the nature of the ubiquitin modification: a single molecule of ubiquitin is not enough to target the substrate to the proteasome, whereas a polyubiquitin chain preferentially targets substrates for degradation. Ubiquitin is usually attached to protein lysine residues, and it has itself seven lysine residues that can be used for this attachment. The fate of the ubiquitylated protein is also dependent on the ubiquitin lysine residue involved in attachment to the substrate protein. In fact, Lys48-linked chains appear to target proteins for degradation, whereas Lys63-linked chains seem to be regulatory (reviewed in Finley et al., 2012). Ubiquitin conjugation involves the E1–E2–E3 enzyme cascade. The reaction starts from the ubiquitin-activating enzyme E1, which forms a high-energy bond with the terminal glycine residue of ubiquitin. Activated ubiquitin is transferred to an ubiquitin-conjugating enzyme E2 (Ubc) by transesterification. Finally, E3 enzymes (ubiquitin ligases) catalyze the formation of isopeptide bonds between lysine residues in substrate proteins and the activated ubiquitin. The selectivity and the type of the modification

are determined by E3 enzymes through physical interaction with the targets. Polyubiquitin chains are then synthesized through successive rounds of conjugation (reviewed in Finley et al., 2012).

The budding yeast E3 ubiquitin ligases Dma1 and Dma2 (known also as Chf1 and Chf2) share 58% of identity and are functionally redundant (Fraschini et al., 2004). They belong to the same FHA-RING E3 ubiquitin ligase family as *S. pombe* Dma1 and human Chfr and Rnf8. All these proteins appear to control different aspects of the mitotic cell cycle, but several molecular details of their functions are still obscure. In particular, *S. pombe* Dma1 is required to prevent precocious septum formation and cytokinesis when the spindle checkpoint is active; it localizes at the cell division site and inhibits the SIN (Septation Initiation Network) by preventing the SIN activator Plo1 (Polo-like kinase) from localizing to the SPB, thus inhibiting cell division (Murone and Simanis 1996; Guertin et al., 2002). Human Rnf8 is involved in cellular response to DNA damage and promotes the assembly of repair complex at DSB site and the activation of the G2-M checkpoint (Huen et al., 2007; Kolas et al., 2007; Wang and Elledge 2007). It also localizes at the spindle midbody and its absence causes failure to arrest the cell cycle in response to nocodazole treatment (Tuttle et al., 2007). Moreover, *RNF8* overexpression causes a cytokinesis delay that is frequently followed by an aberrant mitosis (Plans et al., 2007). The other human homologue of the *S. cerevisiae* Dma proteins, Chfr, is a mitotic checkpoint protein. It

delays entry into metaphase when the mitotic spindle is damaged, and it has been found to be mutated or unproperly expressed in different tumor lines (Scolnick and Halazonetis, 2000; Chaturvedi et al., 2002). Like their homologues in *S. pombe* and in human cells, also the *S. cerevisiae* Dma proteins are involved in mitotic checkpoints. While deletion of only one of the two *DMA* genes does not cause any detectable defect, concomitant deletion of both *DMA1* and *DMA2* causes defects in spindle positioning, septin ring dynamics, spindle positioning checkpoint (SPOC) and cytokinesis (Fraschini et al., 2004; Merlini et al., 2012). Unlike their *S. pombe* homolog, the *S. cerevisiae* Dma proteins do not appear to be involved in the spindle assembly checkpoint (SAC), as nocodazole treated *dma1Δ dma2Δ* cells arrest properly in G2 as wild type cells, indicating that the SAC is proficient in these cells (Fraschini et al., 2004).

All these proteins share two main domains: FHA domains that are phosphothreonine-binding modules (Hofmann and Bucher, 2005) frequently found in DNA repair and checkpoint proteins (Durocher and Jackson, 2002; Lorick et al., 1999) and RING domains, which are typical of a class of E3 ubiquitin ligases (Lorick et al., 1999) (Fig. 9). The presence of an FHA phospho-peptide binding domain implies that one or more protein kinases function upstream of these proteins. Moreover, intact FHA and RING domains are required for checkpoint function of all characterized FHA-RING ubiquitin ligases. In particular, point mutation in either the FHA or the RING domain of

S. cerevisiae Dma1 and Dma2 are sufficient to cause a complete loss of their activity (Bieganowsky et al., 2004). Despite their involvement in a lot of processes important for cell cycle progression and regulation, the mechanisms and the targets of *S. cerevisiae* Dma1 and Dma2 are still unknown. Their *in vitro* ubiquitin ligase activity has been described (Loring et al., 2008) and it has been reported that their *in vitro* interaction with the E2 enzymes Ubc4 and Ubc13 is required for their function in G1 and in G2, respectively (Loring et al., 2008). Nevertheless their *in vivo* targets are still unknown, as well as the kind of ubiquitylation that they are able to catalize. The double association with Ubc4 and Ubc13 suggests that Dma1 and Dma2 might catalize both Lys48 and Lys63 ubiquitylation depending on the E2 enzyme they interact with. In fact, Ubc4 promotes ubiquitin polimerization through Lys48, while Ubc13 promotes Lys63 polimerization (Loring et al., 2008).

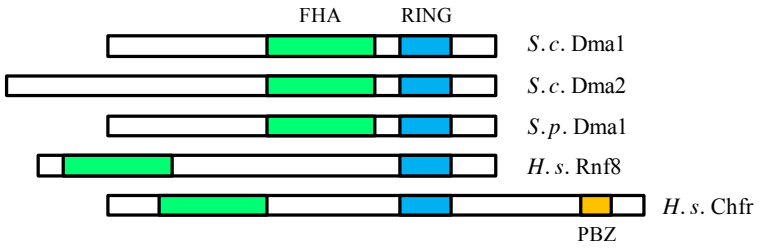

Figure 9: Domain structure of FHA-RING ubiquitin ligases. Dma proteins and their homologues share two main domains: an FHA domain (green) and a RING domain (blue) (see text for details). Moreover *H. s.* Chfr has a C-terminal PBZ domain (poly(ADPribose)-binding zinc finger). (Brooks et al., 2008)

Chapter 1

Budding yeast Dma1 and Dma2 participate in regulation of Swe1 levels and localization

Mol Biol Cell. 2011 Jul 1;22(13):2185-97. Epub 2011 May 11.
Erica Raspelli, Corinne Cassani, Giovanna Lucchini and Roberta Fraschini

Budding yeast Dma1 and Dma2 participate in regulation of Swe1 levels and localization

The Dma proteins control Swe1 protein levels

In order to gain insights into the role of the Dma proteins in cell cycle progression and checkpoints, we looked for synthetic effects between their complete absence (*dma1Δ dma2Δ*) and available mutations in mitotic genes. Interestingly, we found that the lack of Dma proteins was lethal at 25°C for cells lacking proteins that negatively regulate Swe1 stability, such as the protein kinase Hsl1 and the Cdc55 regulatory subunit of protein phosphatase 2A. In fact, we could never recover viable *dma1Δ dma2Δ hsl1Δ* or *dma1Δ dma2Δ cdc55Δ* spores in meiotic tetrads from diploid strains heterozygous for the deletions under analysis (Table 1). In addition, these lethal effects were suppressed by *SWE1* deletion, indicating that they might be due to Swe1 accumulation (Table 1 and Fig. 10A). We then managed to analyze the terminal phenotype caused by the *dma1Δ dma2Δ hsl1Δ* combination using a *dma1Δ dma2Δ* strain where the *HSL1* gene was replaced by a *MET3-HSL1* construct, whose expression can be turned off by the addition of methionine that represses the *MET3* promoter (Masselot *et al.*, 1977). Methionine addition inhibited *dma1Δ dma2Δ MET3-HSL1* cell growth (Fig. 10A)

and caused these cells to arrest with very elongated buds (Fig. 10B), a phenotype that resembled that observed in cells unable to degrade Swe1 (Lim *et al.*, 1996). This elongated bud phenotype was completely reversed by deletion of *SWE1* (Fig. 10B) that also allowed *dma1Δ dma2Δ MET3-HSL1* to grow normally in the presence of methionine (Fig. 10A). Altogether, these genetic interactions suggest that Dma1 and Dma2 might participate, together with Hsl1 and Cdc55, in Swe1 down-regulation.

The lack of Dma proteins turned out to be very toxic also for cells lacking the phosphatase Mih1 (Table 1 and Fig. 10C) that counteracts Swe1-dependent inihibitory phosphorylation of Cdc28 (Russel *et al.*, 1989).

GENOTYPE	PHENOTYPE AT 25°C
dma1Δ dma2Δ hsl1Δ	lethal
dma1Δ dma2Δ hsl1Δ swe1Δ	healthy
dma1Δ dma2Δ cdc55Δ	lethal
dma1Δ dma2Δ cdc55Δ swe1Δ	healthy
dma1Δ dma2Δ mih1Δ	sick
dma1Δ dma2Δ mih1Δ swe1Δ	healthy

Table 1: Swe1-dependent effects of the lack of Dma proteins on viability/growth efficiency of *hsl1Δ, cdc55Δ* and *mih1Δ* cells. Haploid *dma1Δ dma2Δ* cells were crossed either with *hsl1Δ*, *cdc55Δ* and *mih1Δ* cells or with *hsl1Δ swe1Δ, cdc55Δ swe1Δ* and *mih1Δ swe1Δ* double mutant strains. The resulting diploid strains were induced to sporulate and meiotic segregants of 15 tetrads for each cross were assayed for their ability to form colonies on rich medium at 25°C, followed by genotyping of the viable spores based on the deletion markers. Lethal, no viable spores with the indicated genotypes were found; sick, spores formed very small colonies; healthy, spore colony size was undistinguishable from wild type.

This synthetic effect could be due to accumulation of the Swe1 kinase concomitantly with loss of Mih1 phosphatase activity in *dma1Δ dma2Δ mih1Δ* cells, leading to strong Cdk1 inhibition. Accordingly, the low viability and elongated bud phenotypes of *dma1Δ dma2Δ mih1Δ* cells were reversed by *SWE1* deletion (Fig. 10C and 10D).

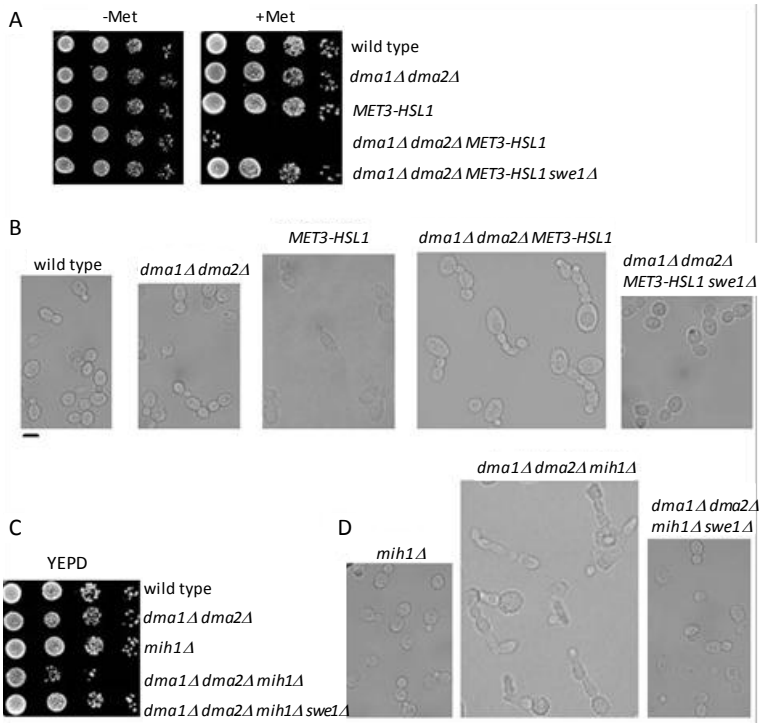

Figure 10. Toxic effects of Dma1/Dma2 lack in cells lacking Hsl1 and Mih1 are counteracted by *SWE1* deletion. A and C: Serial dilutions of stationary phase cultures of strains with the indicated genotypes were spotted on plates containing either synthetic medium without (-Met) or with (+Met) 2 mM methionine, or YEPD (C), which were then incubated for 2 days at 25°C. B and D: The morphology at 25°C of cells with the indicated genotypes was examined by differential interference contrast (DIC) microscopy. All cell cultures were exponentially growing in YEPD medium with the exception of those carrying the *MET3-HSL1* construct integrated at the *HSL1* locus (B), whose cellular morphology was analyzed after shut off of the *MET3* promoter for 3 hours by addition of 2 mM methionine to synthetic growth medium lacking methionine. bar: 5µm.

The above observations prompted us to compare Swe1 protein levels in wild type and *dma1Δ dma2Δ* cells during a single cell cycle. To this end, synchronous cultures of cells expressing a functional HA-tagged Swe1 variant (Swe1-3HA) from the *SWE1* promoter were released from α-factor-induced G1 arrest, followed by re-addition of α-factor 85 minutes later, when 95% of cells were budded, to arrest cells in the next G1 phase. Samples were taken at different times after release to monitor the kinetics of DNA replication by FACS analysis (Fig. 11A), budding, nuclear division and septin ring formation (Fig. 11B) and Swe1 protein levels (Fig. 11C). Wild type and *dma1Δ dma2Δ* cells showed very similar profiles of budding, DNA replication and nuclear division, while septin ring deposition appeared to take place with somewhat reduced efficiency, although with similar kinetics, in *dma1Δ dma2Δ* cells compared to wild type. Swe1 amount increased in both cultures after release in the cell cycle, concomitantly with cells entering S phase, and decreased as cells started nuclear division. Nonetheless, *dma1Δ dma2Δ* cells appeared to be partially defective in targeting Swe1 to degradation, as Swe1 levels were higher in these cells than in wild type throughout the duration of the experiment. Because localization of Swe1 is important for its turnover, we also analysed this issue in the above experiment (Fig. 11B).

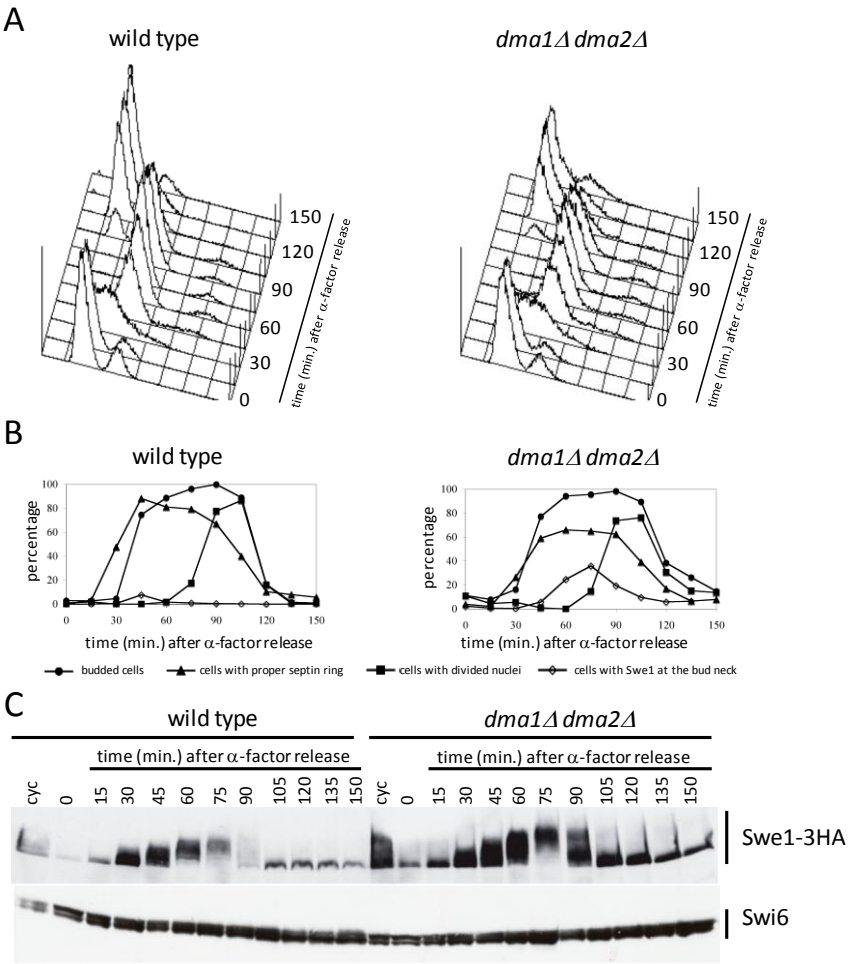

Figure 11. The lack of Dma proteins causes Swe1 stabilization. Exponentially growing (cyc) cultures of *SWE1-3HA* and *dma1Δ dma2Δ SWE1-3HA* cells were arrested in G1 by α-factor and released from G1 arrest in YEPD at 25°C (time 0), followed by α-factor readdition after 85 minutes. At the indicated times after release, cell samples were taken for FACS analysis of DNA contents (A), for scoring budding, nuclear division, septin ring formation and Swe1-3HA localization (B) and for determining Swe1 levels by western blot analysis with anti-HA and anti-Swi6 (loading control) antibodies (C).

As expected, Swe1 was found transiently at the bud neck in a very small percentage (8% maximum) of wild type cells, because it is targeted to degradation as soon as it reaches that location (McMillan *et al.*, 2002). Conversely, bud neck localized Swe1 was detected in a significant percentage (up to 38%) of *dma1Δ dma2Δ* cells. Thus, the Dma proteins seem to contribute to proper Swe1 down-regulation under unperturbed conditions, likely by acting after Swe1 recruitment at the bud neck.

The Dma proteins are essential for Swe1 degradation in response to DNA replication stress

Several mutants partially impaired in Swe1 degradation, such as *hsl1Δ, hsl7Δ, cla4Δ* and *cdc55Δ* mutants, were reported to show Swe1-dependent hypersensitivity to the ribonucleotide reductase inhibitor hydroxyurea (HU) (Liu and Wang, 2006) that causes stalling of DNA replication forks due to deoxyribonucleotide depletion (Rosenkranz and Levy, 1965). Also *dma1Δ dma2Δ* cells, which are as sensitive as wild type to either methyl methanesulfonate, phleomycin or UV radiation treatments (our unpublished observation), turned out to be more sensitive to HU than wild type (Fig. 12A). This hypersensitivity was not due to inability of *dma1Δ dma2Δ* cells to arrest cell cycle progression in response to incomplete DNA replication through the S-phase checkpoint, which prevents mitotic entry in response to HU (Weinert *et al.*, 1994). In

fact, when cell cultures were released from α–factor into HU-containing medium, neither *dma1Δ dma2Δ* nor wild type cells did elongate the mitotic spindle (Fig. 12B, and data not shown), as expected when the S-phase checkpoint is proficient. The hypersensitivity to HU was not even due to inability of *dma1Δ dma2Δ* cells to recover from the HU-induced arrest. In fact, when cell cultures were arrested with 200 mM HU for 120 minutes, followed by release into fresh medium containing α-factor to arrest cells in the next G1 phase, mitotic spindle elongation kinetics after HU removal were very similar in wild type and *dma1Δ dma2Δ* cells (Suppl. Fig. 1). Thus, the Dma proteins are not required for cell recovery from HU, at least after exposure to HU for a short time. As expected, similarly treated *hsl1Δ* cells, which are partially defective in recovery from S-phase arrest (Liu and Wang, 2006), entered anaphase after HU removal with some delay compared to wild type cells (Suppl. Fig. 1).

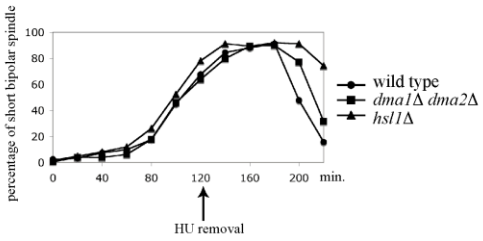

Suppl. figure 1: Recovery from hydroxyurea treatment of *dma1Δ dma2Δ* cells. Exponentially growing cultures of wild type, *hsl1Δ* and *dma1Δ dma2Δ* cells were arrested in G1 by α-factor and released from G1 arrest in YEPD containing 200 mM HU at 25°C (time = 0). After 120 minutes, cells were released from HU (arrow). Cell samples were taken at the indicated times after release from α-factor to determine mitotic spindle formation and elongation by indirect immunofluorescence with anti-tubulin antibodies.

As expected, incubation for 8 hours in the presence of 200 mM HU led wild type cells to accumulate as dumbbells with a big round bud, single nucleus, short mitotic spindle and normal septin ring (Fig. 12B, 91% of 190 cells). Interestingly, under the same conditions a significant percentage of *dma1Δ dma2Δ* cells (35% of 216 cells) accumulated as cells with misshapen elongated buds, single nucleus, short mitotic spindle and mispositioned septin rings (Fig. 12B). In particular, HU-treated *dma1Δ dma2Δ* cells first assembled a proper septin ring at the bud neck, but then a new septin ring appeared at the bud tip, also causing a restriction in the growing bud, followed by disassembly of the first assembled ring. This phenotype resembles that of cells with misorganized septins and elevated Swe1 levels (Gladfelter *et al.* 2005), suggesting that both the elongated bud phenotype and the mispositioned septin ring could be due to high Swe1 levels causing low mitotic Cdk1 activity, thus inhibiting isotropic bud growth (Booher *et al.*, 1993) and allowing assembly of a new septin ring at the bud tip (Gladfelter *et al.* 2005). Indeed, although deletion of *SWE1* only partially suppressed the hypersensitivity to HU of cells lacking the Dma proteins (Fig. 12A), it restored both the round bud phenotype and proper septin ring positioning in the same cells (Fig. 12B, 89% of 205 cells), suggesting that their morphology and septin ring defects were likely due to Swe1 accumulation.

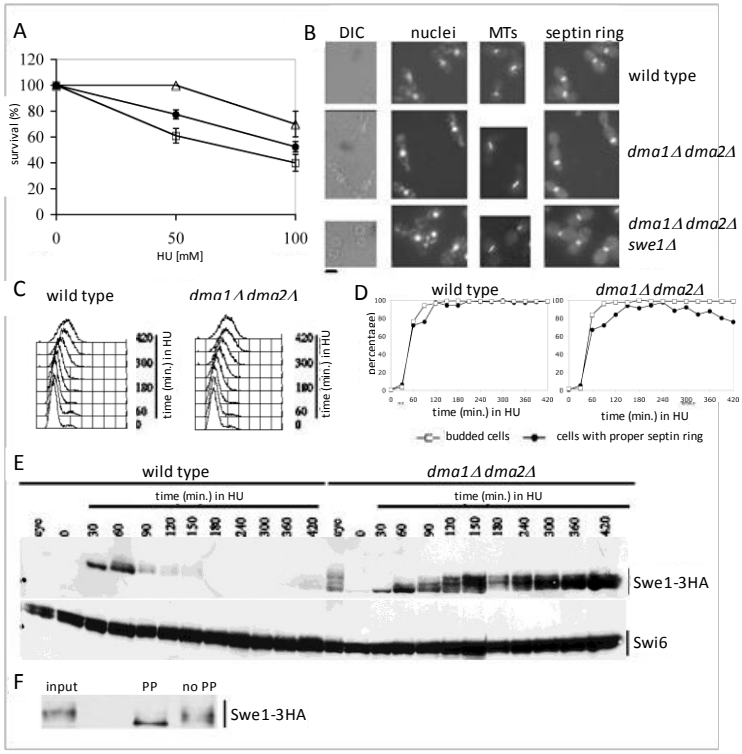

Figure 12. **Effect of the lack of Dma proteins on cell viability, cell morphology and Swe1 stability in HU-treated cells**. A: Serial dilutions of stationary phase cultures of the indicated strains were spotted on YEPD plates containing the indicated HU concentrations and incubated for 2 days at 25°C. Colony forming units were then counted to determine cell viability. Plotted values are the mean values ± SD (bars) from three independent experiments. B: Exponentially growing cultures of wild type, *dma1Δ dma2Δ*, and *dma1Δ dma2Δ swe1Δ* cells were transferred to YEPD medium containing 200 mM HU at 25°C. After 7 hours, cell samples were taken for cell morphology analysis (DIC) and for *in situ* immunofluorescence analysis of nuclei, mitotic spindles (MTs) and septin ring deposition by using DAPI staining, anti-tubulin antibodies and anti-Cdc11 antibodies, respectively. bar: 5μm. C-E: Exponentially growing (cyc) cultures of *SWE1-3HA* and *dma1Δ dma2Δ SWE1-3HA* cells were arrested in G1 by α-factor and released from G1 arrest at 25°C in YEPD medium containing 200 mM HU (time 0). At the indicated times, cell samples were taken for FACS analysis of DNA contents (C), for scoring budding and septin ring formation (D) and for determining Swe1 levels by western blot analysis with anti-HA and anti-Swi6 (loading control) antibodies (E). F: protein extracts of *dma1Δ dma2Δ SWE1-3HA* cells grown for 3 hours in HU containing medium (input) were immunoprecipitated with anti-HA antibodies and the immunoprecipitate was incubated for 30 minutes at 30°C with 20 unit/μl λ-phosphatase (PP) or with reaction buffer only (no PP).

To further investigate whether the Dma proteins are involved in controlling Swe1 protein levels under DNA replication stress conditions, synchronous cultures of wild type and *dma1Δ dma2Δ* cells expressing *SWE1-3HA* were released from α-factor arrest into HU-containing medium. After entry into S phase of both cell cultures with similar kinetics, DNA replication was stalled because of the lack of deoxyribonucletides, as shown by FACS analysis of DNA content (Fig. 12C). Also budding and septin ring deposition after release in the presence of HU took place with similar kinetics in the two strains (Fig. 12D), although septin ring deposition seemed to be slightly less efficient in *dma1Δ dma2Δ* cells than in wild type. Swe1 levels increased in both cell cultures after transfer to HU (Fig. 12E) concomitantly with cells entering S phase, and then Swe1 disappeared in wild type cells, as previously reported (Enserink *et al.*, 2006), about 90 minutes after transfer to HU. Strikingly, high levels of the same protein progressively accumulated throughout the duration of the experiment in *dma1Δ dma2Δ* cells, suggesting that the Dma proteins are required for Swe1 degradation in response to interrupted DNA synthesis.

Swe1 seemed to undergo posttranslational modifications in HU-treated *dma1Δ dma2Δ* cells, which accumulated Swe1 species with low electrophoretic mobility (Fig. 12E), which were transiently observed also during an unperturbed cell cycle (Fig. 11C). Because Swe1 must be localized at the bud neck and phosphorylated by

multiple kinases in order to be degraded (Keaton and Lew, 2006), we asked whether the slowly migrating Swe1 species might be due to phosphorylation events. Indeed, such species disappeared after lambda phosphatase treatment of Swe1 immunoprecipitates from HU-treated *dma1Δ dma2Δ* cells (Fig. 12F), indicating that the lack of Dma proteins allows accumulation of phosphorylated Swe1 in the presence of HU.

Swe1 is restrained at the bud neck of HU-treated cells lacking the Dma proteins

Swe1 must be localized at the bud neck and interact with specific factors in order to be phosphorylated, and this phosphorylation is essential for subsequent Swe1 degradation (Sakchaisri *et al.*, 2004). To fully rule out the possibility that Dma proteins might regulate degradation of Swe1 in HU-treated cells by controlling its localization, we initially checked the localization at the bud neck of a functional myc-tagged variant (Hsl1-18myc) of the Hsl1 kinase that is essential for Swe1 recruitment at the septin ring (Shulewitz *et al.*, 1999; Longtine *et al.*, 2000). Hsl1 localization in HU-treated cells was unaffected by the lack of Dma proteins, as 85% of wild type cells (n=250) and 86% of *dma1Δ dma2Δ* cells (n=260) showed precise co-localization of Hsl1-18myc with the septin ring protein Cdc11 (Fig. 13A).

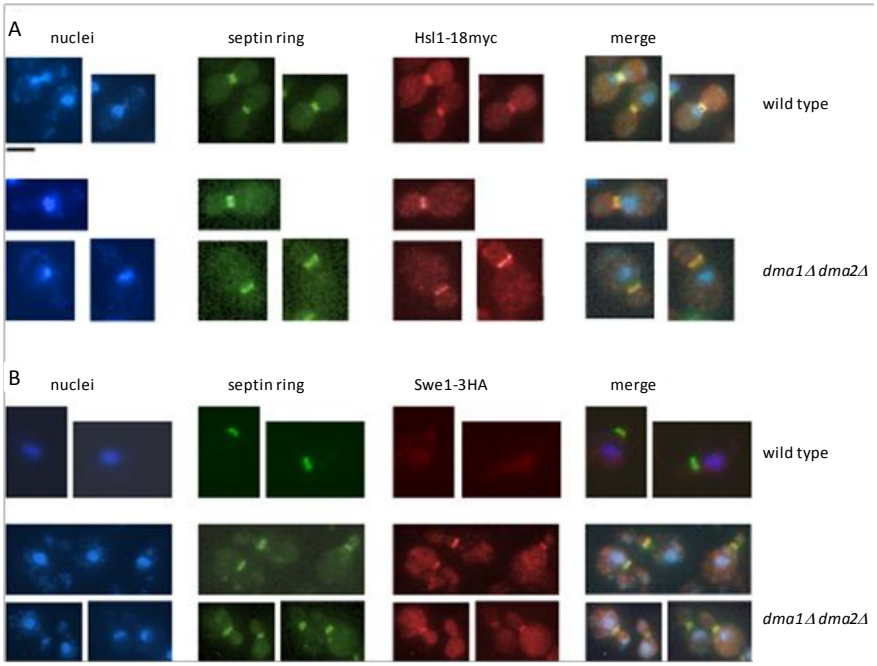

Figure 13. The lack of Dma proteins causes Swe1 retention at the bud neck in HU-treated cells. Exponentially growing cell cultures of *HSL1-18MYC* and *dma1Δ dma2Δ HSL1-18MYC* strains (A), or *SWE1-3HA* and *dma1Δ dma2Δ SWE1-3HA* strains (B) were transferred to YEPD medium containing 200 mM HU at 25°C. After 3 hours, nuclei and septin ring deposition were analyzed as in Figure 12, while Hsl1-18MYC and Swe1-3HA were visualized by indirect immunofluorescence with anti-Myc and anti-HA antibody, respectively. bar: 5μm.

We then analysed directly Swe1 subcellular localization after incubation for 3 hours in the presence of HU of cells expressing *SWE1-3HA*. As expected, because treatment with HU triggers Swe1 degradation (Enserink *et al.*, 2006; Fig. 12E), Swe1 was undetectable at the bud neck of wild type cells under these conditions (Fig. 13B). The same protein was instead properly localized at the bud side of the mother-bud neck in 50% of *dma1Δ dma2Δ* cells (n=170) (Fig. 13B), indicating that the lack of Dma proteins stabilizes Swe1 at the

bud neck, in agreement with the previously observed accumulation of its phosphorylated forms (Fig. 12E). These data are consistent with the accumulation of bud neck localized Swe1 we previously observed in *dma1Δ dma2Δ* cells undergoing an unperturbed cell cycle (Fig. 11B), indicating that the Dma proteins are somehow involved in promoting Swe1 release from the bud neck.

Swe1 stabilization in *dma1Δ dma2Δ* cells is not due to morphogenesis checkpoint activation

Perturbations of the septin ring architecture and/or actin cytoskeleton cause activation of the morphogenesis checkpoint that prevents nuclear division by inhibiting Swe1 recruitment at the bud neck and therefore Swe1 degradation (Keaton and Lew, 2006). For example, shift of temperature-sensitive *cla4-75* mutant cells to the restrictive temperature (37°C) causes septin ring defects (Kadota *et al.*, 2004), which in turn trigger activation of the morphogenesis checkpoint (Lew, 2003). As cells lacking the Dma proteins show partial septin ring defects, we compared Swe1 protein levels and localization in *dma1Δ dma2Δ* and *cla4Δ cla4-75* cells. Synchronous cultures of cells producing Swe1-3HA were released from α-factor into HU-containing medium at 37°C. As expected, Swe1 appeared to be stabilized in both cell cultures (Fig. 14A) but, strikingly, it accumulated phosphorylated forms (Fig. 14A) and localized at the septin ring (Fig. 14B) specifically in *dma1Δ dma2Δ* cells, and not in

cla4-75 cells, where its stabilization is known to depend on morphogenesis checkpoint activation (Longtine *et al*., 2000).

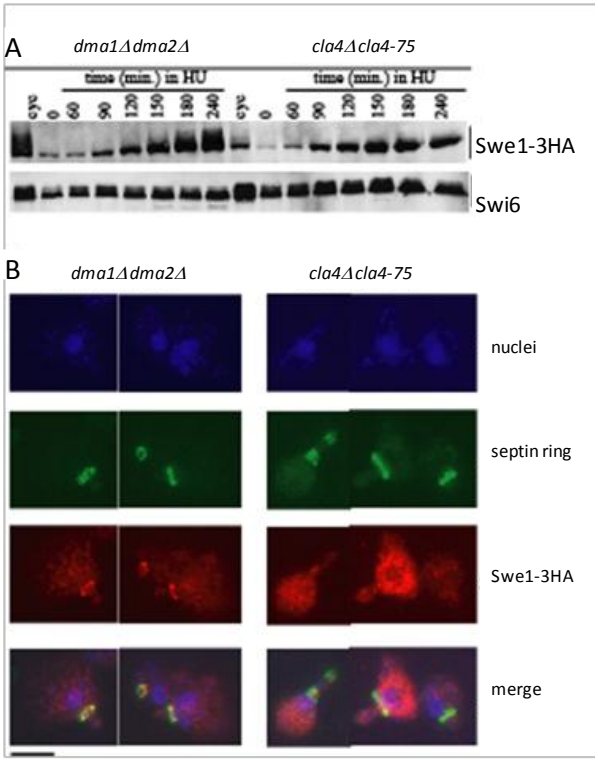

Figure 14. Different patterns of Swe1 stabilization in HU-treated *dma1Δ dma2Δ* and *cla4-75* cells. Exponentially growing (cyc) cell cultures of *dma1Δ dma2Δ SWE1-3HA* and *cla4-75 SWE1-HA3* strains were arrested in G1 by α-factor at 25°C (time 0) and released from G1 arrest at 37°C in YEPD medium containing 150 mM HU. Samples were taken at the indicated times after release for determining Swe1 levels (A) as in Figure 11C, *in situ* immunofluorescence analysis (B) of nuclei, septin ring deposition and Swe1-HA3 localization, as in Figure 13. Representative micrographs were taken at t=180 min. bar: 5μm.

We also analyzed Swe1 regulation in *cdc12-1* and *cdc12-6* conditional mutants, where the morphogenesis checkpoint is activated by septin ring disassembly (Barral *et al*., 2000). Synchronous cell cultures were

released from α-factor into HU-containing medium at 23°C, permissive temperature for the *cdc12* mutants. As expected, *cdc12-1* and *cdc12-6* cells were defective in septin ring deposition even at this temperature (Fig. 15A), consistently with Cdc12 role in septin ring architecture (Dobbelaere *et al.*, 2003).

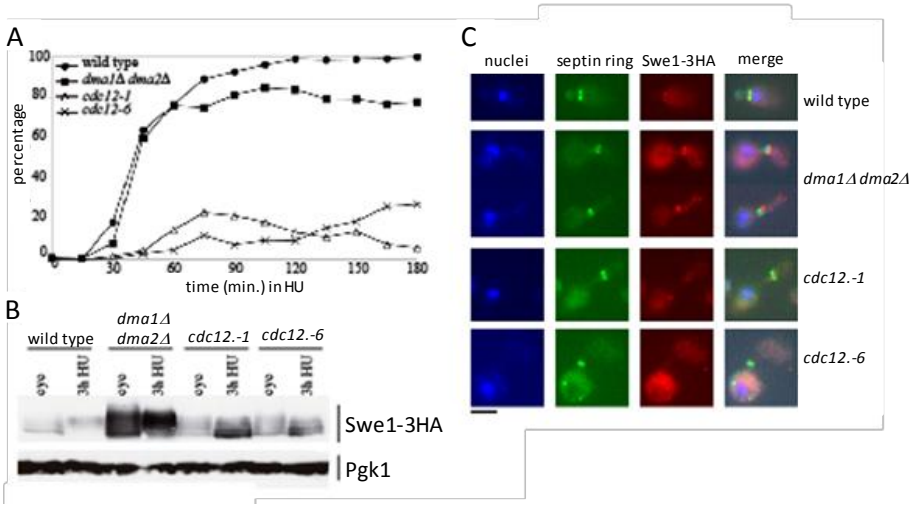

Figure 15. Septin mutants do not accumulate hyperphosphorylated Swe1 in the presence of HU. Exponentially growing (cyc) cultures of *SWE1-3HA*, *dma1Δ dma2Δ SWE1-3HA*, *cdc12-1 SWE1-3HA* and *cdc12-6 SWE1-3HA* cells were arrested in G1 by α-factor at 23°C and released in YEPD medium containing 200 mM HU. Samples were taken at the indicated times to determine the kinetics of septin ring deposition (A), as well as Swe1 levels (B) by western blot analysis with anti-HA (Swe1-3HA) and anti-Pgk1 (loading control) antibodies, and for *in situ* immunofluorescence analysis (C) of nuclei, septin ring and Swe1-3HA as in Figure 13. Representative micrographs were taken at t=180 min. bar: 5μm.

Importantly, neither septin mutant accumulated hyperphosphorylated Swe1 within 3 hours after release in the presence of HU, while high levels of slowly migrating Swe1 species were detectable in similarly treated *dma1Δ dma2Δ* cells (Fig. 15B). Accordingly, these conditions did not allow detection of Swe1 at the

bud neck of *cdc12* cells, while the same protein co-localized with the septin ring in *dma1Δ dma2Δ* cells (Fig. 15C).

Altogether, the data above strengthen the hypothesis that the mechanism leading to Swe1 stabilization in cells lacking the Dma proteins is different from the one triggered by morphogenesis checkpoint activation and does not involve inhibition of Swe1 recruitment at the bud neck.

Because HU-treated *dma1Δ dma2Δ* cells seemed to be slightly impaired in septin ring deposition (Fig. 12C), we wished to fully rule out the possibility that Swe1 stabilization in these cells might merely be a consequence of septin ring problems. To this end, we stabilized the septin ring in *dma1Δ dma2Δ* cells by overexpressing the *BNI5* gene, whose product acts as a septin regulator and has been implicated in septin ring stabilization (Lee *et al.*, 2002). Cells carrying high copy number plasmids, either empty or containing *BNI5*, were grown under selective conditions for plasmid maintenance, arrested in G1 by α-factor and then released from G1 arrest into HU-containing medium. As shown in Figure 16, both strains showed similar budding kinetics after release (Fig. 16A). Moreover, Swe1 accumulation in *dma1Δ dma2Δ* cells carrying the empty vector (Fig. 16C) was similar to that observed in isogenic cells without any plasmid in previous experiments (see Fig. 12E and 14A). Strikingly, high copy number *BNI5* suppressed the slight septin ring deposition defect in *dma1Δ dma2Δ* cells (Fig. 16B), as expected, but did not

decrease accumulation of phosphorylated Swe1 in the same cells (Fig. 16C). Thus, Swe1 stabilization in HU-treated cells lacking the Dma proteins is independent of septin ring defects.

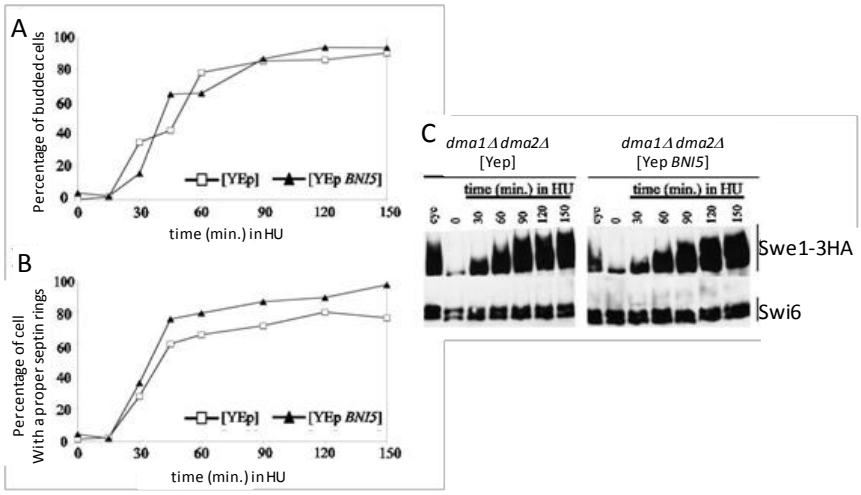

Figure 16. Septin ring stabilization in *dma1Δ dma2Δ* cells does not restore Swe1 degradation in the presence of HU. Exponentially growing (cyc) cultures of *SWE1-3HA dma1Δ dma2Δ* cells containing the 2m plasmid YEplac181, either empty (YEp) or carrying the *BNI5* gene (YEp-*BNI5*), were grown at 25°C in synthetic medium lacking leucine, arrested in G1 by α-factor and released from G1 arrest in YEPD medium containing 200 mM HU (time 0). Samples were taken at the indicated times after release for determining the kinetics of budding (A) and septin ring deposition (B) and for analysis of Swe1 levels (C) as in Figure 11C.

The Dma proteins contribute to Swe1 ubiquitylation *in vivo*

Dma1 and Dma2 act as E3 ubiquitin ligases *in vitro* (Loring *et al.*, 2008) and Swe1 likely undergoes ubiquitylation *in vivo*, because incubation of purified Swe1 with a ubiquitylation cocktail in the presence of wild type cell lysates yields polyubiquitylated Swe1 (Kaiser *et al.*, 1998). As polyubiquitylated proteins are targeted to

proteasome-mediated degradation (Driscoll and Goldberg, 1990), we wondered whether the Dma proteins might control Swe1 ubiquitylation. To address this question, *SWE1-3HA* and *SWE1-3HA dma1Δ dma2Δ* cells were transformed with high copy number plasmids carrying a construct expressing 6xHIS-tagged ubiquitin from the *CUP1* inducible promoter (YEp-*CUP1-6xHIS-UBI4*, Callis and Ling, 2005). Addition of 250 μM $CuSO_4$ to cultures of the transformant clones, exponentially growing under selective conditions (see Materials and methods) was used to induce the *CUP1* promoter, followed by addition, 30 minutes later, of the proteasome inhibitor MG132 (Gaczynska and Osmulski, 2005) to promote accumulation of ubiquitylated proteins. After 3 hours, total protein extracts from $CuSO_4$-induced and uninduced cell cultures were incubated with Nichel resin that selectively binds 6xHIS-tagged proteins and therefore purifies the ubiquitylated proteins in our induced cell extracts. The resin eluates were then subjected to SDS polyacrylamide gel electrophoresis and western blot analysis with anti-HA antibody to detect Swe1. These experimental conditions allowed Swe1 accumulation in both wild type and *dma1Δ dma2Δ* cells (Fig. 17A, lanes 1-4) but, interestingly, Swe1 ubiquitylated forms, which clearly accumulated in the $CuSO_4$-induced wild type eluates (Fig. 17A, lane 6), were only slightly detectable in the eluates deriving from similarly treated *dma1Δ dma2Δ* cells (Fig. 17A, lane 8). Thus, accumulation of Swe1 ubiquitylated forms in cycling cells

under conditions of proteasome inhibition is at least partially dependent on Dma1 and Dma2.

We also tried to assess whether Swe1 accumulation in HU-treated *dma1Δ dma2Δ* cells correlated with defective Swe1 ubiquitylation. Unfortunately, we were unable to obtain significant results, because ubiquitylated Swe1 was undetectable in wild type cells in the absence of proteasome inhibitors, likely because it is immediately degraded. On the other hand, combining HU with MG132, under the growth conditions required for treatment with the latter (see Materials and methods), dramatically affected cell growth and did not allow to recover acceptable Swe1 inputs even in wild type cell extracts. Nonetheless, the data above indicate that the lack of Dma proteins interferes with Swe1 ubiquitylation *in vivo*, suggesting that these proteins might be involved in promoting this event.

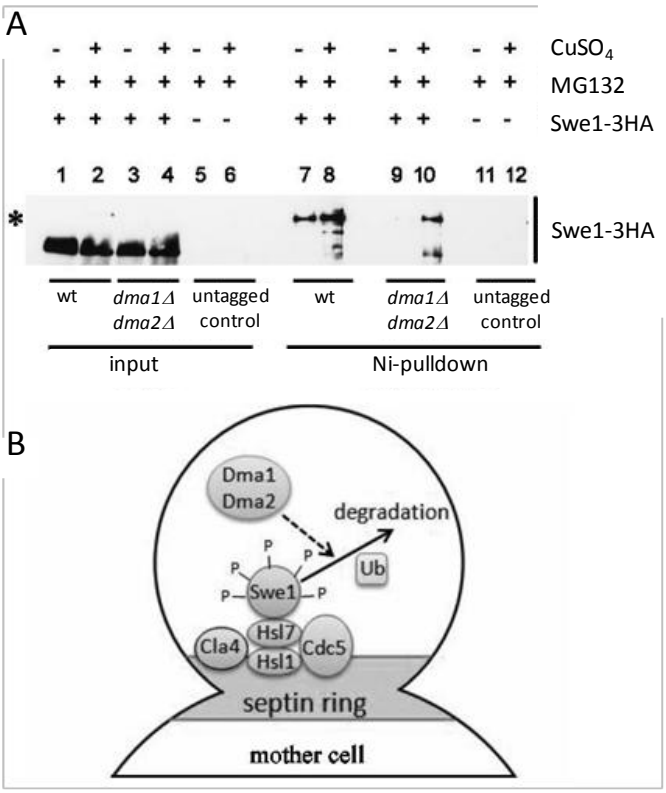

Figure 17. Swe1 ubiquitylation is partially dependent upon the Dma proteins. A: Exponentially growing cultures of *SWE1-3HA* and *dma1Δ dma2Δ SWE1-3HA* cells, all carrying a high copy number plasmid with the *CUP1-6xHIS-UBI4* construct, were incubated for 3 hours in the presence of the proteasome inhibitor MG132 and with (lane 2, 4, 6, 8) or without (lane 1, 3, 5, 7) 250 μM $CuSO_4$ that induces overproduction of 6xHIS-ubiquitin. Cells were then lysed and aliquots of the lysates were incubated with Ni-NTA beads to purify the proteins bound by 6xHIS-ubiquitin (Ni-pulldown), followed by SDS polyacrilamide gel electrophoresis and western blot analysis with anti-HA antibody of the bead eluates. Equivalent aliquots of the lysates were also loaded on the gel (input). The asterisk marks Swe1 ubiquitylated bands.

B: A model for Swe1 down-regulation by the Dma proteins. Swe1 is recruited by the Hsl1/Hsl7 complex to the septin ring, where it interacts with the protein kinases Cla4 and Cdc5, undergoing multiple,phosphorylation events (P). Phosphorylated Swe1 is then likely polyubiquitylated, followed by degradation. The Dma1 and Dma2 proteins partially trigger this degradation by acting after Swe1 recruitment to the bud neck and its phosphorylation, possibly by controlling, directly or indirectly, Swe1 ubiquitylation.

Discussion

Swe1 degradation in budding yeast relieves Swe1-dependent inhibitory phosphorylation of the Cdk1 catalytic subunit Cdc28, thus allowing nuclear division. Swe1 is recruited to the bud neck and undergoes stepwise phosphorylations by multiple kinases (Keaton and Lew, 2006) that likely trigger its ubiquitylation and subsequent degradation. These events are critical for coordinating proper bud morphology with cell cycle progression, and localization of the Hsl1/Hsl7 complex at the bud neck provides a platform for Swe1 degradation, which requires also the Cdc55 regulatory subunit of protein phosphatase PP2A (Yang et al., 2000).

We now show that also the FHA-RING ubiquitin ligases Dma1 and Dma2 are involved in Swe1 down-regulation. In fact, their absence is lethal for cells lacking either Hsl1 or Cdc55. Moreover, cells concomitantly lacking the Dma proteins and either Hsl1 or the phosphatase Mih1, which counteracts Swe1-mediated Cdc28 phosphorylation, exhibit very elongated buds and Swe1-dependent growth arrest or very slow growth, respectively. As these harmful synthetic effects are relieved by SWE1 deletion, the Dma proteins likely contribute to promote Swe1 turnover. Indeed, their absence partially alters Swe1 degradation and localization also during an unperturbed cell cycle of otherwise wild type cells. In fact, even if kinetics of Swe1 accumulation, phosphorylation and degradation are similar in wild type and *dma1Δ dma2Δ* cells, the latter contain higher

amounts than wild type of total and bud neck-localized Swe1. However, this larger amount of Swe1 does not significantly affect cell cycle progression of unperturbed *dma1Δ dma2Δ* cells, likely because multiple redundant pathways are involved in Swe1 down-regulation. Accordingly, partial impairment of Swe1 degradation in *hsl1Δ* or *hsl7Δ* mutants does not cause any detectable G2 delay under unperturbed conditions (McMillan et al., 1999).

How do the Dma proteins control Swe1 protein levels? Because Dma1 and Dma2 have been implicated in septins dynamics (Fraschini et al., 2004) and a functional septin ring is required for Swe1 recruitment to the bud neck and subsequent degradation (Keaton and Lew, 2006), septin ring defects in *dma1Δ dma2Δ* cells might activate the morphogenesis checkpoint, which causes stabilization of Swe1 by interfering with its localization at the bud neck (Longtine et al., 2000). Strikingly, Swe1 recruitment to the septin ring is enhanced by the lack of the Dma proteins, which therefore appear to control Swe1 degradation by a mechanism that does not involve Swe1 displacement from the bud neck.

Both DNA replication and mitotic spindle elongation are blocked in wild type cells treated with the DNA synthesis inhibitor HU, due to activation of a specific S-phase checkpoint that responds to stalled DNA replication forks (Weinert et al., 1994). Interestingly, Swe1 is properly targeted to the bud neck and degraded under these conditions, and these events seem to be essential for proper cell

recovery from HU. In fact, wild type cells maintain normal cell morphology during HU-induced S-phase block and high viability after HU treatment, while abnormally elongated buds and low viability are observed under the same conditions in mutants that are defective in Swe1 degradation when treated with HU (Enserink et al., 2006). We found that HU-treated *dma1Δ dma2Δ* cells are less viable than wild type, form abnormally elongated buds and accumulate very high amounts of Swe1. Moreover, SWE1 deletion fully restores proper cell morphology and partially recovers viability of HU-treated *dma1Δ dma2Δ* cells. These data indicate that the Dma proteins participate in Swe1 down-regulation in response to DNA replication stress, and this regulation is important for cell survival and proper cell morphology. They might also play some more direct role in DNA damage response, as previously shown for their human homolog Rnf8 (Al-Hakim et al., 2010), thus explaining why SWE1 deletion does not completely restore cell viability in HU-treated *dma1Δ dma2Δ* cells.

Activation of the morphogenesis checkpoint in HU-treated *cla4-75*, *cdc12-1* and *cdc12-6* cells leads to accumulation of Swe1 that does not localize at the bud neck and is not phosphorylated, as expected by the current model of morphogenesis checkpoint action (Lew, 2003). On the contrary, HU-treated *dma1Δ dma2Δ* cells properly localize Hsl1 and Swe1 to the septin ring and accumulate phosphorylated Swe1. Moreover, the septin ring defects observed in *dma1Δ dma2Δ* cells after HU-treatment are likely the consequence,

and not the cause, of Swe1 stabilization. In fact, *BNI5* overexpression restores a proper septin ring in HU-treated *dma1Δ dma2Δ* cells, but does not change their pattern of Swe1 stabilization. Thus, the mechanism by which the lack of Dma proteins causes Swe1 accumulation in response to DNA replication stress is different from the one promoted by morphogenesis checkpoint activation. This mechanism seems different also from that involving the DNA damage checkpoint protein Rad53, which promotes Swe1 degradation in HU-treated cells likely by acting on the septin ring (Enserink et al., 2006; Smolka et al., 2006). In particular, the Dma proteins seem to participate in a step of Swe1 degradation that is downstream of Swe1 recruitment at the division site and its subsequent phosphorylation (Fig. 17B).

Swe1 is likely polyubiquitylated in vivo (Kaiser et al., 1998), suggesting that its degradation occurs via the ubiquitin-proteasome pathway. However, how bud neck-localized Swe1 is targeted to degradation after phosphorylation is still unclear. Specific E3 ubiquitin ligases, among which the key yeast cell cycle regulators SCF (Skp1-cullin-F box) and anaphase-promoting complex (APC), dictate the specificity of substrate recognition for ubiquitin conjugation (for review see Deshaies and Joazeiro, 2009). Intensive analysis of yeast strains bearing F-box gene deletions that abolish substrate specificity of SCFs failed to identify ubiquitin ligases directly required for Swe1 ubiquitylation (McMillan et al., 2002). On the other hand, APC seems

unlikely to mediate Swe1 degradation, which is unaffected when the spindle checkpoint keeps inactive APC (Sia et al., 1998). In addition, Swe1 variants have been described that do not undergo degradation although they show proper bud neck localization, phosphorylation and interaction with known Swe1 regulators (McMillan et al., 2002), indicating that still unknown Swe1 regulators exist.

As the Dma proteins have ubiquitin ligase activity in vitro (Loring et al., 2008) and their absence allows accumulation of Swe1 under conditions that normally trigger its degradation, an intriguing hypothesis is that Dma1 and Dma2 might be involved in Swe1 ubiquitylation. Indeed, the amount of Swe1 ubiquitylated species we detect under conditions inhibiting the proteasome is strongly reduced in cells lacking the Dma proteins compared to wild type. In spite of our efforts to unravel possible in vivo physical interactions between Swe1 and Dma1 or Dma2, we did not yet obtain reproducible results. Therefore, further experiments will be required in order to assess whether Dma proteins directly ubiquitylate Swe1. It is anyhow important to point out that both ubiquitylation and release of Swe1 from the bud neck are inhibited in the absence of the Dma proteins, indicating that these events might be coupled (Fig. 17B).

As *dma1Δ dma2Δ* cells are viable, while Swe1 degradation is essential for cell viability, other yet unidentified ubiquitin ligases likely ubiquitylate Swe1 during an unperturbed cell cycle. Nonetheless, Dma-dependent control of Swe1 degradation seems to

be crucial for Swe1 down-regulation in response to DNA replication stress. It will be challenging to investigate whether these evolutionarily conserved proteins play similar roles also in other eukaryotes.

Chapter 2

Search for new targets of the protein kinase Swe1 in mitotic spindle elongation

The non phosphorylatable *cdc28-Y19F* allele does not restore proper spindle elongation in *SWE1* overexpressing cells, but is sufficient to restore cell viability.

In *S. cerevisiae*, entry and progression into mitosis are controlled by the cyclin-dependent kinase Cdc28 bound to B-type cyclins (Cdk1). Swe1 inhibits entry into mitosis by phosphorylating the Tyr19 (Y19) residue of the catalitic subunit of Cdk1, Cdc28 (Booher et al., 1993) and this inhibitory phosphorylation is reversed by the Mih1 phosphatase (Russell et al., 1989), leading to Cdk1 activation and entry into mitosis. Cdc28 activity in budding yeast is required not only for G2-M transition, but also for the switch from polarized to isotropic bud growth, so when Cdc28 is inactive also this step is inhibited. Therefore, Swe1 overexpression from the *GAL1* promoter (*GAL1-SWE1*) is lethal for cells, because it inhibits Cdc28 totally, thus blocking both switch from polar to isotropic bud growth and separation of the microtubule organizing centers (Spindle Pole Bodies, SPBs, in yeast) thus causing cells to arrest with elongated buds, undivided nuclei and monopolar spindle (Lim et al., 1996).

Cdc28 is the only known target of the protein kinase Swe1. To test if Swe1 could be involved also in other processes or if it could have also other targets we constructed a strain carrying both the *GAL1-SWE1* construct and a non phosphorylatable allele of *CDC28* in which the Y19 is substituted by a phenalanine, *cdc28-Y19F*, and characterized its phenotype in galactose containing medium. For this purpose, wild

type, *GAL1-SWE1*, *cdc28-Y19F* and *GAL1-SWE1 cdc28Y19F* cells were inoculated in YEPR, arrested in G1 with α-factor and released in galactose containing medium (YEPRG). Samples were taken at different time points after release to monitor the kinetics of DNA replication by Fluorescence Activated Cell Sorter (FACS) analysis, budding, nuclear division and spindle assembly and elongation. Wild type and *cdc28-Y19F* cells showed very similar profiles of budding, DNA replication and nuclear division (Fig. 18A, 18B and 18C); *GAL1-SWE1* cells, as expected, replicated their DNA but failed to divide and, after 240 minutes, accumulated cells with very elongated buds, 2C DNA content, undivided nuclei and monopolar spindle (Fig. 18A, 18B and 18C). Interestingly, *GAL1-SWE1 cdc28-Y19F* cells were able to elongate mitotoc spindle, separate nuclei and divide, but with some defect (Fig. 18A). In particular they were about 30-45 minutes delayed respect to wild type cells in reaccumulating the 1C DNA peak (this difference was always reproducible and observed in different *GAL-SWE1 cdc28-Y19F* segregants; our observations) and were also delayed in dividing nuclei and in elongating the mitotic spindle (Fig. 18A, 18B and 18C). These results indicate that Cdc28 seems not to be the only target of Swe1 kinase, as the substitution of the residue phosphorylated by Swe1 into a not phosphorylatable one does not restore a proper cell cycle in Swe1 overproducing cells. Moreover, we observed that the major defect of *GAL1-SWE1 cdc28-Y19F* cells is in mitotic spindle elongation, as they were able to assemble a short

mitotic spindle with the same kinetics of wild type cells but fail to elongate it, resulting in a small percentage of cells with an elongated mitotic spindle and a high percentage of cells with short or stretched bipolar spindle throughout the entire experiment (Fig. 18C).

However, despite the defects described above, and in particular despite the spindle elongation defect, *GAL1-SWE1 cdc28-Y19F* cells were still able to divide and to form colonies on galactose containing plates, although not with the same efficiency of wild type cells, while Swe1 overproducing cells as expected were not able to growth in the same conditions (Fig. 18D).

Interestingly, we obtained the same results also using another Cdc28 allele, *cdc28-E12K*, that could not physically interact with Swe1 (McMillan et al., 1999) and therefore could not be phosphorylated and inhibited by Swe1 (data not shown). Altogether our data suggest that the protein kinase Swe1 is involved in mitotic spindle elongation and that it has other targets apart from Cdc28.

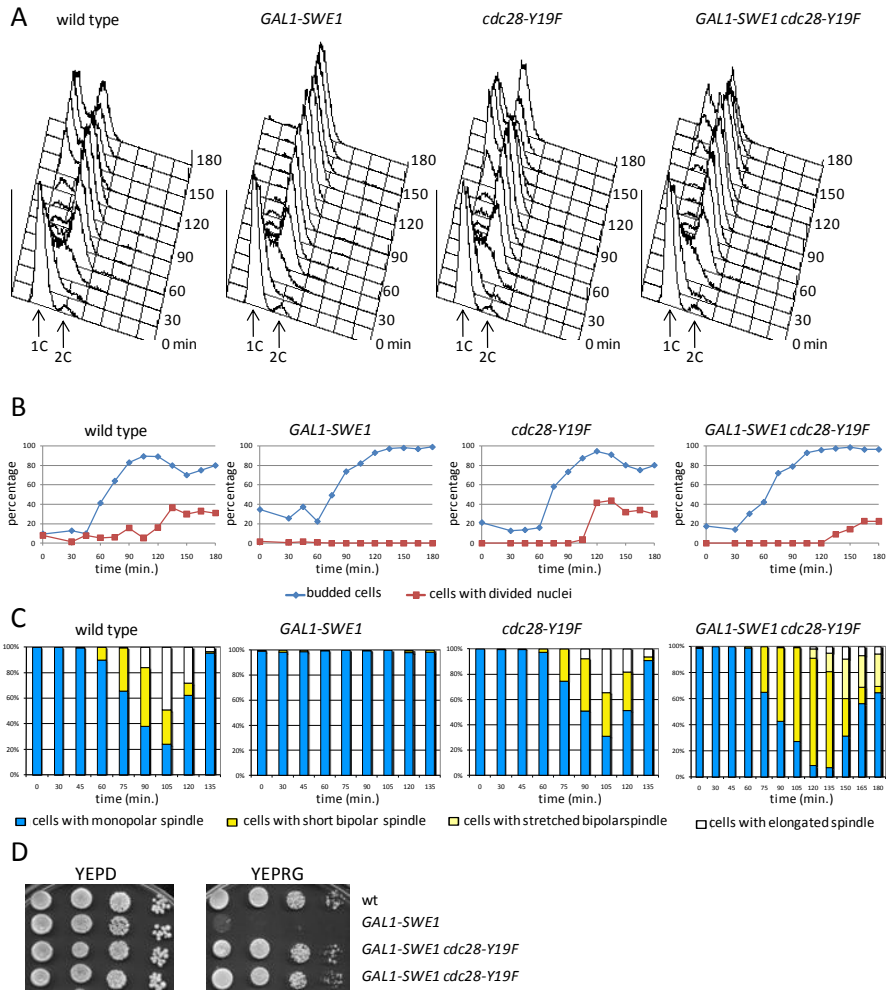

Figure 18: *cdc28-Y19F* allele is sufficient to restore cell viability but not proper spindle elongation in *SWE1* overexpressing cells. Exponentially growing cultures of wild type, *GAL1-SWE1, cdc28-Y19F* and *GAL1-SWE1 cdc28-Y19F* cells were arrested in G1 by α-factor in YEPR and released from G1 arrest in YEPRG at 25°C (time 0) to induce *SWE1* overexpression. At the indicated times after release, cell samples were taken for FACS analysis of DNA content (A) and for scoring budding, nuclear division (B) and mitotic spindle formation and elongation with immunofluorescence using anti-tubulin antibodies (C). D: Serial dilutions of stationary phase cultures of strains with the indicated genotypes were spotted on YEPD or YEPRG plates which were then incubated for 2 days at 25°C.

The spindle elongation defect of *GAL-SWE1 cdc28-Y19F* cells is not due to a defect in sister chromatids cohesion removal

In yeast, the initiation of anaphase is marked by the separation of sister chromatids, which is brought about by proteolytic cleavage of the cohesin subunit Scc1 by the protease separase. Cohesin remains associated with chromosomes until the onset of anaphase, however it must be removed for sister chromatids to separate, because it is a structural barrier that opposes the pulling forces of the microtubules. So, for proper spindle elongation, is required a proper timely removal of the cohesion between sister chromatids. We asked therefore if the spindle elongation defect of *GAL1-SWE1 cdc28-Y19F* cells could be due to a delay in cohesin removal.

To analyze sister chromatids cohesion, we used the TetO/TetR system (Michaelis et al., 1997); briefly, 336 sequences of Tet operators are inserted adjacent to the centromere of chromosome V in cells that expresses a Tet repressor fused to GFP, so the Tet operators are visible as green fluorescent dots within the nuclei of cells. In particular, they appear as a single dot when the sister chromatids are bound together by cohesin and as two dots when the cohesion between them is removed.

Wild type, *GAL1-SWE1, cdc28-Y19F* and *GAL1-SWE1 cdc28Y19F* cells, all carrying the TetO/TetR system, were inoculated in YEPR, arrested in G1 with α-factor and released in YEPRG to induce Swe1 overexpression. Samples were taken at different time points after

release to monitor the kinetics of DNA replication by FACS analysis (Fig. 19A), budding, nuclear division (Fig. 19B) and sister chromatids separation (Fig. 19C). All the four strains had the same behaviour as the previous experiment as far as FACS analysis of the DNA content, the kinetics of budding and nuclear division are concerned (Fig. 19A and 19B, Fig 18A and 18B). Interestingly, *GAL1-SWE1 cdc28-Y19F* cells are able to separate sister chromatids with a kinetic similar to wild type and *cdc28-Y19F* cells (Fig. 19C), indicating that the spindle elongation defects of these cells is not due to a persistence in sister chromatids cohesion but to a defect in spindle dynamics.

We therefore decided to further analyze this aspect both by performing a genetic screen and by searching directly for possible targets of the protein kinase Swe1 in spindle elongation.

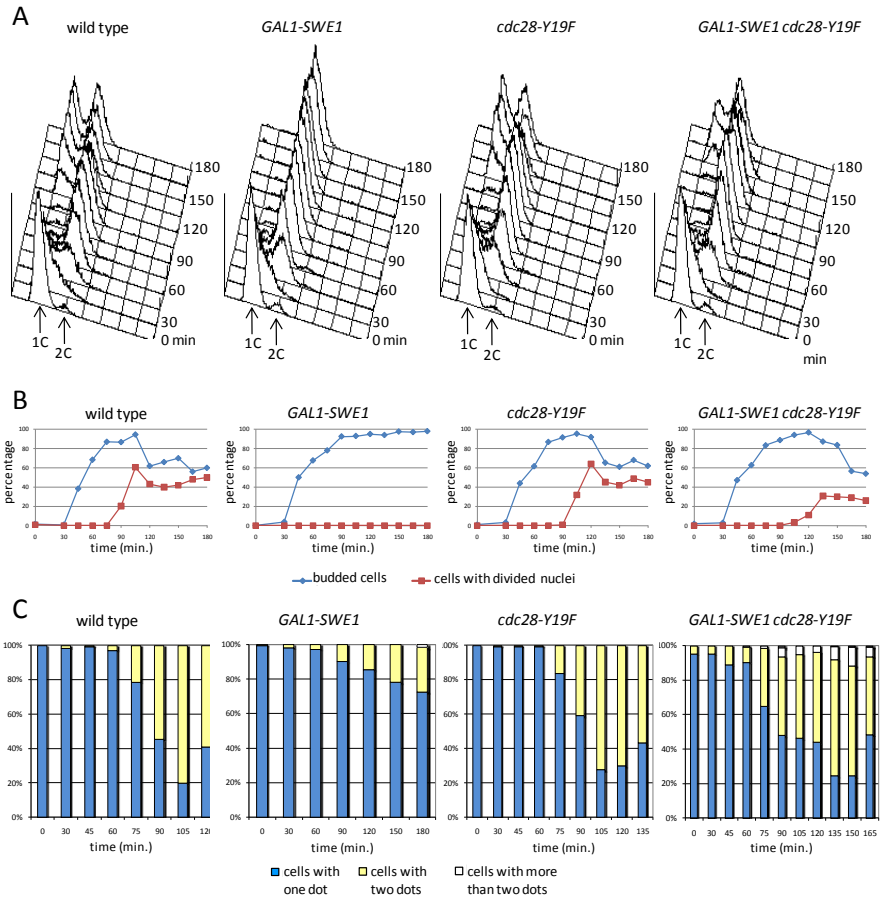

Figure 19: The spindle elongation defect of *GAL1-SWE1 cdc28-Y19F* cells is not due to a persistence of sister chromatids cohesion. Exponentially growing cultures of wild type, *GAL1-SWE1, cdc28-Y19F* and *GAL1-SWE1 cdc28-Y19F* cells were arrested in G1 by α-factor in YEPR and released from G1 arrest in YEPRG at 25°C (time 0) to induce *SWE1* overexpression. At the indicated times after release, cell samples were taken for FACS analysis of DNA content (A) and for scoring budding, nuclear division (B) and sister chromatids separation (C) using the system described above.

CDH1 deletion restores spindle pole bodies (SPBs) separation but not cell viability of Swe1 overproducing cells

As the spindle elongation defect of *GAL-SWE1 cdc28-Y19F* cells is not due to a defect in sister chromatids separation but rather to a direct involvement of the protein kinase Swe1 in mitotic spindle dynamics, we decided to perform a genetic screen to search for potential Swe1 targets involved in this process. Unfortunately, we could not use *GAL1-SWE1 cdc28-Y19F* strain because these cells in our background were able to form colonies on galactose containing plates despite their defects (Fig. 18D). Instead, the search for suppressors of *GAL1-SWE1* lethality in galactose would lead to the finding of *CDC28* mutants; moreover these cells have monopolar spindles (Fig. 18C), while we were interested in investigating mitotic spindle elongation. So, in order to set up the best conditions for the genetic screen, we tried to force SPBs separation in *SWE1* overexpressing cells.

The microtubule associated proteins (MAPs) Cin8, Kip1 and Ase1 are all required for SPBs separation. They are all are targeted for degradation by the E3 ubiquitin ligase APC (Anaphase Promoting Complex) associated to its regulatory subunit Cdh1. To be able to separate the SPBs, cells have to accumulate these MAPs by inhibiting their degradation through inactivation of Cdh1. For these reasons, the deletion of *CDH1* in cells that are unable to separate the SPBs is sufficient to allow Cin8, Kip1 and Ase1 accumulation and SPBs separation (Crasta et al., 2006). Therefore, we asked if *CDH1* deletion

is also able to restore SPBs separation also in *SWE1* overexpressing cells without restoring cell viability.

To verify our hypothesis, wild type, *GAL1-SWE1* and *GAL1-SWE1 cdh1Δ* cells were inoculated in YEPR, arrested in G1 with α-factor and released in YEPRG to induce *SWE1* overexpression. Samples were taken at different times after release to monitor the kinetics of DNA replication by FACS analysis, budding, nuclear division and spindle assembly and elongation by immunofluorescence. Wild type and *GAL1-SWE1* cells behave as in the experiments described above (Fig. 20A and 20B). Interestingly, *GAL1-SWE1 cdh1Δ* arrested as budded cells (Fig. 20B) with 2C DNA content (Fig. 20A) and undivided nuclei (Fig. 20B), but they were able to separate the SPBs and to form a short bipolar spindle, while *GAL1-SWE1* cells arrested with monopolar spindle as expected (Fig 20C). As *GAL1-SWE1 cdh1Δ* cannot form a functional mitotic spindle nor complete mitosis in galactose containing medium, likely they are not viable in these conditions. As shown in Figure 20D, *GAL1-SWE1 cdh1Δ* cells were not able to form colonies on galactose containing plate, like *GAL1-SWE1* cells.

At this point, we found a condition in which cells that have high levels of Swe1 were able to separate the SPBs but not to divide and form colonies; this strain could be used for a screening to search for targets of the protein kinase Swe1 in spindle elongation.

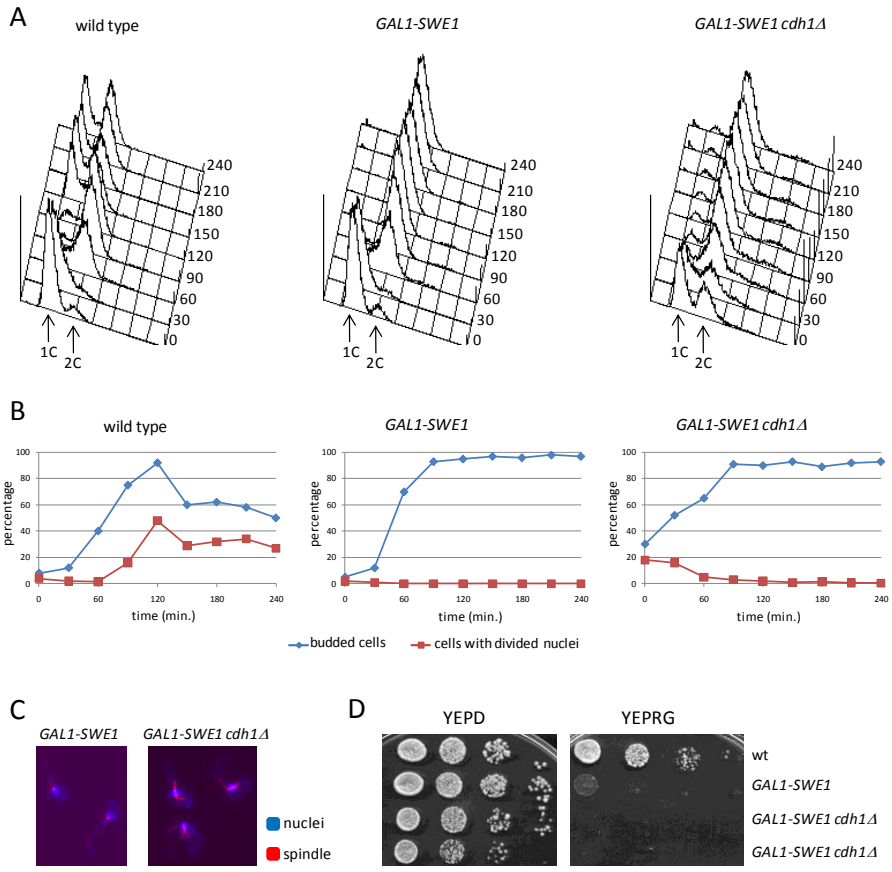

Figure 20: *CDH1* deletion is sufficient to restore SPBs separation but not cell viability in *SWE1* overexpressing cells. Exponentially growing cultures of wild type, *GAL1-SWE* and *GAL1-SWE1 cdh1Δ* cells were arrested in G1 by α-factor in YEPR and released from G1 arrest in YEPRG at 25°C (time 0) to induce *SWE1* overexpression. At the indicated times after release, cell samples were taken for FACS analysis of DNA content (A) and for scoring budding, nuclear division (B) and spindle formation and elongation with immunofluorescence using anti-tubulin antibodies. Representative micrographs were taken at 240 minutes after release in YEPRG (C). D: Serial dilutions of stationary phase cultures of strains with the indicated genotypes were spotted on plates containing either YEPD or YEPRG which were then incubated for 2 days at 25°C.

Genetic screen to search for Swe1 targets involved in mitotic spindle elongation

As *CDH1* deletion allows SPBs separation in *SWE1* overexpressing cells, it is possible to perform a genetic screen to search for mutants that are able to elongate the mitotic spindle of *GAL1-SWE1 cdh1Δ* cells and therefore to divide. As we were searching for targets inhibited by Swe1 phophorylation, we assumed that a mutation(s) in a residue(s) that is phosphorylated by Swe1 into a non phosphorylatable one could restore spindle elongation and therefore viability of *GAL1-SWE1 cdh1Δ* cells in galactose containing medium. For this reason, we chose to search for spontaneous mutations, that normally are generated at every cell cycle, that could allow *GAL1-SWE1 cdh1Δ* cells to grow on YEPRG plates.

The ability of these mutants to grow on galactose containing plates could be due to an inactivation of the *GAL1* promoter or to an increased Swe1 degradation, rather than to mitotic spindle elongation. To exclude the former two possibilities, we constructed a strain in which the coding sequence of *SWE1* under *GAL1* promoter is fused in frame with 3 PK epitopes, recognized by commercial antibodies, that allow us to analyze Swe1 levels in the future isolated mutants by western blot analysis. We decided to perform search for spontaneous mutations both on a *MATa* and on a *MATalpha* strains to be able to cross the suppressors and to divide them into complementation groups. To select diploids for the dominance and

the complementation tests, we deleted the *LYS2* gene with a *TRP1* cassette in one of the two strains. These are the two strains used for the screening:

MATa GAL1-SWE1-3PK cdh1Δ

MATalpha GAL1-SWE1-3PK cdh1Δ lys2::TRP1

These two strains were grown in permissive conditions and plated on YEPD to isolate single colonies. During all the division cycles that lead to the formation of a colony starting from a single cell, mutations accumulate and some of them could allow the growth of *GAL1-SWE1 cdh1Δ* cells in galactose containing medium. We collected 14 independent colonies for each strain from YEPD plates and after properly dilutions we plated about 1-1,5x10^5 viable cells coming from a single colony on a YEPRG plate. After five days of incubation at 25°C, on each plate there were some colonies, and we called them suppressors. As general rule, the suppressors coming from the same plate are classified as identical because they most likely originated from the same cell and therefore carry the same mutation. Instead, we observed that the colonies grown on each YEPRG plate had two different morphologies: smooth and rough. Colonies with a rough morphology are formed of cells with elongated bud, which is typical of cells with high Swe1 levels. We decided therefore to collect 3 smooth and 3 rough colonies and we retested their ability to growth on YEPRG plates to confirm the suppression phenotype. The results of the screening are listed in table 2:

	plates	suppressors	morphology
MATa	14	72	42 smooth 30 rough
MATalpha	14	74	42 smooth 32 rough

Table 2: Summary of the suppressors isolated respectively from the *MATa* and the *MATalpha* strains and the morphology of their colonies. See text for details.

As first thing, we tested if the ability of each suppressor to growth on YEPRG plates was due to a dominant or to a recessive mutation(s). For this purpose, we crossed each suppressor with the starting strain of the opposite mating type to obtain homozygous *GAL1-SWE1 cdh1Δ* cells, then we selected the diploids on –Lys –Trp plates and tested their ability to growth on YEPRG plates. If the mutation(s) responsible for the suppression is dominant, the diploid will be able to grow in this condition, if it is recessive the diploid will not be able to form colonies on YEPRG plates. We classified intermediary situations as semidominants. The results of the dominance test are summarized in the table below (Table 3):

	dominants	semidominants	recessives
MATa	48	13	11
MATalpha	12	30	32

Table 3: Each suppressor was crossed with a *GAL1-SWE1 cdh1Δ* strain, diploids were selected on opportune plates and the ability of the diploids to form colonies on galactose containing plates was assayed. See text for details.

Later, we analyzed Swe1 levels in all the suppressors after incubation in galactose containing medium, to verify that the ability of the suppressors to growth on YEPRG plates was not due to a decrease in Swe1 levels. For this purpose, all the suppressors strains were grown

in YEPR and shifted in YEPRG for three hours; after this time, samples were collected to analyze Swe1 levels by western blot analysis. *GAL1-SWE1-3PK cdh1Δ* cells were used as a control. The results are listed in the table below (Table 4):

	high Swe1 levels	low Swe1 levels
MATa	27	45
MATalpha	30	44

Table 4: Each suppressor was grown in YEPR medium and then shifted in galactose containing medium for 3 hours; samples were collected to analyze Swe1 levels by western blot analysis using anti-PK antibodies. See text for details.

Based on the analysis described above, we determined that all the colonies with the same morphology that were picked up from the same YEPRG plate behave in the same way, so we considered them identical. For this reason, we continued the analysis on just one of the three suppressors with the same colony morphology coming from each YEPRG plate. Interestingly, almost all the suppressors with high levels of Swe1 formed rough colonies. We decided to focus on recessive suppressors (because recessive mutation are easier to clone respect to dominants or semidominants one) with high Swe1 levels (not mutated in *GAL1* promoter or in Swe1 degradation pathway) listed in the table below (Table 5).

MATa	***mut516***	***mut517***	***mut518***	***mut546***	***mut555***	***mut567***
MATalpha	***mut51***	***mut60***	***mut63***	***mut66***	***mut69***	***mut72***

Table 5: Summary of the recessive suppressors that have high Swe1 levels. See text for details

All the isolated suppressors are able to form colonies on galactose containing plates

While we were performing the screening, we tested the ability of all the suppressors to form colonies on YEPRG just on a quality levels (patch). We therefore performed a drop test to better characterize the 12 suppressor that we selected from the preliminary analysis (Table 5); we tested their ability not only to growth on YEPRG plates but also to growth at different temperatures.

Wild type cells formed colonies efficiently at all the tested temperature both on YEPD and YEPRG, while *GAL1-SWE1 cdh1Δ* cells were able to form colonies only on YEPD (Fig 21A and 21B). As we expected from our preliminary results, all the twelve suppressors were able to form colonies both on YEPD and on YEPRG plates, although with low efficiency compared to wild type cells especially on YEPRG (Fig. 21A and 21B). Interestingly, *mut66* lost viability both on YEPD and YEPRG at 37°C, indicating that it is a termosensitive mutant (Fig. 21B). However further analysis revealed that its termosensitivity did not segregate together with the ability to growth on YEPRG, indicating that these two features are independent.

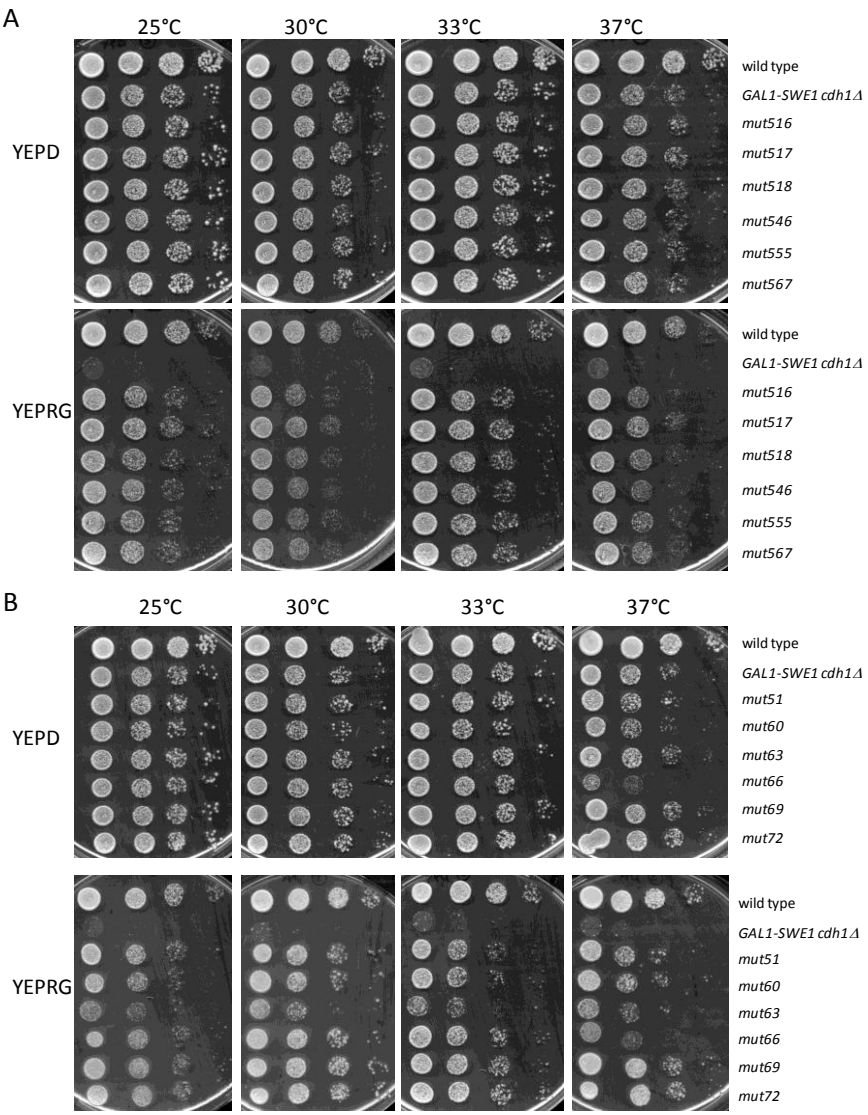

Figure 21: All the suppressors were able to form colonies on galactose containing plates. Serial dilutions of stationary phase cultures of strains with the indicated genotypes were spotted on YEPD or YEPRG plates which were then incubated for 2 days at the indicated temperature. (A) *MATa* suppressors and (B) *MATalpha* suppressors.

All the suppressors are able to elongate the mitotic spindle and to complete mitosis in galactose containing medium

At this time, we had just tested the ability of the twelve mutants to suppress the lethality of *SWE1* overexpression in cells lacking *CDH1* on galactose containing plates. Therefore, we decided to further analyze the phenotype of these mutants and to see if they are really able to allow mitotic spindle elongation and to divide in liquid medium. We analyzed separately the *MATa* and the *MATalpha* suppressors, because we synchronized them in different ways.

First, *GAL1-SWE1 cdh1Δ, mut516, mut517, mut518, mut546, mut555* and *mut567* cells were inoculated in YEPR, arrested in G1 with α-factor and released in galactose containing medium (YEPRG). Samples were taken at different time points after release to monitor the kinetics of DNA replication by FACS analysis and spindle assembly and elongation. *GAL1-SWE1 cdh1Δ* cells arrested as expected with 2C DNA content (Fig. 22A) and short bipolar spindle (Fig. 22B), as previously described (Fig. 20). On the contrary, all the suppressors were able to divide, as they reaccumulate the 1C DNA peak (Fig. 22A); moreover, they elongate the mitotic spindle (Fig. 22B), indicating that they are really able to suppress the phenotype of *GAL1-SWE1 cdh1Δ* cells in galactose containing medium.

We then tested the ability of *MATalpha* suppressors to elongate the mitotic spindle. We could not synchronize these mutants with α-factor because they are not sensitive to this pheromone, so we

patched *GAL1-SWE1 cdh1Δ, mut51, mut60, mut63, mut66, mut69* and *mut72* cells on YEPR plates and incubated at 25°C for two days to let them growth to stationary phase. Then, we released all the strains from stationary phase arrest in YEPRG at 25°C (time 0) to induce *SWE1* overexpression. Samples were taken at different time points after release to monitor the kinetics of DNA replication by FACS analysis and spindle assembly and elongation. Also in this case, all the suppressors are able to replicate the DNA and to divide, although with different efficiencies (Fig. 23A) and all assembled a short mitotic spindle and elongated it (Fig. 23B), indicating that they are able to suppress the spindle elongation defect of *GAL-SWE1 cdh1Δ* cells also in liquid medium.

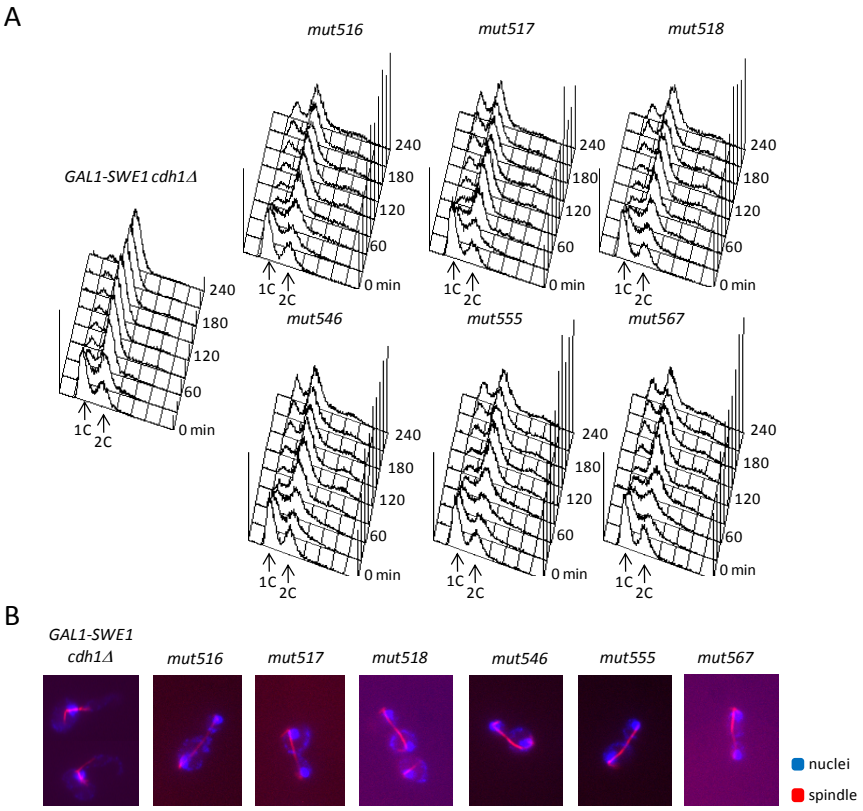

Figure 22: All the *MATa* suppressors are able to elongate the mitotic spindle and to complete mitosis in galactose containing medium. Exponentially growing cultures of *GAL1-SWE1 cdh1Δ, mut516, mut517, mut518, mut546, mut555* and *mut567* cells were arrested in G1 by α-factor in YEPR and released from G1 arrest in YEPRG at 25°C (time 0) to induce *SWE1* overexpression. At the indicated times after release, cell samples were taken for FACS analysis of DNA content (A) and to follow mitotic spindle formation and elongation with immunofluorescence using anti-tubulin antibodies. Representative micrographs were taken at 240 minutes after release in YEPRG (B).

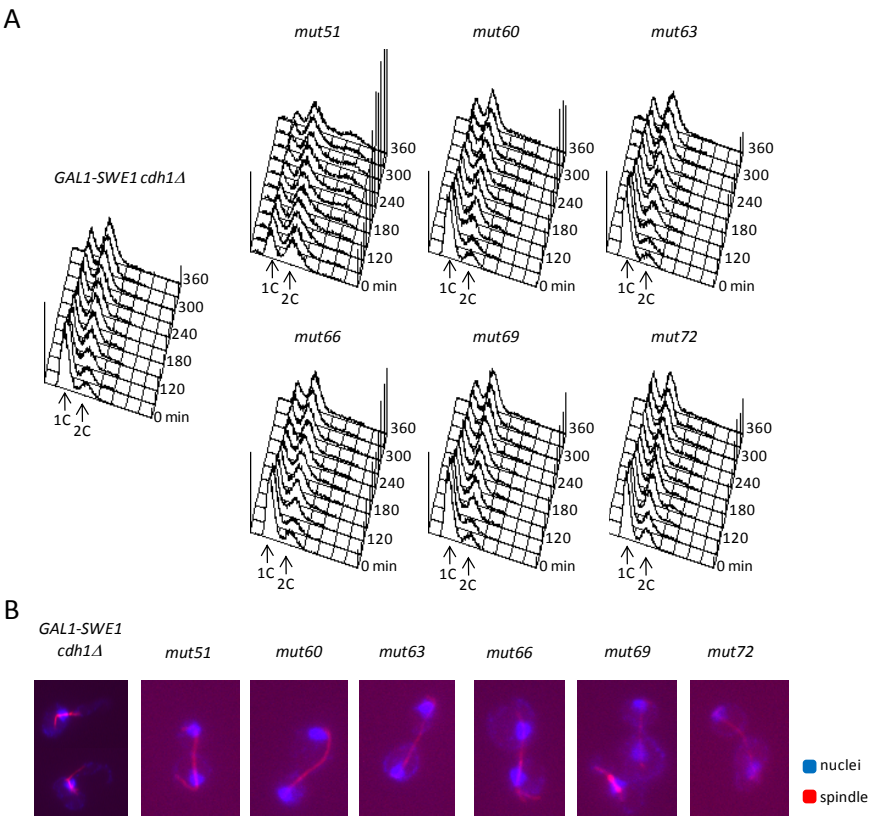

Figure 23: The *MATalpha* suppressors are able to elongate the mitotic spindle and to complete mitosis in galactose containing medium. *GAL1-SWE1 cdh1Δ, mut51, mut60, mut63, mut66, mut69* and *mut72* cells were patched on YEPR plates and incubated at 25°C for two days to let them growth to stationary phase; than they were released from stationary phase arrest in YEPRG at 25°C (time 0) to induce *SWE1* overexpression. At the indicated times after release, cell samples were taken for FACS analysis of DNA content (A) and to follow mitotic spindle formation and elongation with immunofluorescence using anti-tubulin antibodies. Representative micrographs were taken at 360 minutes after release in YEPRG (B).

All the suppressors are mutated in the same gene

From the previous experiments, we determined that all the twelve recessive suppressors that we isolated are really able to elongate the mitotic spindle and therefore to suppress the phenotype of *GAL1-SWE1 cdh1Δ* cells in galactose containing medium. We crossed them with a *GAL1-SWE1 cdh1Δ* strain and after sporulation and tetrads analysis we determined that the suppression phenotype is due to a single mutated gene in all the suppressors. As they are all recessive and all mutated in only one gene, we made a complementation test to see if some *MATa* suppressors carried the same mutated gene as some *MATalpha* suppressors. We therefore crossed all the *MATa* with all the *MATalpha* suppressors, selected the diploids on –Lys –Trp plates and tested their ability to growth on YEPRG plates. All the diploids formed colonies on YEPRG plates, indicating that all the twelve suppressors are mutated in the same gene (Fig. 24).

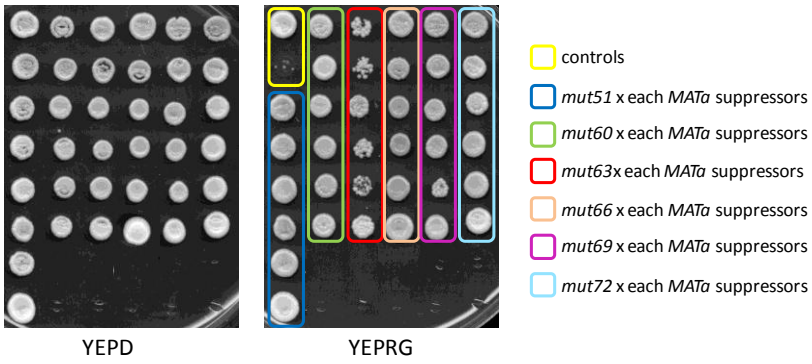

Figure 24: All the suppressors are mutated in the same gene. Each *MATa* suppressor was crossed with every *MATalpha* suppressor and diploids were selected on proper plates; the ability of the diploids to form colonies on galactose containing plates was assayed, to divide the suppressors into complementation groups.

Cloning strategy

From this genetic screen we found twelve recessive suppressors with high levels of Swe1 and they are all mutated in the same gene that is responsible for the suppression phenotype. We decided therefore to try to clone the gene from one suppressor; we chose the *mut546* suppressor.

We will clone the gene by complementation, transforming the *mut546* with a library of centromeric plasmids in which is cloned the entire yeast genomic DNA (genomic library) and identifying the plasmid in which is cloned the gene that is mutated in the suppressors. Exponentially growing cultures of *mut546* cells will be transformed with a yeast centromeric library and transformants will be selected on opportune plates. These plates will be replicated on YEPRG plates and we will search for transformants that will not be able to grow in the presence of galactose, like *GAL1-SWE1 cdh1Δ* cells (Fig. 25). We will test if the inability of these transformants to form colonies on YEPRG is due to the library plasmid and we will identify and collect the plasmids that are responsible for that phenotype. We will sequence the genomic insert of the plasmids, and targeted strategies will be applied to identify the gene. Once identified, we will set up the best strategy to study the interactions between this gene product and Swe1, and to better characterize the role of the protein kinase Swe1 in mitotic spindle elongation.

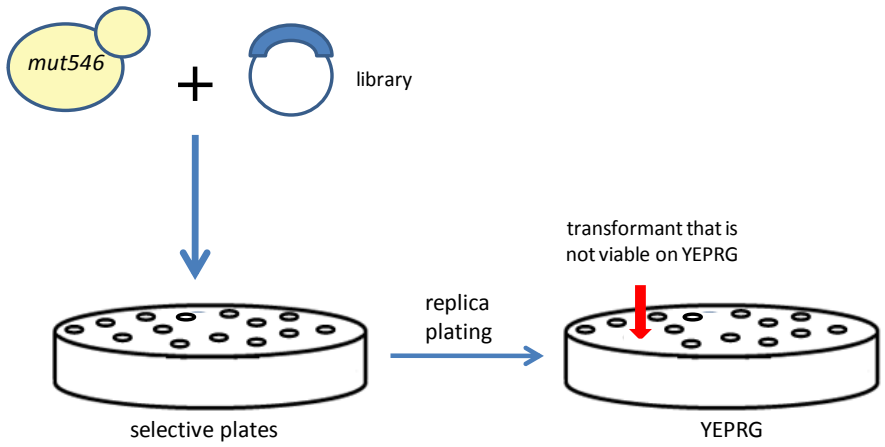

Figure 25: Cloning strategy. Exponentially growing culture of *mut546* cells will be transformed with a centromeric yeast genomic library and transformants will be selected on proper plates. These plates will be replicated on YEPRG and transformants that are not viable in this condition will be identified (red arrow). See text for details.

SWE1 overexpression reduces Bik1 phosphorylation

As this kind of the genetic screen allows only the identification of proteins inhibited by Swe1, in parallel we used an alternative approach to find other Swe1 targets in mitotic spindle elongation process. In particular we took advantage of highthroughput screenings published in literature and whose results available on line, searching for microtubule associated proteins or factors that are involved in mitotic spindle dynamics. A proteome chip array identified a number of proteins phosphorylated by Swe1 (Bodenmiller et al., 2010); among these there is the microtubule associated protein (MAP) Bik1. Bik1 is a microtubule plus-end tracking protein (+TIP) that is required for microtubule function during mitosis; it plays a negative role in microtubule assembly through inhibition of growth rates and by enhancing frequency of catastrophes, it produces preanaphase pulling force on kinetochores and it is required for spindle elongation during anaphase. Considering the result of the proteome chip array, we asked if Bik1 phosphorylation depends on Swe1, and in particular if it is increased in *SWE1* overexpressing cells and decreased in *swe1Δ* cells. To answer this question, wild type, *swe1Δ* and *GAL1-SWE1* cells were inoculated in YEPR and shifted in YEPRG for three hours. Samples were collected from both YEPR and YEPRG cultures for analyzing Bik1 phosphorylation by western blot analysis. Surprisingly, Bik1 phosphorylation did not increase in cells with high Swe1 levels

respect to wild type and instead it decreased in *GAL1-SWE1* cells in YEPRG respect to the same cells in YEPR and to the wild type, while it increased in *swe1Δ* cells compared to wild type (Fig. 26A, left panel). These results indicate that Swe1 does not directly phosphorylates Bik1, as it was suggested by the data found in literature. As Bik1 contain a CDK consensus sequence, we asked if the mobility shift of Bik1 could be due to phosphorylation by Cdk1 rather than by Swe1. To answer this question, we analyzed Bik1 phosphorylation in cells with high Swe1 levels and expressing either a non phosphorylatable allele of Cdc28, *cdc28-Y19F*, or an allele coding for a Cdc28 variant that could not physically interact with Swe1, *cdc28-E12K*. We decided to use *swe1Δ* cells as a positive control because, as these two alleles codify for two Cdc28 variants that should not be inhibited by Swe1, they mimic the absence of Swe1 as far as Cdc28 kinase activity is concerned. For this purpose, exponentially growing cultures of *swe1Δ, GAL1-SWE1, GAL1-SWE1 cdc28-Y19F* and *GAL1-SWE1 cdc28-E12K* cells were shifted in galactose containing medium for three hours, then samples were collected for analyzing Bik1 phosphorylation as described above. Neither the Y19F nor the E12K substitutions were able to restore Bik1 phosphorylation in *SWE1* overexpressing cells as it appears in *swe1Δ* cells (Fig. 26A, right panel) indicating that an other protein kinase(s) apart from Cdc28 is responsible for Bik1 phosphorylation.

However, high levels of Swe1 seems to inhibit Bik1 phosphorylation totally and independently from Cdk1. We decided therefore to analyze Bik1 phosphorylation during the whole cell cycle both in wild type and in *SWE1* overexpressing cells. For this purpose, wild type and *GAL1-SWE1* cells were inoculated in YEPR, arrested in G1 with α-factor and released in YEPRG to induce Swe1 overproduction. Samples were taken at different time points after the release to monitor the kinetics of DNA replication by FACS analysis and Bik1 phosphorylation by western blot analysis. Both strains progressed through the cell cycle as in the previous experiments (see Fig. 18) according to FACS analysis of DNA content (Fig 26B). In wild type cells, Bik1 appears as a single band, likely corresponding to its unphosphorylated form, in G1 and in early S phase then at about 60 minutes after the release, a slower migrating band appears (Fig. 26C, left). In *SWE1* overexpressing cells Bik1 remained unphosphorylated for all the time course of the experiment, confirming the previous result (Fig. 26C, right). Thus, Swe1 does not directly phosphorylates Bik1 but somehow acts modifying its phosphorylation state; in fact, Bik1 is no more phosphorylated in the presence of high Swe1 levels, while its phosphorylation increases in cells lacking Swe1 (Fig. 26A and 26C). Moreover, the introduction of *cdc28-Y19F* or of *cdc28-E12K* allele in *SWE1* overexpressing cells did not restore Bik1 phosphorylation (Fig. 26A, right panel) indicating that Swe1 influences Bik1 phosphorylation independently of its inhibitory

activity on Cdc28. Further analysis will be required to better understand the molecular details of the indirect Swe1 action on Bik1 phosphorylation. In particular, we could hypothesize either an inhibitory action of Swe1 on another protein kinase or, intriguingly, an activating action on a protein phosphatase.

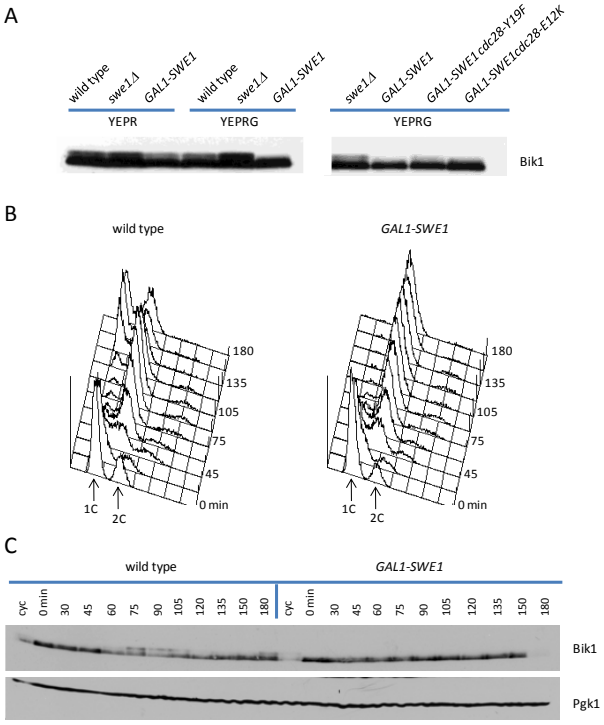

Figure 26: Bik1 phosphorylation is reduced in *SWE1* overexpressing cells. A: wild type, *swe1Δ* and *GAL1-SWE1* or *swe1Δ*, *GAL1-SWE1, GAL1-SWE1 cdc28-Y19F* and *GAL1-SWE1 cdc28-E12K* cells were inoculated in YEPR and shifted in YEPRG for three hours. Then, samples were collected both from YEPR and YEPRG cultures for analyzing Bik1 phosphorylation by western blot analysis using anti-Bik1 antibodies. B and C: Exponentially growing cultures of wild type and *GAL1-SWE1* cells were arrested in G1 by α-factor in YEPR and released from G1 arrest in YEPRG at 25°C (time 0) to induce *SWE1* overexpression. At the indicated times after release, cell samples were collected for FACS analysis of DNA content (B) and for analyzing Bik1 phosphorylation (C) using anti-Bik1 antibodies and anti-Pgk1 antibodies as a loading control.

***CDC5* overexpression partially restores spindle elongation and viability of *SWE1* overexpressing cells in the presence of functional Mih1**

Preliminary results obtained in our laboratory indicated that the overproduction of the Polo kinase Cdc5 partially restores viability of *SWE1* overexpressing cells; moreover, *CDC5* overexpression was sufficient to partially restore viability of *GAL1-SWE1* cells on galactose containing plates but surprisingly the lack of the protein phosphatase Mih1 inhibits Cdc5 action. In fact, as shown in figure 27A, the deletion of *MIH1* completely abolished the viability of *GAL1-SWE1 GAL1-CDC5* cells on YEPRG plates. Mih1 is the protein phosphatase that counteracts Swe1 action on Cdc28; it reverses the inhibitory phosphorylation on Y19 of Cdc28 (Russell *et al.*, 1989), leading to Cdk1 activation and entry into mitosis. We therefore decided to gain insight this aspect, to better understand why *CDC5* overexpression allows *GAL1-SWE1* cells to form colonies on galactose containing plates, and the role of the protein phosphatase Mih1 in this process.

For this purpose wild type, *GAL1-SWE1*, *GAL1-SWE1 GAL1-CDC5* and *GAL1-SWE1 GAL1-CDC5 mih1Δ* cells were inoculated in YEPR, arrested in G1 with α-factor and released in galactose containing medium (YEPRG). Samples were taken at different time points after release to monitor the kinetics of DNA replication by FACS analysis (Fig. 27B), budding, nuclear division (not shown) and spindle

assembly and elongation (Fig. 27C). As shown in previous experiments (for example see Fig. 18), wild type cells properly replicated their DNA and divided, while *SWE1* overexpressing cells accumulated with 2C DNA content and monopolar spindle (Fig. 27B and 27C). *GAL1-SWE1 GAL1-CDC5* cells, as in preliminary experiments, partially elongated mitotic spindle and divided (Fig. 27C), although not with the same efficiency as wild type cells, as *CDC5* overexpression is partially toxic for cells. Interestingly, cells overexpressing both *SWE1* and *CDC5* but lacking *MIH1* accumulated as budded cells (data not shown) with 2C DNA content like *GAL1-SWE1* cells (Fig. 27B), but differently from this strain, they were able to separate the SPBs and to form a short bipolar spindle (Fig. 27C).

Therefore, the overexpression of *CDC5* is sufficient to allow SPBs separation in *SWE1* overexpressing cells but the protein phosphatase Mih1 is required for these cells to elongate the mitotic spindle. This suggested that high levels of Cdc5 could suppress the lethal effects due to *SWE1* overexpression, in particular the spindle elongation defect, acting through the phosphatase Mih1.

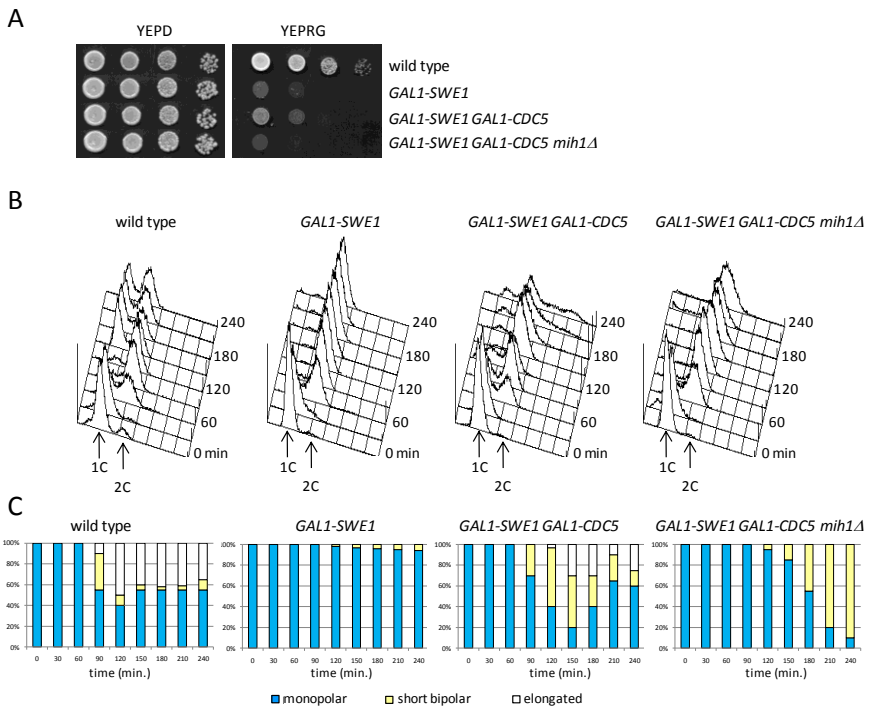

Figure 27: *CDC5* overexpression partially restores viability of *SWE1* overexpressing cells, but it requires Mih1. A: Serial dilutions of stationary phase cultures of strains with the indicated genotypes were spotted on YEPD or YEPRG plates which were then incubated for 2 days at 25°C. B and C: Exponentially growing cultures of wild type, *GAL1-SWE1*, *GAL1-SWE1 GAL1-CDC5* and *GAL1-SWE GAL1-CDC5 mih1Δ* cells were arrested in G1 by α-factor in YEPR and released from G1 arrest in YEPRG (2% galactose) at 25°C (time 0) to induce *SWE1* and *CDC5* overexpression. At the indicated times after release, cell samples were taken for FACS analysis of DNA content (B) and for scoring mitotic spindle formation and elongation with immunofluorescence using anti-tubulin antibodies (C).

***CDC5* overexpression does not causes a decrease of Swe1 levels in *SWE1* overexpressing cells**

During an unperturbed cell cycle, Swe1 is subjected to multiple regulations that change its phosphorylation state, subcellular localization and protein levels. In particular, Swe1 is degraded at the G2/M transition after multiple phosphorylation by different kinases. Among others, the Polo kinase Cdc5 has an important role in Swe1 phosphorylation, targeting it to proteasome-mediated degradation. We asked therefore if the partial ability of *GAL1-SWE1 GAL1-CDC5* cells to form colonies on YEPRG and to elongate the mitotic spindle in galactose containing medium could be due to lower levels of Swe1 in these cells respect to *GAL1-SWE1* cells. For this purpose, we constructed a strain in which the coding sequence of *SWE1* under *GAL1* promoter is fused in frame with 3 PK epitopes recognized by commercial antibodies, that allowed us to analyze Swe1 levels by western blot analysis. *GAL1-SWE1-3PK* and *GAL1-SWE1-3PK GAL1-CDC5* cells were inoculated in YEPR, arrested in G1 with α-factor and released in YEPRG. Samples were taken at different time points after release to monitor the kinetics of DNA replication by FACS analysis and Swe1 levels. Both *GAL1-SWE1* and *GAL1-SWE1 GAL1-CDC5* cells behave as in the previous experiment (Fig. 27B) as determined by FACS analysis of DNA content (Fig. 28A). Importantly, Swe1 levels remained high until the end of the experiment both in *GAL1-SWE1* and in *GAL1-SWE1 GAL1-CDC5* cells (Fig. 28B), indicating that the

restored spindle elongation in cells overexpressing both *CDC5* and *SWE1* that we observed in the previous experiment (Fig. 27C) is not due to a decrease in Swe1 levels. Interestingly, the pattern of the modified Swe1 forms (that correspond to different phosphorylation) are different between the two strains. In particular, in *CDC5* overexpressing cells Swe1 is more phosphorylated, consistent with the fact that Cdc5 phosphorylates Swe1.

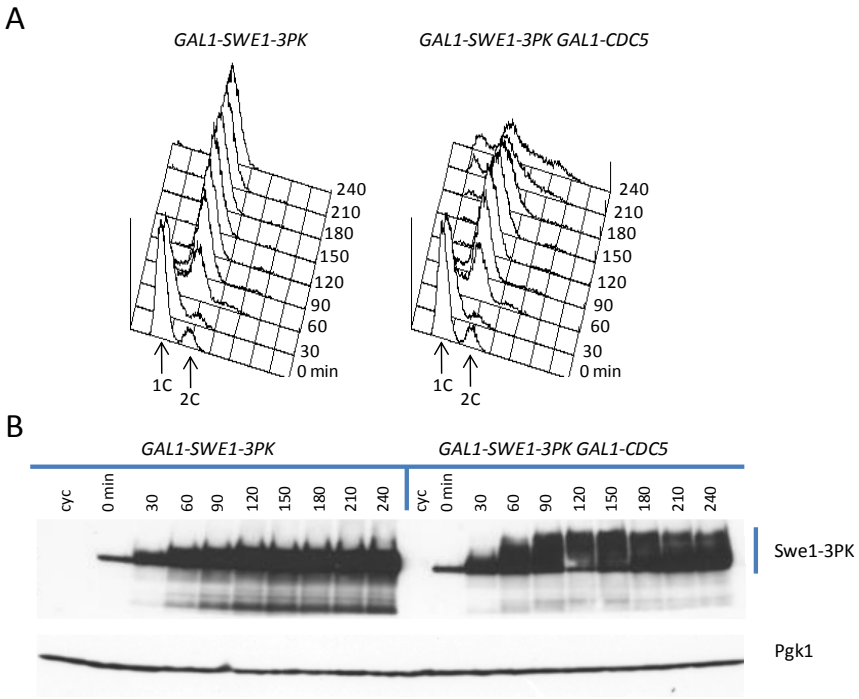

Figure 28: The restored spindle elongation and partial viability of *GAL1-SWE1 GAL1-CDC5* cells are not due to a decrease in Swe1 levels. Exponentially growing cultures of wild type, *GAL1-SWE1-3PK* and *GAL1-SWE1-3PK GAL1-CDC5* cells were arrested in G1 by α-factor in YEPR and released from G1 arrest in YEPRG (2% galactose) at 25°C (time 0) to induce *SWE1* and *CDC5* overexpression. At the indicated times after release, cell samples were taken for FACS analysis of DNA content (A) and for determining Swe1 levels by western blot analysis with anti-HA and for loading control with anti-Pgk1 antibodies (B).

***SWE1,* and not *CDC5,* overexpression changes the balance between phosphorylated and unphosphorylated forms of Mih1**

From the previous experiments, we found that the overexpression of *CDC5* is sufficient to partially restore both spindle elongation and viability of *GAL1-SWE1* cells in galactose containing medium. In mammalian cells, the homologue of budding yeast Cdc5, PLK, phosphorylates CDC25B, the homologue of the phosphatase Mih1, thus promoting CDK activation and entry into mitosis (Lobjois et al., 2009 and 2011). We asked therefore if the Polo kinase phosphorylates the phosphatase of CDK also in budding yeast, like in mammalian cells.

We decided therefore to analyze Mih1 phosphorylation in wild type and in *CDC5* overexpressing cells. For this purpose, we constructed a strain in which the coding sequence of *MIH1* is fused in frame with 3 HA epitopes recognized by commercial antibodies, that allowed us to analyze Mih1 levels and phosphorylation. *MIH1-3HA* and *MIH1-3HA GAL1-CDC5* cells were inoculated in YEPR, arrested in G1 with α-factor and released in YEPRG; 90 minutes after release, we readded α-factor to the cultures to arrest cells in the next G1 phase, thus analyzing a single cell cycle. Samples were taken at different time points after release to monitor the kinetics of DNA replication by FACS analysis and Mih1 levels and phosphorylation by western blot analysis. Wild type cells expressing *MIH1-3HA* normally progressed through the cell cycle and arrested in the next G1, as shown by FACS

analysis of DNA content (Fig. 29A). On the other side, *CDC5* overexpressing cells replicated their DNA but partially failed to divide, as in the previous experiments, because high levels of Cdc5 are toxic for cells (Fig. 29A). However, despite this difference in the last phases of the cell cycle, both in wild type and in *CDC5* overexpressing cells the phosphorylation pattern of Mih1 is almost the same (Fig. 29B). In fact, soon after the release from G1 arrest Mih1 is fully phosphorylated, while after 45 minutes from the release the less phosphorylated forms appeared. As Mih1 has a lot of phosphorylation sites, it appears as a series of bands at different molecular weight. It's interesting to notice that both in wild type and in *GAL1-CDC5* cells the pattern of phosphorylation is almost the same during the whole time course of the experiment, indicating that the overexpression of *CDC5* does not change the balance between different Mih1 phosphorylation forms and that thus, likely, the yeast Polo kinase Cdc5 does not directly phosphorylates Mih1.

We then asked if there were some changes in the pattern of Mih1 phosphorylation between cells that overexpress only *SWE1* or both *SWE1* and *CDC5*, the latter being the condition in which Mih1 becomes essential for mitotic spindle elongation (Fig. 27). *GAL1-SWE1 MIH1-3HA* and *GAL1-SWE1 GAL1-CDC5 MIH1-3HA* cells were inoculated in YEPR, arrested in G1 with α-factor and released in YEPRG. Samples were taken at different time points after release to monitor the kinetics of DNA replication and Mih1 levels and

phosphorylation as in the experiment described above. Both strains behave as in the experiments previously described for what concern the kinetics of DNA replication (Fig. 29C, compare with Fig. 27); in *SWE1* overexpressing cells hyperphosphorylated Mih1 persisted throughout the experiment, conversely 60 minutes after the release, the unphosphorylated forms of Mih1 appeared in cells overexpressing both *SWE1* and *CDC5* (Fig. 29D).

In summary, our data show that the overproduction of the protein kinase Swe1, rather than the overexpression of the Polo kinase Cdc5, changes the phosphorylation pattern of the protein phosphatase Mih1. This is very important because a change in Mih1 phosphorylation changes its activity: in fact, both the fully phosphorylated and the not phosphorylated forms of Mih1 are inactive, so a proper balance of Mih1 phosphorylated forms is important for its activity. We can hypothesize that in *SWE1* overexpressing cells Mih1 is inactive, as it accumulates at a higher molecular weight (Fig. 29D). The overexpression of *CDC5* in these cells restores Mih1 phosphorylation pattern and likely Mih1 activity, allowing mitotic spindle elongation and cell division at least partially. This leads to the hypothesis that active Mih1 is required to allow spindle elongation in *SWE1* overexpressing cells.

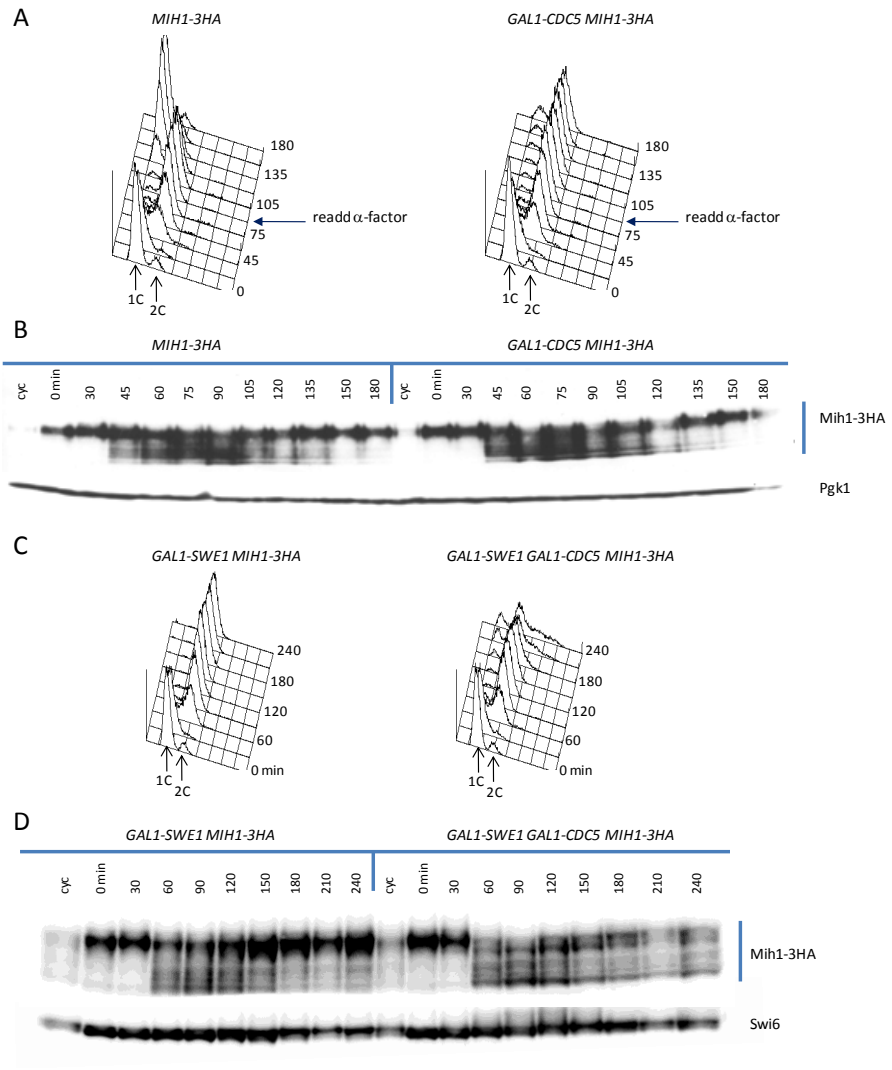

Figure 29: *SWE1,* and not *CDC5,* overexpression changes the balance between phosphorylated and not phosphorylated forms of Mih1. Exponentially growing cultures of *MIH1-3HA* and *GAL1-CDC5 MIH1-3HA* (A and B) or *GAL1-SWE1 MIH1-3HA* and *GAL1-SWE1 GAL1-CDC5 MIH1-3HA* (C and D) cells were arrested in G1 by α-factor in YPR and released from G1 arrest in YEPRG at 25°C (time 0) to induce *SWE1* (A and B) or *SWE1* and *CDC5* (C and D; 2% galactose used) overexpression. At the indicated times after release, cell samples were taken for FACS analysis of DNA content (A and C) and for determining Swe1 levels by western blot analysis (C and D) with anti-HA and for loading control with anti-Pgk1 (B) or anti-Swi6 (D) antibodies.

Discussion

In *S. cerevisiae*, entry and progression into mitosis are controlled by the cyclin-dependent kinase Cdc28 bound to B-type cyclins (Cdk1). Swe1 blocks entry into mitosis through inhibitory phosphorylation on Tyr19 (Y19) residue of the catalytic subunit of the cyclin-dependent kinase Cdk1, Cdc28, and this modification is reversed by the protein phosphatase Mih1. Cdc28 activity is required both for entry into mitosis and for the switch from polar to isotropic bud growth, so when Cdc28 is phosphorylated on Y19 both these events are inhibited. Therefore, Swe1 overexpression from the *GAL1* promoter (*GAL1-SWE1*) is lethal for cells, because it blocks both switch from polar to isotropic bud growth and separation of the SPBs thus causing cells to arrest with elongated buds, undivided nuclei and monopolar spindle (Lim et al., 1996).

Cdc28 is the only known target of the protein kinase Swe1; however, we showed that the introduction of a non phosphorylatable allele of Cdc28, *cdc28-Y19F*, in cells overexpressing *SWE1* is not sufficient to restore proper cell cycle in these cells. In fact, although able to divide, they are delayed in mitotic spindle elongation, nuclear division and progression into mitosis respect to wild type cells. We demonstrated that spindle elongation defects of *GAL1-SWE1 cdc28-Y19F* cells is not due to a defect in sister chromatids cohesion removal, as these cells separate sister chromatids with the same kinetics as wild type cells in galactose containing medium. The

introduction of another *CDC28* allele that could not physically interact with Swe1 (*cdc28-E12K*) in cells overexpressing *SWE1,* is not sufficient to restore proper cell cycle nor proper spindle elongation in these cells, thus it seems likely that the protein kinase Swe1 is involved in mitotic spindle dynamics and that it has other targets apart from Cdc28. We therefore tried to identify these targets using complementary approaches, both by performing a genetic screen and by analyzing putative candidates among factors known to be involved in spindle dynamics. Unfortunately, we could not use *GAL1-SWE1 cdc28-Y19F* strain for the screening because these cells in our genetic background were viable on galactose containing plates. In order to set up the best conditions, we forced SPBs separation in *SWE1* overexpressing cells by deleting the APC regulatory subunit *CDH1*; the lack of Cdh1 allows *GAL1-SWE1* cells to separate the SPBs in galactose containing medium without restoring cell viability. As we were searching for targets inhibited by Swe1 phosphorylation, we assumed that a spontaneous mutation(s) in a residue(s) that is phosphorylated by Swe1 into a non phosphorylatable one could restore mitotic spindle elongation in *GAL1-SWE1 cdh1Δ* cells and therefore cell viability. We analyzed about 5 x 10^6 cells and found about 56 different suppressors. Among these, we characterized 12 recessive suppressors that were effectively able to restore mitotic spindle elongation of *GAL1-SWE1 cdh1Δ* cells in galactose containing medium. Interestingly, the suppression phenotype of all these

mutants was due to the same mutated gene. We are now trying to clone this gene and, once identified, we will set up the best strategy to study the interactions between this gene product and Swe1, and to better characterize the role of the protein kinase Swe1 in mitotic spindle elongation.

As this kind of the genetic screen allows only the identification of proteins inhibited by Swe1, we used an alternative approach to find other Swe1 targets in mitotic spindle elongation process. We searched in literature for microtubule associated proteins or factors that are involved in mitotic spindle dynamics that are somehow related to Swe1. In particular, a proteome chip array identified several proteins phosphorylated by Swe1 (Bodenmiller et al., 2010) among which the MAP Bik1. In order to prove that Bik1 phosphorylation is dependent upon Swe1 activity, we analyzed it in *SWE1* overexpressing cells and in *swe1Δ* cells. Surprisingly, Bik1 phosphorylation decreased in the presence of high Swe1 levels respect to wild type, while it increased in *swe1Δ* cells. As Bik1 phosphorylation is not restored by Cdc28 variants that escape Swe1 inhibition, further analysis will be required to better understand the molecular details of the indirect Swe1 action on Bik1 phosphorylation. Since both the hyperactivation of a phosphatase and the inactivation of a kinase could explain the indirect action of Swe1 in Bik1 phosphorylation, an intriguing hypothesis is that Swe1 could directly activate a protein phosphatase, or inhibit another

protein kinase different from Cdc28. Further experiments are needed to discriminate between these two possibilities.

Preliminary results obtained in our laboratory showed that high levels of the Polo kinase Cdc5 were sufficient to allow mitotic spindle elongation and to partially restore viability of *SWE1* overexpressing cells. Surprisingly the lack of the protein phosphatase Mih1 inhibits Cdc5 action. In fact, the deletion of *MIH1* completely abolished spindle elongation and cell division of *GAL1-SWE1 GAL1-CDC5* cells in galactose containing medium, and therefore cell viability on YEPRG plates. Interestingly, *GAL1-SWE1 GAL1-CDC5 mih1Δ* cells arrested in galactose containing medium with short bipolar spindle, and not with monopolar spindle as *GAL1-SWE1* cells; therefore, the overexpression of *CDC5* is sufficient to allow SPBs separation in *SWE1* overexpressing cells but the protein phosphatase Mih1 is required for these cells to elongate the mitotic spindle. This suggest that high levels of Cdc5 could suppress the lethal effects due to *SWE1* overexpression, in particular the spindle elongation defect, acting through the phosphatase Mih1. As in mammalian cells the homologue of budding yeast Cdc5, phosphorylates the homologue of the phosphatase Mih1 thus promoting CDK activation and entry into mitosis, we asked if the Polo kinase phosphorylates the phosphatase of CDK also in budding yeast. Differently from mammalian cells, in budding yeast the Polo kinase likely does not phosphorylate Mih1, as *CDC5* overexpression and inactivation did not change the balance

between different Mih1 phosphorylation forms. However, we found that *SWE1* overexpression causes the accumulation of fully phosphorylated Mih1, that is not functional, and that *CDC5* overexpression in these cells restores the proper balance between Mih1 phosphorylation forms, and so its functionality. From these data, we could hypothesize a direct kinase activity of Swe1 on Mih1 or on Mih1 regulators. In particular, Swe1 could inactivate the phosphatase of Mih1, Cdc55, or somehow activate CK kinase. Further analysis will be required to better understand the interaction between Swe1, Cdc5 and the protein phosphatase Mih1.

In summary, our data indicate a role of Swe1 in mitotic spindle elongation independently of its action on Cdc28 and put the basis for the identification of Swe1 new target(s).

Materials and Methods

Abbreviations

DAPI: 4,6-Diamidino-2-phenylindole

kDa: kilodalton

DMSO: dimetilsolfossido

SDS: sodium dodecil sulphate

Kphos: phosphate buffer

TRIS: Tris(hydroxymethyl)aminomethane

PEG: Polyethylene glycol

OD: optical density

YNB: yeast nitrogen base

rpm: rounds per minute

bp: base pairs

aa: aminoacid

O/N: overnight

HU: hydroxyurea

MMS: metil methan sulfonate

EDTA: Ethylenediaminetetraacetic acid

TCA: trichloroacetic acid

BFB: bromophenol blue

Bacterial strains

E. coli DH5α^{TM} (F^-, Φ 80dlacZΔM15, ΔlacZTA-argF) U169, deoR, recA1, endA1, hsdR17, (rK^-, mK^+) supE44, λ-, thi-1, gyrA96, relA1 strain was used as a bacterial host for plasmid construction and amplification.

Yeast strains

All yeast strains were derivatives of W303 (MATa or MATalpha, ade2-1, can1-100, trp1-1, leu2-3,112, his311,15, ura3.) or were backcrossed at least three times to W303. The strains used are listed in the table below:

yRF 1	*MATa, ade2-1, trp1-1, can1-100, leu2-3,112, his3-11,15, ura3*
yRF 33	*MATa, swe1::LEU2*
yRF 41	*MATa, dma2::LEU2, dma1::TRP1*
yRF 42	*MATalpha, dma2::LEU2, dma1::TRP1*
yRF 122	*MATa, HSL1myc18::klTRP1*
yRF 124	*MATa, swe1::LEU2, dma2::LEU2, dma1::TRP1*
yRF 135	*MATa, his3::GAL-CDC5-HIS3, ura3::URA3::GAL-SWE1 (single integration)*
yRF 149	*MATa, mih1::LEU2, his3::GAL-CDC5-HIS3, ura3::URA3::GAL-SWE1 (single integration)*
yRF 182	*MATa, SWE1HA3::klURA3*
yRF 324	*MATa, CEN5::tetO2X112::HIS3 (1,4Kb), LEU2::tetR-GFP*
yRF 661	*MATa, dma2::LEU2, dma1::TRP1, SWE1-HA3::klURA3*
yRF 672	*MATa, dma2::HPHMx, dma1::LEU2kl, HSL1myc18::klTRP1*

yRF 690	*MATa, cla4::kanMX4, SWE1HA3::klURA3, cla4-75 in YCplac22*
yRF 693	*MATa, ura3::URA3::GAL-SWE1-3PK (SpHIS) (single integration)*
yRF 702	*MATa, ura3::URA3::GAL-SWE1 (single integration)*
yRF 710	*MAT a, dma1::TRP1, dma2::HPHMx, SWE1-HA3::klURA3,* [YEp351 *BNI5*]
yRF 714	*MAT a, dma1::TRP1, dma2::HPHMx, SWE1HA3::klURA3,* [YEplac181 *(LEU2)*]
yRF 816	*MATa, cdc12-1, SWE1-HA3::klURA3*
yRF 828	*MATa, cdc12-6, SWE1-HA3::klURA3*
yRF 841	*MATa, mih1::LEU2*
yRF 852	*MAT a, dma1::TRP1, dma2::HPHMx, mih1::LEU2*
yRF 862	*MATa, SWE1-HA3::klURA3, hsl1::MET-HSL1::TRP1*
yRF 865	*MATa, SWE1-HA3::klURA3,dma2::HPHMx, dma1::LEU2kl, hsl1::MET-HSL1::TRP1*
yRF 957	*MATa, SWE1-HA3::klURA3,* [YEp96 *CUP1 6HIS-UBI (TRP1 AMP LYS2)*]
yRF 959	*MATa, SWE1-HA3::klURA3, dma2::HPHMx, dma1::LEU2kl,* [YEp96 *CUP1 6HIS-UBI (TRP1 AMP LYS2)*]
yRF 1040	*MATalpha, cdc28F19-TRP1 (at CDC28 locus)*
yRF 1042	*MAT a, dma1::TRP1, dma2::HPHMx, mih1::LEU2, swe1::kanMX4.*
yRF 1045	*MATa, cdc28F19-TRP1 (at CDC28 locus), ura3::URA3::GAL-SWE1 (single integration)*
yRF 1107	*MATa, cdc28F19-TRP1 (at CDC28 locus), CEN5::tetO2X112::HIS3 (1,4Kb), LEU2::tetR-GFP,*
yRF 1135	*MATa, ura3::URA3::GAL-SWE1 (single integration), CEN5::tetO2X112::HIS3 (1,4Kb), LEU2::tetR-GFP , cdc28F19-TRP1 (at CDC28 locus)*
yRF 1138	*MATa,* [YEp96 *CUP1 6HIS-UBI (TRP1 AMP LYS2)*]
yRF 1153	*MATa, ura3::URA3::GAL-SWE1 (single integration), CEN5::tetO2X112::HIS3 (1,4Kb), LEU2::tetR-GFP*

yRF 1200	*MATa, his3::GAL-CDC5-HIS3, MIH1-HA3-KlTRP1*
yRF 1220	*MATa, cdh1::LEU2, ura3::URA3::GAL-SWE1 (single integration)*
yRF 1280	*MATa, MIH1-HA3-KlTRP1*
yRF 1324	*MATa, ura3::URA3::GAL-SWE1 (single integration), cdc28E12K*
yRF 1460	*MATalpha, ura3::GAL-SWE1-3PK (SpHIS) (single integration), lys2::K.l.TRP1, cdh1::nat*
yRF 1461	*MATa, ura3::GAL-SWE1-3PK (SpHIS) (single integration), cdh1::nat*
yRF 1505	*MATa, ade2-1, ura3::URA3::GAL-SWE1-3PK (SpHIS) (single integration), his3::GAL-CDC5-HIS3*
yRF 1604	*MATa, ura3::URA3::GAL-SWE1 (single integration), MIH1-HA3-KlTRP1*
yRF 1606	*MATa, ura3::URA3::GAL-SWE1 (single integration), his3::GAL-CDC5-HIS3, MIH1-HA3-KlTRP1*

Plasmids

RF 1	*MET-HSL1;* N-terminal fragment of *HSL1* in *c2436*
SP 173	YEplac181
SP 211	*cla4-75 in YCplac22*
SP 605	*YEp96 CUP1 6HIS-UBI (TRP1 AMP LYS2)*
SP 629	YEp351 *BNI5*

Growth media

All media were sterilized with autoclave and stored at room temperature.

Media for *E. coli*

LD:

1% Bactotryptone

0.5% yeast extract

0,5% NaCl (pH 7,25)

LD+ampicillin was obtained adding 2,5g/L of ampicillin to LD medium.

Agar to 1% was added to obtain solid medium

Media for *S. cerevisiae*:

YEP (Yeast Extract Peptone)

Yeast extract 1%

Bactopeptone 2%

Adenine 50mg/l

Just before use, YEP was supplemented with the appropriate carbon source: 2% glucose (YEPD), 2% raffinose (YEPR), 2% raffinose and 1% galactose (YEPRG). Were indicated, for YEPRG 2% glucose was added. Unless differently stated, hydroxyurea was used at 200mM to obtain YEP+HU. Agar to 2% was added to obtain solid medium.

Synthetic medium

Yeast Nitrogen Base (YNB) 0,7% without aminoacids

Just before use, synthetic medium was supplemented with the appropriate carbon source (as YEP) and with 25mg/l of the appropriate aminoacids and nitrogen base. Agar to 2% was added to obtain solid medium.

Sporulation medium

$CH3COONa^{+}$ $3H_2O$ 1.36%

KCl 0.19%

$MgSO4^{2-}$ $7H_2O$ 0.0035%

NaCl 0.12%

pH 7.0

2% agar was added to obtain solid medium

Buffers and solutions

SDS-PAGE running buffer 5X: Glycine 2M, TRIS 0.25M, SDS 0.02M, pH 8.3

TBS 10X: 1.5M NaCl, 0.5M TRIS-HCl, pH 8

TE: 10mM TRIS-HCl, 1mM EDTA, pH 7.4

TAE: 0.04M Tris acetate, 0.001M EDTA

Laemli buffer 3X: TRIS 0.187M, SDS 6%, 2-mercaptoethanol 15%, glycine 30%, BFB 0.003%

BSA/PBS: BSA 1%, K_2HPO_4 0.04M, KH_2PO_4 0.01M, NaCl 0.15M

Genetic manipulations

Standard techniques were used for genetic manipulations (Maniatis *et al.*, 1992; Sherman, 1991). Gene deletions were generated by one-step gene replacement (Wach *et al.*, 1994). One-step tagging techniques were used to create 3HA-, 3PK- and 18MYC- tagged variants of Swe1, Mih1 and Hsl1 (Janke *et al.*, 2004). All gene replacements and tagging were controlled by PCR based methods or Southern blot analysis.

Generation of diploid strains and sporulation

Diploid strains were generated by crossing the appropriate haploid strains on YEPD plates. After 24 hours, diploids were transferred to VB plates to induce sporulation, and incubated for 2 days at 25°C. After zymolase digestion, tetrads were dissected with a micromanipulator on the appropriate plates.

Synchronization with α-factor

MATa strains were inoculated in the appropriate medium to reach a concentration of 5 x 10^6 cells/ml. α-factor was added to a final concentration of 2μg/ml. when more than 95% of cells arrested as unbudded (about 2 hours after α-factor adding), the pheromone was removed and cells were washed once with opportune fresh medium and resuspended and incubated in the opportune fresh medium. Unless differently stated, synchronization were performed at 25°C

and galactose, when requested, was added 15 minutes before α-factor release.

Yeast transformation

Cells were inoculated in the opportune medium an incubated overnight at 25 or 30°C, allowing them to reach the stationary phase. Cell cultures were diluted and incubated again at 25 or 30°C for at least two hours, until they reached a concentration of about 1 x 10^6 cells/ml. 50ml of the culture were than centrifuged for 2 minutes at 3500 rpmand pellet was washed with 1ml of 1M LiAc to eliminate the growth medium. The pellet was then resuspended in about 200μl of 1M LiAC (depending on the amount of cells). For each transformation we used: 12μl cells in LiAc v/v, 4μl carrier DNA (SS DNA), 45μl 50% PEG , 1-5μl DNA. After mixing, the tubes were incubated at room temperature for 30-60 minutes. Than, 6ml of 60% glycerol were added to each tube, followed by mixing and incubation for 30-60 minutes at room temperature. After a 5-15 minutes heat shock at 42°C (the time of the heat shock depends on the strain used) cells were plated on the opportune selective medium.

Drop test

Cell cultures were grown overnight at the appropriate temperature until they reached stationary phase. They were diluted to 1.25 x10^6, 1.25 x 10^5, 1.25 x 10^4 and 1.25 x 10^3 cells/ml. For each dilution, 5ml of

cell suspension were spotted on opportune plates and incubated at the appropriate temperatures.

FACS analysis

$5x10^6$ cells were collected each time point by centrifugation and resuspended in 1ml of 70% ethanol, prior to 1 hour of incubation at room temperature. Cells were than washed once with 50mM TRIS pH 7.5; the pellets were resuspended in 0.5ml of 50mM TRIS pH7.5 and 50µl of 10mg/ml RNAse was added to each sample. After incubation overnight al 37°C, cells were collected by centrifugation, pellets were resuspended in 0.5 ml of 5mg/ml pepsin (freshly dissolved in 55mM HCl) and incubated at 37°C for 30 minutes. Cells were than washed once with FACS buffer (200mM TRIS pH7.5, 211mM NaCl, 78mM $MgCl_2$) and resuspended in 0.5ml of FACS buffer containing 55µl of 0.5mg/ml propidium iodide. Samples were finally analyzed with a FACS-Scan.

In situ immunofluorescence and fluorescence microscopy

Cells were fixed in 1ml of IF buffer (0.1M Kphos pH6.4, 0.5mM $MgCl_2$) containing 3.7% formaldehide at 4°C overnight (for anti-Cdc11 and anti-tubuline staining) or 15-60 minutes (for anti-HA and anti-myc staining). Samples were than washed three times with IF buffer and once with IF buffer containing 1.2M sorbitol. Cells were spheroplasted by incubating 10-30 minutes in 0.2ml of

spheroplasting solution (1.2M sorbithol, 0.1M Kphos pH7.4, 0.5mM $MgCl_2$) containing 5µl of 10mg/ml 100T zymolase and 0.2% β–mercaptoethanol (only for overnight incubation). Spheroplasts were checked microscopically by mixing cells with an equal amount of 10% SDS. Spheroplasts were than washed one time in IF buffer containing 1.2M sorbitol and resuspended in 0.2ml of the same solution.

A 30 well slide was coated with 0.1% polylysine; a drop of cells reasonably cloudy (not too dense) was added to each well and, after 5-10 minutes of incubation at room temperature, was removed. The slide was put into a MeOH bath at -20°C for 6 minutes, then into an acetone bath at -20°C for 30 seconds. The slide was then removed from acetone bath and let dry.

Primary antibody was added to each well and the slide was incubated at 4°C in the dark from 2 hours to overnight. Than, the primary antibody was aspirated of and each well was washed three times with BSA/PBS, followed by the addition of the appropriate secondary antibody. Slides were incubated at 4°C in the dark for 2 hours, than the secondary antibody was aspirated off and each well was washed three times with BSA/PBS. For DAPI staining, DAPI was diluted in ANTIFADE (0.1%phenylenediamine, 10% PBS pH8 in glycerol) to a final concentration of 0.05 mg/ml and added to each well. A coverslip was placed over and sealed using nail enamel. Slides were stored at -20°C in the dark until use. Visualization of septin rings was performed

using anti-Cdc11 polyclonal antibodies (1:200, sc-7170 Santa Cruz) followed by indirect immuno-fluorescence with Alexa Fluor 488-conjugated anti-rabbit antibody (1:100, Invitrogen). *In situ* immunofluorescence of myc-tagged proteins was done with the 9E10 mAb, whereas that of HA-tagged proteins was done with the 16B12 mAb (Babco), followed by indirect immunofluorescence using CY3-conjugated goat anti–mouse antibody (1:1,000; GE Healthcare) and tertiary donkey anti-goat CY3-conjugated antibodies (1:500, Santa Cruz) to visualize Swe1. To detect spindle formation and elongation, α-tubulin immunostaining was performed with the YOL34 monoclonal antibody (Serotec) followed by indirect immunofluorescence using rhodamine-conjugated anti-rat Ab (1:500 Pierce Chemical Co). Digital images were taken with a Leica DC350F charge-coupled device camera mounted on a Nikon Eclipse 600 and controlled by the Leica FW4000 software or with the MetaMorph imaging system software on a fluorescent microscope (Eclipse 90i; Nikon), equipped with a charge-coupled device camera (Coolsnap, Photometrics) with an oil 100X 0,5-1.3 PlanFluor oil objective (Nikon).

Protein extracts and analysis

For most experiments total protein extracts were prepared by TCA precipitation. Briefly, cells were washed with 1ml of 20% TCA and resuspended in about 200μl of 20% TCA. After addition of an equal amount of glass beads, cells were disrupted by vortexing for 10 min.

Glass beads were washed once with 400 μl of 5% TCA and the resulting extract was centrifuged for 10 min at 3000 rpm. The pellet was resuspended in 100μl of Laemmli buffer 2X, neutralized by adding 50μl of 1M TRIS base, boiled for 3 min, and finally clarified by centrifugation for 5 minutes at 13000 rpm. For the phosphatase treatment in Figure 12F protein extracts were made in the following breaking buffer: 50mM Hepes, 150mM NaCl, 20% glycerol, 5mM EDTA, 60mM β-glycerophosphate and 1mM Na ortovanadate, supplemented with protease inhibitors (Complete Boheringer). Swe1-3HA was immunoprecipitated from 1μg of cleared extracts upon incubation with anti-HA antibodies for 1 hour at 4°C followed by incubation with protein A-sepharose for 1 hour at 4°C. The slurry was washed three times in PBS, resuspended in 60μl of phosphatase buffer containing 20 units of lambda phosphatase (Biolabs) and2mM $MnCl_2$ and incubated 30 minutes at 30°C before loading.

For Western blot analysis, proteins were transferred to Protran membranes (Schleicher and Schuell) were probed with monoclonal anti-HA (1:3000), anti-PK (1:1000), anti-Bik1 (1:5000), anti-Swi6 (1:100000) and anti-Pgk1 antibodies (1:40000). Secondary antibodies were purchased from Amersham and proteins were detected by an enhanced chemioluminescence system according to the manufacturer.

Detection of ubiquitin conjugates *in vivo*

For the experiments involving the expression of 6xHIS-ubiquitin, cells were grown to log phase at 25°C in selective medium containing 0.17% YNB without ammonium sulfate, 0.1% L-proline and 2% glucose, followed by dilution to 8x106 cells/ml in the same medium containing also 0.003% SDS, as described (Liu et al., 2007). After further incubation for 3 hours, 6xHIS-Ubiquitin expression was induced by addition of 250μM $CuSO_4$ to half of each culture, and 75μM MG-132 (C2211, supplied by Sigma-Aldrich) was added 30 minutes later to all cultures. After 3 further hours, yeast cells were then washed in water, and protein extracts were prepared under denaturing conditions as described (Yaffe and Schatz, 1984), TCA precipitates were resuspended in buffer A (6M guanidium, 100mM NaPO4 pH 8, 10mM Tris-HCl pH 8) and the debris removed by centrifugation. Ni-pull down was performed as described (Ulrich and Davies, 2009). Briefly, lysates were incubated overnight at room temperature with Ni-NTA agarose beads (QIAGEN), in the presence of 15mM imidazole and 0.05% Tween 20. Beads were then washed twice with buffer A plus 0.05% Tween 20 and 4 times with buffer C (8M urea, 100mM $NaPO_4$ pH 6.3, 10mM Tris-HCl pH 6.3, 0.05% Tween 20). Bound proteins were eluted by addition of 30μl of HU buffer (8M urea, 200mM Tris-HCl pH 6.8, 1mM EDTA, 5% SDS, 0.1% BFB, 1.5% DTT), and then subjected to SDS-PAGE followed by western blot analysis with anti-HA antibody.

References

References

Adams IR and Kilmartin JV. **Localization of core spindle pole body (SPB) components during SPB duplication in S*accharomyces cerevisiae.*** J Cell Biol. 1999 May 17;145(4):809-23.

Al-Hakim A, Escribano-Diaz C, Landry MC, O'Donnell L, Panier S, Szilard RK and Durocher D. **The ubiquitous role of ubiquitin in the DNA damage response.** DNA Repair (Amst). 2010 Dec 10;9(12):1229-40.

Amon A, Surana U, Muroff I and Nasmyth K. **Regulation of p34CDC28 tyrosine phosphorylation is not required for entry into mitosis in *S. cerevisiae*.** Nature. 1992 Jan 23;355(6358):368-71.

Asano S, Park JE, Sakchaisri K, Yu LR, Song S, Supavilai P, Veenstra TD and Lee KS. **Concerted mechanism of Swe1/Wee1 regulation by multiple kinases in budding yeast.** The EMBO journal, 2005 Jun 15;24(12):2194-204.

Ayad NG, Rankin S, Murakami M, Jebanathirajah J, Gygi S and Kirschner MW. **Tome-1, a trigger of mitotic entry, is degraded during G1 via the APC.** Cell, 2003 Apr 4;113(1):101-13.

Barral Y, Parra M, Bidlingmaier S and Snyder M. **Nim1-related kinases coordinate cell cycle progression with the organization of the peripheral cytoskeleton in yeast.** Genes Dev. 1999 Jan 15;13(2):176-87.

Barral Y, Mermall V, Mooseker MS and Snyder M. **Compartmentalization of the cell cortex by septins is required for maintenance of cell polarity in yeast.** Molecular cell, 2000 May;5(5):841-51.

Bieganowski P, Shilinski K, Tsichlis PN and Brenner C. **Cdc123 and checkpoint forkhead associated with RING proteins control the cell cycle by controlling eIF2gamma abundance.** The journal of biological chemistry, 2004 Oct 22;279(43):44656-66.

Bodenmiller B, Wanka S, Kraft C, Urban J, Campbell D, Pedrioli PG, Gerrits B, Picotti P, Lam H, Vitek O, Brusniak MY, Roschitzki B, Zhang C, Shokat KM, Schlapbach R, Colman-Lerner A, Nolan GP, Nesvizhskii AI, Peter M, Loewith R, von Mering C and Aebersold R. **Phosphoproteomic analysis reveals interconnected system-wide responses to perturbations of kinases and phosphatases in yeast.** Sci Signal. 2010 Dec 21;3(153):rs4.

Booher RN, Deshaies RJ and Kirschner MW. **Properties of Saccharomyces cerevisiae wee1 and its differential regulation of p34CDC28 in response to G1 and G2 cyclins.** EMBO J. 1993 Sep;12(9):3417-26.

Brooks L 3rd, Heimsath EG Jr, Loring GL and Brenner C. **FHA-RING ubiquitin ligases in cell division cycle control.** Cell Mol Life Sci. 2008 Nov;65(21):3458-66.

Callis J and Ling R. **Preparation, characterization, and use of tagged ubiquitins.** Methods Enzymol. 2005;399:51-64.

Cao L, Yu W, Wu Y and Yu L. **The evolution, complex structure and function of septin proteins.** Cellular and molecular life science, 2009 Oct;66(20):3309-23.

Caudron F and Barral Y. **Septins and the lateral compartmentalization of eukaryotic membranes.** Developmental cell. 2009 Apr;16(4):493-506.

Caviston JP, Longtine M, Pringle JR and Bi E. **The role of Cdc42p GTPase-activating proteins in assembly of the septin ring in yeast.** Molecular biology of the cell, 2003 Oct;14(10):4051-66.

Chaturvedi P, Sudakin V, Bobiak ML, Fisher PW, Mattern MR, Jablonski SA, Hurle MR, Zhu Y, Yen TJ and Zhou BB. **Chfr regulates a mitotic stress pathway through its RING-finger domain with ubiquitin ligase activity.** Cancer research, 2002 Mar 15;62(6):1797-801.

Cid VJ, Shulewitz MJ, McDonald KL and Thorner J **Dynamic localization of the Swe1 regulator Hsl7 during the *Saccharomyces cerevisiae* cell cycle.** 2001 Jun;12(6):1645-69.

Ciliberto A, Novak B and Tyson JJ. **Mathematical model of the morphogenesis checkpoint in budding yeast.** J Cell Biol. 2003 Dec 22;163(6):1243-54.

Cooper JA and Kiehart DP. **Septins may form a ubiquitous family of cytoskeletal filaments. The Journal of cell biology,** 1996 Sep;134(6):1345-8.

Crasta K, Huang P, Morgan G, Winey M and Surana U. **Cdk1 regulates centrosome separation by restraining proteolysis of microtubule-associated proteins.** EMBO J 2006; 25:1551-63.

Crasta K, Lim HH, Giddings TH Jr, Winey M and Surana U. **Inactivation of Cdh1 by synergistic action of Cdk1 and polo kinase is necessary for proper assembly of the mitotic spindle.** Nat Cell Biol 2008; 10:665-75.

Crasta K, Lim HH, Zhang T, Nirantar S and Surana U. **Consorting kinases, end of destruction and birth of a spindle. Cell Cycle.** 2008 Oct;7(19):2960-6. Epub 2008 Oct 13.

de Gramont A and Cohen-Fix O. **The many phases of anaphase.** Trends Biochem Sci. 2005 Oct;30(10):559-68.

DeMarini DJ, Adams AE, Fares H, De Virgilio C, Valle G, Chuang JS and Pringle JR. **A septin-based hierarchy of proteins required for localized deposition of chitin in the *Saccharomyces cerevisiae* cell wall. The Journal of cell biology,** 1997 Oct 6;139(1):75-93.

Deshaies RJ and Joazeiro CA. **RING domain E3 ubiquitin ligases.** Annu Rev Biochem. 2009;78:399-434.

De Virgilio C, DeMarini DJ and Pringle JR. ***SPR28*, a sixth member of the septin gene family in *Saccharomyces cerevisiae* that is**

expressed specifically in sporulating cells. Microbiology. 1996 Oct;142 (Pt 10):2897-905.

De Wulf P, Montani F and Visintin R. **Protein phosphatases take the mitotic stage.** Curr Opin Cell Biol. 2009 Dec;21(6):806-15.

Dobbelaere J, Gentry MS, Hallberg RL and Barral Y. **Phosphorylation-dependent regulation of septin dynamics during the cell cycle.** Developmental cell, 2003 Mar;4(3):345-57.

Driscoll J and Goldberg AL. **The proteasome (multicatalytic protease) is a component of the 1500-kDa proteolytic complex which degrades ubiquitin-conjugated proteins.** J Biol Chem. 1990 Mar 25;265(9):4789-92.

Durocher D and Jackson SP. **The FHA domain.** FEBS Lett. 2002 Feb 20;513(1):58-66.

Elledge SJ, Winston J and Harper JW. **A question of balance: the role of cyclin-kinase inhibitors in development and tumorigenesis.** Trends in cell biology, 1996 Oct;6(10):388-92.

Enserink JM, Smolka MB, Zhou H and Kolodner RD. **Checkpoint proteins control morphogenetic events during DNA replication stress in *Saccharomyces cerevisiae*. The Journal of cell biology,** 2006 Dec 4;175(5):729-41.

Fares H, Goetsch L and Pringle JR. **Identification of a developmentally regulated septin and involvement of the septins in spore formation in *Saccharomyces cerevisiae*.** J Cell Biol. 1996 Feb;132(3):399-411.

Finley D, Ulrich HD, Sommer T, Kaiser P. **The Ubiquitin-Proteasome System of *Saccharomyces cerevisiae.*** Genetics. 2012 Oct;192(2):319-60.

Fitch I, Dahmann C, Surana U, Amon A, Nasmyth K, Goetsch L, Byers B and Futcher B. **Characterization of four B-type cyclin genes of the**

budding yeast *Saccharomyces cerevisiae*. Mol Biol Cell. 1992 Jul;3(7):805-18

Fraschini R, Bilotta D, Lucchini G and Piatti S. **Functional characterization of Dma1 and Dma2, the budding yeast homologues of *Schizosaccharomyces pombe* Dma1 and human Chfr.** Molecular biology of the cell, 2004 Aug;15(8):3796-810.

Fraschini R, Venturetti M, Chiroli E and Piatti S. **The spindle position checkpoint: how to deal with spindle misalignment during asymmetric cell division in budding yeast.** Biochemical society transactions, 2008 Jun;36(Pt 3):416-20.

Gaczynska M and Osmulski PA. **Small-molecule inhibitors of proteasome activity.** Methods Mol Biol. 2005;301:3-22.

Gheber L, Kuo SC and Hoyt MA. **Motile properties of the kinesin-related Cin8p spindle motor extracted from *Saccharomyces cerevisiae* cells.** J Biol Chem 1999; 274:9564-72.

Gladfelter AS, Kozubowski L, Zyla TR and Lew DJ. **Interplay between septin organization, cell cycle and cell shape in yeast. Journal of cell science**, 2005 Apr 15;118(Pt 8):1617-28.

Guertin DA, Venkatram S, Gould KL and McCollum D. **Dma1 prevents mitotic exit and cytokinesis by inhibiting the septation initiation network (SIN).** Dev Cell. 2002 Dec;3(6):779-90.

Harvey SL, Charlet A, Haas W, Gygi SP and Kellogg DR. **Cdk1-dependent regulation of the mitotic inhibitor Wee1.** Cell, 2005 Aug 12;122(3):407-20.

Hartwell LH. **Genetic control of cell division cycle in yeast. IV. Genes controlling bud emergence and cytokinesis.** Experimental cell research, 1971 Dec;69(2):265-76.

Hartwell LH and Weinert TA. **Checkpoints: controls that ensure the order of cell cycle events.** Science. 1989 Nov 3;246(4930):629-34.

Higuchi T, Uhlmann F. **Stabilization of microtubule dynamics at anaphase onset promotes chromosome segregation.** Nature. 2005 Jan 13;433(7022):171-6.

Hofmann K and Bucher P. **The FHA domain: a putative nuclear signalling domain found in protein kinases and transcription factors.** Trends Biochem Sci. 1995 Sep;20(9):347-9.

Huen MS, Grant R, Manke I, Minn K, Yu X, Yaffe MB and Chen J. **RNF8 transduces the DNA-damage signal via histone ubiquitylation and checkpoint protein assembly.** Cell. 2007 Nov 30;131(5):901-14.

Huang S and Ingber DE. **The structural and mechanical complexity of cell-growth control.** Nature cell biology, 1999 Sep;1(5):E131-8.

Jacobs CW, Adams AE, Szaniszlo PJ and Pringle JR. Functions of microtubules in the *Saccharomyces cerevisiae* cell cycle. J Cell Biol. 1988 Oct;107(4):1409-26.

Janke C, Magiera MM, Rathfelder N, Taxis C, Reber S, Maekawa H, Moreno-Borchart A, Doenges G, Schwob E, Schiebel E and Knop M. **A versatile toolbox for PCR-based tagging of yeast genes: new fluorescent proteins, more markers and promoter substitution cassettes.** Yeast. 2004 Aug;21(11):947-62.

Jaspersen SL and Winey M. The budding yeast spindle pole body: structure, duplication, and function. Annu Rev Cell Dev Biol. 2004;20:1-28.

Johnson ES and Blobel G. Cell cycle-regulated attachment of the ubiquitin-related protein SUMO to the yeast septins. The Journal of cell biology, 1999 Nov 29;147(5):981-94.

Kadota J, Yamamoto T, Yoshiuchi S, Bi E and Tanaka K. **Septin ring assembly requires concerted action of polarisome components, a PAK kinase Cla4p, and the actin cytoskeleton in *Saccharomyces cerevisiae*.** Molecular biology of the cell, 2004 Dec;15(12):5329-45.

Kaiser P, Sia RA, Bardes EG, Lew DJ and Reed SI. **Cdc34 and the F-box protein Met30 are required for degradation of the Cdk-inhibitory kinase Swe1.** Genes & development, 1998 Aug 15;12(16):2587-97.

Keaton MA and Lew DJ**, Eavesdropping on the cytoskeleton: progress and controversy in the yeast morphogenesis checkpoint,** Current Opinion in Microbiology, 2006 Dec;9(6):540-6.

Keaton MA, Szkotnicki L, Marquitz AR, Harrison J, Zyla TR and Lew DJ. **Nucleocytoplasmic trafficking of G2/M regulators in yeast.** Mol Biol Cell. 2008 Sep;19(9):4006-18.

Khmelinskii A, Lawrence C, Roostalu J and Schiebel E. **Cdc14-regulated midzone assembly controls anaphase B.** J Cell Biol. 2007 Jun 18;177(6):981-93.

Khmelinskii A and Schiebel E. **Assembling the spindle midzone in the right place at the right time.** Cell Cycle. 2008 Feb 1;7(3):283-6.

Khmelinskii A, Roostalu J, Roque H, Antony C and Schiebel E. **Phosphorylation-dependent protein interactions at the spindle midzone mediate cell cycle regulation of spindle elongation.** Dev Cell. 2009 Aug;17(2):244-56.

Kinoshita M. **The septins.** Genome Biol. 2003;4(11):236.

Kolas NK, Chapman JR, Nakada S, Ylanko J, Chahwan R, Sweeney FD, Panier S, Mendez M, Wildenhain J, Thomson TM, Pelletier L, Jackson SP and Durocher D. **Orchestration of the DNA-damage response by the RNF8 ubiquitin ligase.** Science, 2007 Dec 7;318(5856):1637-40.

Kops GJ, Weaver BA and Cleveland DW. **On the road to cancer: aneuploidy and the mitotic checkpoint.** Nat Rev Cancer. 2005 Oct;5(10):773-85.

Kusch J, Meyer A, Snyder MP and Barral Y. **Microtubule capture by the cleavage apparatus is required for proper spindle positioning in yeast.** Genes & Development, 2002 Jul 1;16(13):1627-39.

Lee PR, Song S, Ro HS, Park CJ, Lippincott J, Li R, Pringle JR, De Virgilio C, Longtine MS and Lee KS. **Bni5p, a septin-interacting protein, is required for normal septin function and cytokinesis in Saccharomyces cerevisiae.** Mol Cell Biol. 2002 Oct;22(19):6906-20.

Lee KS, Asano S, Park JE, Sakchaisri K, Erikson RL. **Monitoring the cell cycle by multi-kinase-dependent regulation of Swe1/Wee1 in budding yeast.** Cell Cycle. 2005 Oct;4(10):1346-9.

Lew DJ. **The morphogenesis checkpoint: how yeast cells watch their figures.** Current opinion in cell biology, 2003 Dec;15(6):648-53.

Lim HH, Goh PY and Surana U. **Spindle pole body separation in *Saccharomyces cerevisiae* requires dephosphorylation of the tyrosine 19 residue of Cdc28.** Mol Cell Biol. 1996 Nov;16(11):6385-97.

Liu C, Apodaca J, Davis LE and Rao H. **Proteasome inhibition in wild-type yeast Saccharomyces cerevisiae cells.**Biotechniques. 2007 Feb;42(2):158, 160, 162.

Liu H and Wang Y. **The function and regulation of budding yeast Swe1 in response to interrupted DNA synthesis.** Molecular biology of the cell, 2006 Jun;17(6):2746-56.

Lobjois V, Jullien D, Bouché JP and Ducommun B. **The polo-like kinase 1 regulates CDC25B-dependent mitosis entry.** Biochim Biophys Acta. 2009 Mar;1793(3):462-8.

Lobjois V, Froment C, Braud E, Grimal F, Burlet-Schiltz O, Ducommun B and Bouche JP. **Study of the docking-dependent PLK1 phosphorylation of the CDC25B phosphatase.** Biochem Biophys Res Commun. 2011 Jun 24;410(1):87-90.

Longtine MS, Theesfeld CL, McMillan JN, Weaver E, Pringle JR and Lew DJ. **Septin-dependent assembly of a cell cycle-regulatory module in *Saccharomyces cerevisiae.*** Molecular and cellular biology, 2000 Jun;20(11):4049-61.

Longtine MS and Bi E. **Regulation of septin organization and function in yeast.** Trends in cell biology, 2003 Aug;13(8):403-9.

Lorick KL, Jensen JP, Fang S, Ong AM, Hatakeyama S and Weissman AM. **RING fingers mediate ubiquitin-conjugating enzyme (E2)-dependent ubiquitination.** Proceeding of the national academy of science of the United States of America, 1999 Sep 28;96(20):11364-9.

Loring GL, Christensen KC, Gerber SA and Brenner C. **Yeast Chfr homologs retard cell cycle at G1 and G2/M via Ubc4 and Ubc13/Mms2-dependent ubiquitination.** Cell cycle, 2008 Jan 1;7(1):96-105.

Maniatis T, Fritsch, and Sambrook J. (1992). **Molecular cloning: a laboratory manual.** Cold Spring Harbor Laboratory Press, Cold Spring Harbor Laboratory, NY.

Martinez JS, Jeong DE, Choi E, Billings BM and Hall MC. **Acm1 is a negative regulator of the Cdh1-dependent anaphase-promoting complex/cyclosome in budding yeast.** Mol Cell Biol 2006; 26:9162-76.

Masselot M and Surdin-Kerjan Y. **Methionine biosynthesis in *Saccharomyces cerevisiae.* II. Gene-enzyme relationships in the sulfate assimilation pathway.** Mol Gen Genet. 1977 Jul 7;154(1):23-30.

Mathias N, Johnson SL, Winey M, Adams AE, Goetsch L, Pringle JR, Byers B and Goebl MG. **Cdc53p acts in concert with Cdc4p and Cdc34p to control the G1-to-S-phase transition and identifies a conserved family of proteins.** Mol Cell Biol. 1996 Dec;16(12):6634-43.

McMillan JN, Sia RA and Lew DJ. **A morphogenesis checkpoint monitors the actin cytoskeleton in yeast. The Journal of cell biology,** 1998 Sep 21;142(6):1487-99.

McMillan JN, Sia RA, and Lew DJ. **Phosphorylation-independent inhibition of Cdc28p by the tyrosine kinase Swe1p in the morphogenesis checkpoint.** Mol Cell Biol. 1999 Sep;19(9):5981-90.

McMillan JN, Longtine MS, Sia RA, Theesfeld CL, Bardes ES, Pringle JR and Lew DJ. **The morphogenesis checkpoint in *Saccharomyces cerevisiae*: cell cycle control of Swe1p degradation by Hsl1p and Hsl7p.** Molecular and cellular biology, 1999 Oct;19(10):6929-39.

McMillan JN, Theesfeld CL, Harrison JC, Bardes ES, Lew DJ. **Determinants of Swe1p degradation in Saccharomyces cerevisiae.** Molecular biology of the cell, 2002 Oct;13(10):3560-75.

Merlini L, Fraschini R, Boettcher B, Barral Y, Lucchini G, Piatti S. **Budding yeast dma proteins control septin dynamics and the spindle position checkpoint by promoting the recruitment of the Elm1 kinase to the bud neck.** PLoS Genet. 2012;8(4):e1002670.

Michaelis C, Ciosk R, Nasmyth K. **Cohesins: chromosomal proteins that prevent premature separation of sister chromatids.** Cell. 1997 Oct 3;91(1):35-45

Mortensen EM, McDonald H, Yates J 3rd, Kellogg DR. **Cell cycle-dependent assembly of a Gin4-septin complex.** Mol Biol Cell. 2002 Jun;13(6):2091-105.

Murone M and Simanis V. **The fission yeast dma1 gene is a component of the spindle assembly checkpoint, required to prevent septum formation and premature exit from mitosis if spindle function is compromised.** The EMBO journal, 1996 Dec 2;15(23):6605-16.

Pereira G and Schiebel E. **Separase regulates INCENP-Aurora B anaphase spindle function through Cdc14.** Science. 2003 Dec 19;302(5653):2120-4. Epub 2003 Nov 6.

Plans V, Guerra-Rebollo M and Thomson TM. **Regulation of mitotic exit by the RNF8 ubiquitin ligase.** Oncogene. 2008 Feb 28;27(10):1355-65. Epub 2007 Sep 3.

Roof DM, Meluh PB and Rose MD. **Kinesin-related proteins required for assembly of the mitotic spindle.** J Cell Biol. 1992 Jul;118(1):95-108.

Roostalu J, Schiebel E and Khmelinskii A. **Cell cycle control of spindle elongation.** Cell Cycle. 2010 Mar 15;9(6):1084-90. Epub 2010 Mar 15.

Rosenkranz HS and Levy JA. **Hydroxyurea: a specific inhibitor of deoxyribonucleic acid synthesis.** Biochim Biophys Acta. 1965 Jan 11;95:181-3.

Russell P, Moreno S and Reed SI. **Conservation of mitotic controls in fission and budding yeasts.** Cell. 1989 Apr 21;57(2):295-303.

Sakchaisri K, Asano S, Yu LR, Shulewitz MJ, Park CJ, Park JE, Cho YW, Veenstra TD, Thorner J and Lee KS. **Coupling morphogenesis to mitotic entry.** Proceeding of the national academy of science of the United States of America, 2004 Mar 23;101(12):4124-9.

Sanders SL and Herskowitz I. **The Bud4 protein of yeast, required for axial budding, is localized to the mother/bud neck in a cell-cycle related manner. The Journal of cell biology,** 1996 Jul;134(2):413-27.

Schuyler SC, Liu JY and Pellman D. **The molecular function of Ase1p: evidence for a MAP-dependent midzone-specific spindle matrix. Microtubule-associated proteins.** J Cell Biol. 2003 Feb 17;160(4):517-28.

Scolnick DM and Halazonetis TD. **Chfr defines a mitotic stress checkpoint that delays entry into metaphase.** Nature, 2000 Jul 27;406(6794):430-5.

Shulewitz MJ, Inouye CJ and Thorner J. **Hsl7 Localizes to a Septin Ring and Serves as an Adapter in a Regulatory Pathway That Relieves**

Tyrosine Phosphorylation of Cdc28 Protein Kinase in *Saccharomyces cerevisiae.* Molecular and cellular biology, 1999 Oct; 19(10):7123-37.

Sia RA, Herald HA and Lew DJ. **Cdc28 tyrosine phosphorylation and the morphogenesis checkpoint in budding yeast.** Molecular biology of the cell, 1996 Nov;7(11):1657-66.

Sia RA, Bardes ES and Lew DJ. **Control of Swe1p degradation by the morphogenesis checkpoint.** The EMBO journal, 1998 Nov 16;17(22):6678-88.

Smolka MB, Chen SH, Maddox PS, Enserink JM, Albuquerque CP, Wei XX, Desai A, Kolodner RD and Zhou H. **An FHA domain-mediated protein interaction network of Rad53 reveals its role in polarized cell growth. The Journal of cell biology,** 2006 Dec 4;175(5):743-53.

Stegmeier F, Visintin R and Amon A. **Separase, polo kinase, the kinetochore protein Slk19, and Spo12 function in a network that controls Cdc14 localization during early anaphase.** Cell. 2002 Jan 25;108(2):207-20.

Tang CS, Reed SI. **Phosphorylation of the septin Cdc3 in G1 by the Cdc28 kinase is essential for efficient septin ring disassembly.** Cell Cycle. 2002 Jan;1(1):42-9.

Theesfeld CL, Zyla TR, Bardes EG and Lew DJ. **A monitor for bud emergence in the yeast morphogenesis checkpoint.** Mol Biol Cell. 2003 Aug;14(8):3280-91.

Trimble WS. **Septins: a highly conserved family of membrane-associated GTPases with functions in cell division and beyond.** The journal of membrane biology, 1999 May 15;169(2):75-81.

Tuttle RL, Bothos J, Summers MK, Luca FC and Halazonetis TD. **Defective in mitotic arrest 1/ring finger 8 is a checkpoint protein that antagonizes the human mitotic exit network.** Mol Cancer Res. 2007 Dec;5(12):1304-11.

Ulrich HD, Davies AA. **In vivo detection and characterization of sumoylation targets in Saccharomyces cerevisiae.** Methods Mol Biol. 2009;497:81-103.

Versele M and Thorner J. **Septin collar formation in budding yeast requires GTP binding and direct phosphorylation by the PAK, Cla4. The Journal of cell biology,** 2004 Mar 1;164(5):701-15.

Wach A, Brachat A, Pöhlmann R and Philippsen P. **New heterologous modules for classical or PCR-based gene disruptions in Saccharomyces cerevisiae.** Yeast. 1994 Dec;10(13):1793-808.

Wang B and Elledge SJ. **Ubc13/Rnf8 ubiquitin ligases control foci formation of the Rap80/Abraxas/Brca1/Brcc36 complex in response to DNA damage.** Proc Natl Acad Sci U S A. 2007 Dec 26; 104(52):20759-63.

Weinert TA, Kiser GL and Hartwell LH. Mitotic checkpoint genes in budding **yeast and the dependence of mitosis on DNA replication and repair.** Genes & development, 1994 Mar 15;8(6):652-65.

Woodbury EL, Morgan DO. **Cdk and APC activities limit the spindle-stabilizing function of Fin1 to anaphase.** Nat Cell Biol. 2007 Jan;9(1):106-12. Epub 2006 Dec 17.

Yaffe MP and Schatz G. **Two nuclear mutations that block mitochondrial protein import in yeast.** Proc Natl Acad Sci U S A. 1984 Aug;81(15):4819-23.

Yang H, Jiang W, Gentry M and Hallberg RL. **Loss of a protein phosphatase 2A regulatory subunit (Cdc55p) elicits improper regulation of Swe1p degradation.** Molecular and cellular biology, 2000 Nov; 20(21):8143-56.

Yeong FM, Lim HH and Surana U. **MEN, destruction and separation: mechanistic links between mitotic exit and cytokinesis in budding yeast.** Bioessays. 2002 Jul;24(7):659-66.

Zhou J, Yao J and Joshi HC. **Attachment and tension in the spindle assembly checkpoint.** J Cell Sci. 2002 Sep 15;115(Pt 18):3547-55.

Publications:

Some of the results presented in this thesis are published in the following papers:

Erica Raspelli, Corinne Cassani, Giovanna Lucchini and Roberta Fraschini. **Budding yeast Dma1 and Dma2 participate in regulation of Swe1 levels and localization.** Mol Biol Cell. 2011 July 1; 22(13): 2185–2197.

Fraschini Roberta, Raspelli Erica, Cassani Corinne. **Protein Phosphorylation is an Important Tool to Change the Fate of Key Players in the Control of Cell Cycle Progression in *Saccharomyces cerevisiae*.** InTech, book "Phosphorylation", ISBN 980-953-307-159-1